UCRL-18887

eg 2

CHEMICAL BIODYNAMICS
Annual Report 1968

Lawrence Radiation Laboratory
University of California - Berkeley

UCRL-18887

eg 2

DISCLAIMER

UCRL-18887
UC-4 Chemistry
TID-4500 (54th Ed.)

UNIVERSITY OF CALIFORNIA

Lawrence Radiation Laboratory
Berkeley, California

AEC Contract No. W-7405-eng-48

CHEMICAL BIODYNAMICS ANNUAL REPORT, 1968

M. Calvin, Director, Laboratory of Chemical Biodynamics

June 1, 1969

Work done under auspices of the
U. S. Atomic Energy Commission

CHEMICAL BIODYNAMICS ANNUAL REPORT, 1968

Contents

*Preceding annual reports: UCRL-18216, UCRL-17520.

Plant Biochemistry

PHOTOSYNTHESIS BY ISOLATED CHLOROPLASTS. REGULATION BY FACTORS FROM LEAF CELLS

R. E. Moore, H. Springer-Lederer, H. C. J. Ottenheym, and J. A. Bassham

Introduction

Previous studies of photosynthesis by isolated spinach chloroplasts in the presence of $^{14}CO_2$- and ^{32}P-labeled inorganic phosphate have established several characteristics. High rates of photosynthesis are possible, and are stimulated by added inorganic pyrophosphate (PP_i).[1] Some intermediate compounds of the photosynthetic carbon-reduction cycle readily diffuse out of the chloroplasts, whereas other intermediate compounds are well retained.[2] With isolated chloroplasts photosynthesizing at high rates [greater than 100 μmoles of CO_2 fixed (mg chlorophyll· hr)$^{-1}$], no stimulation of the photosynthetic rate was found upon the addition of any of several intermediates of the photosynthetic carbon-reduction cycle.[3] No stimulation was seen upon the addition of ATP, ADP, AMP, or NADP. Little conversion of intermediates of the photosynthetic carbon-reduction cycle to secondary metabolic compounds such as amino acids and free sugars was seen.[1] It appeared that substances required for such conversion were missing from the isolated chloroplasts.

Preliminary studies showed that addition of clarified spinach juice caused inhibition of the rates of photosynthesis by isolated chloroplasts. Several fractions have now been obtained which have large effects on the rate of CO_2 photosynthesis by isolated chloroplasts. Certain characteristic properties of the inhibitory fractions described below suggest that they contain factors which play a role in the regulation of photosynthesis.

Methods and Materials

Spinach leaves are harvested from a nearby farm and brought on ice to the laboratory soon after being picked. The leaves are stored at 0°C for as long as 7 days.

Buffers and biochemical compounds are purchased from Calbiochem, Los Angeles, California. Buffers include MES [2-(N-morpholino)-ethane-sulfonic acid] and HEPES [N-2-hydroxyethylpiperazine-N'-2-ethane-sulfonic acid].

Each of the three solutions used in the isolation and assay of chloroplasts[1] contains the following: 0.33 M sorbitol, 0.002 M $NaNO_3$, 0.002 M EDTA (dipotassium salt), 0.002 M sodium isoascorbate (added on day of use), 0.001 M $MnCl_2$, 0.001 M $MgCl_2$, and 0.0005 M K_2HPO_4.

In addition, Soln A contains 0.02 M NaCl and 0.05 M MES, adjusted with NaOH to pH 6.1; Soln B contains 0.02 M NaCl and 0.05 M HEPES, adjusted with NaOH to pH 6.7; Soln C contains 0.005 M $Na_4P_2O_7 \cdot 10\ H_2O$ (added on day of use) and 0.05 M HEPES, adjusted with NaOH to pH 7.6.

All solutions are stored at 4°C.

Spinach Leaf Juice

Spinach leaf juice is prepared with a juicer (Model 6001, Acme Juicer Mfg. Co., Sierra Madre, California). This apparatus contains a flat circular grater which rotates at high speed and against which the leaves are pressed. Surrounding the rotating grater is a rotating screen against which the shredded leaves and juice are thrown by centrifugal action. This

apparatus is precooled to 4°C, and the juice emerging from the apparatus is collected in a chilled tube. Usually, 0.2 ml of Soln C minus PP_i is mixed with each gram of leaves as they are shredded by the juicer. About 0.7 ml juice is obtained per gram of leaves. This is adjusted to pH 7.6 with sodium hydroxide, and the juice is then clarified by centrifugation at 200 000×g for 1 hr.

Chloroplast Preparation

In a cold room, at 4°C, 12 g of leaves are washed and cut after removal of the midribs. The leaf strips and 33 ml chilled Soln A are placed in a "semimicro" Monel container on a Waring Blendor, Model 1120, and blended for 5 sec at high speed. The slurry is poured and pressed through six layers of cheesecloth (42 threads per inch), and the resulting juice is centrifuged for 50 sec at 2000×g. The chloroplasts in the resulting pellet are resuspended in Soln B at 0° to give a suspension which contains 2 to 3 mg chlorophyll per ml. This suspension is used for assay within 2 hr.

Extract from Sonicated Chloroplasts

Chloroplast extract is prepared from chloroplasts isolated from spinach leaves as described above, with the following modifications: the leaves are ground for 7 sec in Soln B instead of Soln A. Centrifuging is carried out for 2.5 min instead of 50 sec. Twelve pellets of chloroplasts, each obtained from 12-g batches of spinach leaves, are resuspended in 9 ml chilled Soln C minus PP_i.

The suspension is placed in a beaker, cooled in crushed ice, and sonicated for four periods of 15 sec, using a precooled probe (Biosonik, Model BP 1, Bronwill Scientific, Rochester, N. Y.). Ten-minute intervals between the sonication periods are allowed, to avoid overheating. The resulting broken chloroplast suspension is checked by phase microscopy for complete destruction of chloroplasts, adjusted with NaOH to pH 7.6, and clarified by centrifugation at 200 000×g for 1 hr.

Assay of Photosynthesis Rate

Photosynthesis is carried out in 15-ml round-bottom flasks stoppered with serum caps. Twenty-five µl of the chloroplast suspension is injected into each flask containing 450 µl of the medium to be assayed.

The basic medium is either complete Soln C, or Soln C deficient in either Mg^{++} or PP_i or both. In those experiments in which the medium contains juice or portions of fractions from gel filtration or dialysis, mixing is done in such a way as to keep the concentrations of all constituents present approximately constant. The amounts of juice or fractions added in various experiments are shown in the figures. In some experiments the medium is the effluent of the gel filtration.

The medium is kept at 4°C until the assay is started. Assays are conducted with flasks mounted on a shaking rack and illuminated from below in a constant-temperature bath, as described before.[1]

The chloroplasts in the swirled flasks are preilluminated for 5 min and are allowed to synthesize with ^{14}C-labeled bicarbonate for 10 min. The reaction is terminated by the addition of 4.5 ml of methanol to each flask.

For determination of total radiocarbon fixed, an aliquot sample of this chloroplast-methanol mixture is spotted on a piece of filter paper, acidified with acetic acid, and dried, and its radioactivity is measured with GM tubes. Alternatively, radioactivity is measured by scintillation counting. From the known counter sensitivities, and from the specific activity of the ^{14}C used, the amount of CO_2 fixed in the 10-min period is calculated.

Another aliquot sample of the original spinach chloroplast suspension is extracted with 80% acetone for the spectrophotometric

determination of chlorophyll content.[4] This figure plus the calculated amount of CO_2 fixed permits calculation of the rate of photosynthesis [μmoles CO_2 fixed (mg chlorophyll· hr)$^{-1}$].

Results

Figure 1 shows how the photosynthesis rate of isolated spinach chloroplasts is changed by the addition of various amounts of spinach juice, in the presence and absence of magnesium ion (1 mM) and of pyrophosphate ion (5 mM). The control rate of 1.0 on the vertical scale [128 μmoles CO_2 fixed (mg chlorophyll· hr)$^{-1}$] is obtained with Mg^{++} and PP_i present (the normal complete medium) and no juice added. In the presence of pyrophosphate, 5 to 15 μl of juice causes a significant enhancement of the rate, either in the presence or absence of Mg^{++}. With increasing amounts of added juice, there is a dramatic drop in the photosynthesis rate. With the addition of 30 μl of juice, the rate is reduced to about 5% of the control rate; it remains at this level with subsequent additions of juice up to 80 μl.

A striking difference is seen upon the omission of PP_i, in either the presence or absence of Mg^{++}. In this case there is little enhancement of the rate, and with larger amounts of juice the inhibition is much less pronounced. Thus we see the potentiating effect of PP_i on the enhancement and particularly on the inhibition caused by added juice.

The more active spinach leaves have been found to contain approximately 0.9 mg Chl/g leaf.[1] When juice is prepared as described under the Methods section, about 0.5 ml undiluted juice is obtained per gram of leaf, which gives a value of 0.55 ml juice/mg Chl. Since there is 73 μg Chl in each flask in the experiment shown in Fig. 1, the amount of juice corresponding to the ratio in vivo is 40 μl.

Figure 2a gives the rate of photosynthesis

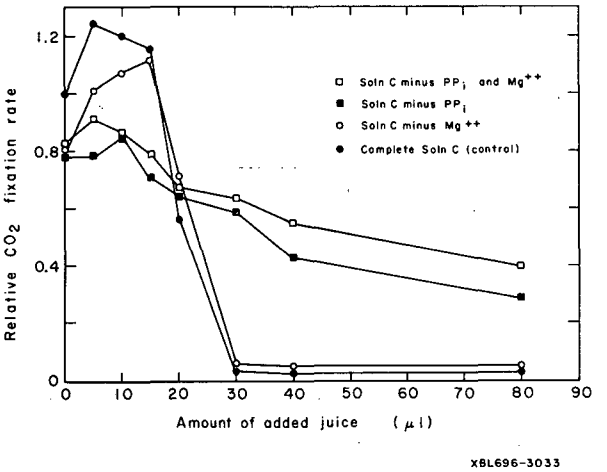

Fig. 1. Dependence of photosynthetic CO_2 fixation rate in isolated chloroplasts on the amount of added spinach juice in presence and absence of Mg^{++} and PP_i.

Each flask contained chloroplasts with 73 μg chlorophyll. Control rate (1.0 on vertical scale) was 128 μmoles CO_2 fixed (mg chlorophyll· hr)$^{-1}$. Control was conducted with complete Soln C as medium.

by isolated chloroplasts relative to the control as a function of various amounts of added juice in the presence of various concentrations of PP_i from 0 to 20 mM. In this experiment, 0.2 ml of Soln C minus PP_i was added per gram of leaves as the juice was being prepared, so that 0.68 ml diluted juice was obtained from each gram of leaves. In this case, therefore, there was 0.75 ml juice/mg Chl. Since there was 56 μg chlorophyll in each flask, the amount of juice per flask, which would again be equivalent to the approximate in vivo amount, is 42 μl.

The results in this experiment show clearly the importance of the ratio of PP_i concentration to amount of added juice in producing stimulation or inhibition of the photosynthetic rate. We have used the amount of juice in each flask corrected to ml juice/mg Chl to calculate the ratio of mM PP_i to ml juice/mg

Chl from the various points on the curves shown in Fig. 2a. The relative rate of photosynthesis is plotted against this ratio in Fig. 2b. With each level of added juice, increasing PP_i concentration causes increasing and then maximum inhibition until a certain threshold ratio is reached. The threshold ratios of mM PP_i to ml juice added/mg Chl range from about 10 to 12 for 5 to 40 µl added juice, to about 14 for 60 µl of juice.

Once the threshold ratio of PP_i/juice is passed, the rate of photosynthesis increases rapidly with increasing PP_i concentration. The maximum rates (> 120% of control) are reached when the ratio of PP_i/juice is very roughly 3 times the threshold ratio, with 5 to 20 µl of added juice.

In another experiment, the results of which are not shown, it was found that when juice is prepared from only the stems of spinach leaves, some enhancement (up to 20%) but no inhibition is seen in the complete medium, which contains PP_i and Mg^{++}. Thus, it seems clear that the inhibitory factor is a constituent of the leaf cells only.

Inhibitory factors can be partially resolved if the spinach juice is placed on a column containing Sephadex G-25, previously equilibrated with complete Soln C, and eluted with this solution into fractions, portions of which are

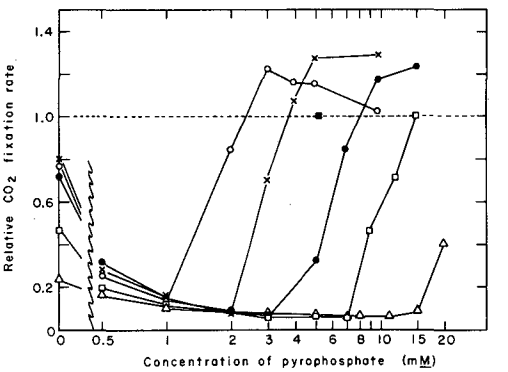

Fig. 2a. Dependence of photosynthetic CO_2 fixation rate in isolated chloroplasts on the concentrations of added spinach juice and PP_i.

56 µg chlorophyll per flask.
Control (complete Soln C): 84 µmoles CO_2 fixed (mg chlorophyll · hr)$^{-1}$.

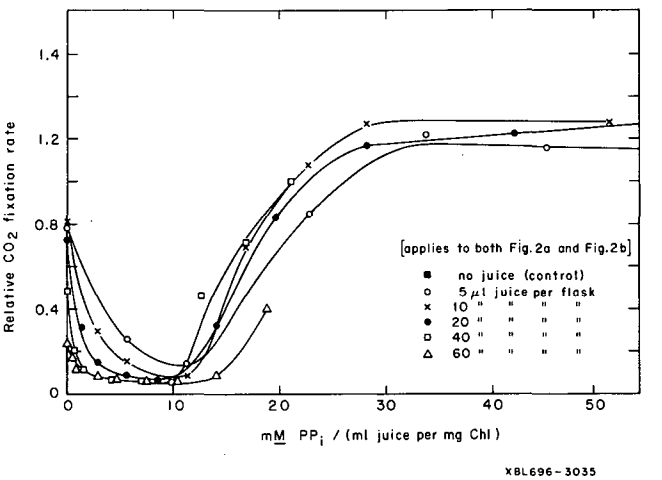

Fig. 2b. Relative rate of photosynthetic CO_2 fixation as a function of the ratio of concentration of added pyrophosphate to the amount of added juice per mg chlorophyll. Plotted points are derived from data shown in Fig. 2a. Forty µl juice per flask correspond to 0.71 µl spinach juice per mg chlorophyll, i.e., the estimated in vivo concentration.

subsequently used as media for the assay of the photosynthetic rate (Fig. 3). The first fraction exhibiting strong inhibitory activity (labeled Fraction A) comes off the column just after an effluent volume corresponding to the void volume of the Sephadex bed. Subsequent fractions are slightly stimulatory, or neutral. Then follows a second inhibitory fraction (labeled Fraction B). The volume of elution of these two fractions is such as to suggest that Fraction A contains an inhibitory compound of high molecular weight, whereas Fraction B contains an inhibitory substance of smaller molecular weight.

When a similar experiment was performed, except that PP_i was omitted from elution and assay, inhibition was seen only with the fractions corresponding to Fraction B. After addition of PP_i to all fractions, inhibition nearly as great as that seen in Fig. 3 was now observed with those fractions corresponding to Fraction A. Thus the inhibitory activity of the presumed large molecule requires the presence of PP_i, whereas inhibition by Fraction B is not dependent on the presence of PP_i.

When Fraction A, obtained as described above (Fig. 3) and left at 4° for 18 hr, was recycled through another column of Sephadex G-25, it was partially recovered as Fraction A, while another part of the inhibitory activity showed up as Fraction B. Thus the inhibitor of presumed smaller molecular weight can be derived from the inhibitory substance of higher molecular weight in Fraction A.

Dialysis of Fraction A against Soln C minus PP_i gave a retentate which upon subsequent analysis was found to be no longer inhibitory, even in the presence of PP_i. In contrast, dialysis of Fraction A against complete Soln C (which contains PP_i) gave a retentate that was still highly inhibitory when assayed with complete Soln C. It may be concluded that the presence of PP_i tends to stabilize a

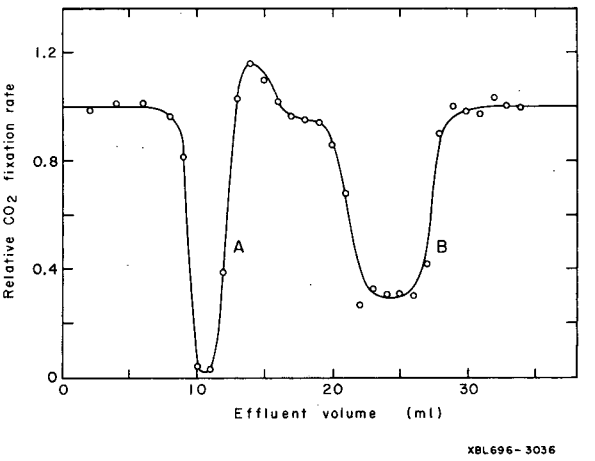

Fig. 3. Photosynthetic CO_2 fixation rates of isolated chloroplasts suspended in portions of effluent fractions of spinach juice separated by gel filtration on Sephadex G-25.

62 μg chlorophyll per flask.
Control (complete Soln C): 129 μmoles CO_2 fixed (mg chlorophyll · hr)$^{-1}$.

complex made up of an inert large molecule and a small molecule. Once this complex dissociates, the small molecule can be removed by dialysis.

The effects of additions to the assay medium of original juice and its dialysis fractions, i.e., retentate and diffusate, and recombined retentate and diffusate, all assayed in the presence and absence of Mg^{++} and PP_i, are shown in Table I, Experiment 1. The effect of PP_i on the inhibitory activity of the various components is seen. Also, the data show that the inhibitory power of the small molecule of the diffusate is greatly increased by the presence of the large inert molecule from the retentate. The reconstitution of inhibitory activity upon recombination of retentate plus diffusate suggests a re-formation of inhibitory complex.

The effects of adding Fraction B and inactive retentate to the assay medium, separately and combined, are shown in Table I, Experiment 2. Although the small molecule

Table I. Relative rates of chloroplast photosynthesis in presence of spinach juice and various juice fractions.

Expt.	Addition to assay medium	PP_i	Relative Rate
1	Original juice, 40 µl	-	0.68
		+	0.06
	Retentate, 40 µl	-	1.38
		+	1.26
	Diffusate, equivalent to 40 µl of original juice	-	0.47
		+	0.43
	Recombined retentate and diffusate	-	0.80
		+	0.08
2	50 µl Fraction B	+	0.93
	100 µl Fraction B	+	0.54
	30 µl retentate	+	1.01
	100 µl retentate	+	0.76
	50 µl Fraction B; 30 µl retentate	+	0.74
	50 µl Fraction B; 100 µl retentate	+	0.12
	100 µl Fraction B; 100 µl retentate	+	0.07
3	100 µl Fraction B	+	1.02
	100 µl retentate of chloroplast extract	+	1.12
	100 µl Fraction B plus 100 µl of chloroplast extract	+	0.16

Assays were made with complete Soln C (+ PP_i) or with Soln C minus PP_i (- PP_i). Retentates were obtained by dialysis of spinach juice (Expts. 1 and 2) or chloroplast extract (Expt. 3) against a hundredfold volume of Soln C minus PP_i. The diffusate (Expt. 1) was prepared by dialysis of spinach juice against a ninefold volume of outer solution. Fraction B (Expts. 2 and 3) was obtained by gel filtration of spinach juice (see text and Fig. 3)
Controls (1.0 relative rate, with complete Soln C): 65 µmoles CO_2 fixed (mg chlorophyll · hr)$^{-1}$ (Expt. 1); 68 (Expt. 2); 89 (Expt. 3).

in Fraction B inhibits by itself, this inhibition is amplified upon the addition of retentate. Thus Fraction B and diffusate exhibit similar potentiating effect, due to the presence of the small molecule in each.

An extract of sonicated, previously isolated chloroplasts was prepared (see Methods). The strong inhibition upon combination of retentate from this extract with Fraction B from spinach juice (Table I, Experiment 3) suggests that the high-molecular-weight component of the inhibition complex is of the same nature in spinach juice and chloroplasts.

Discussion

The dependence of the rate of photosynthesis in isolated chloroplasts on the amount of added clarified spinach juice in our usual assay medium is remarkable. A 20% or more stimulation with 5 to 10 µl of juice is changed to a 95% inhibition with 30 µl of juice. The latter amount is probably less than the amount of juice in the leaves corresponding to the amount of chlorophyll in the flask to which the juice was added. A doubling in concentration of some constituents (which accompanies the doubling of added juice from 15 to 30 µl) is

responsible for a twentyfold change in rate of photosynthesis. This large rate change with a small increase in the amount of added juice suggests a regulatory function of the juice. Such control might occur through the regulation of some enzymic activity or some delicately poised process such as transport through a membrane.

This hypothesis gains support from the strong potentiation of the inhibitory effect by small amounts of pyrophosphate and by the strict dependence of the effect on the ratio of pyrophosphate to added juice.

Further indication of a regulatory function is found in the nature of the most effective inhibitory component, a dissociable complex which is both stabilized and activated by pyrophosphate. It appears to be a molecule of high molecular weight which by itself is inert and an activating compound of smaller molecular weight.

This smaller molecule, found in Fraction B and in the diffusate, seems to have some inhibitory activity by itself, but its inhibitory activity is greatly enhanced upon formation of the complex with the high-molecular-weight compound. It may be that this compound of smaller molecular weight exhibits inhibitory activity only by virtue of its ability to complex with the large molecule, which could be present already in the isolated chloroplasts. The activation of the inhibitory complex on addition of Fraction B only to isolated chloroplasts presumably would require endogenous PP_i in the chloroplasts.

The isolated chloroplasts may have lost much of the small inhibitory molecule but retained some of the high-molecular-weight compound necessary for the potentiation of the activity of the small molecule. In support of this hypothesis, addition of Fraction B obtained from spinach juice, together with the retentate of the extract from sonicated, previously isolated chloroplasts, causes large inhibition.

The strict dependence of inhibitory activity on the ratio of pyrophosphate relative to the level of inhibitory substance suggests an important role for pyrophosphate in the operation of the regulatory mechanism in vivo. Although it is often assumed that pyrophosphate, formed by biosynthetic reactions, is immediately hydrolyzed, this seems not always to be the case in photosynthesis. Previous studies with algae photosynthesizing under steady-state conditions[5] show that there is a measurable steady-state level of pyrophosphate which can fluctuate between light and dark.

Pyrophosphate is produced during biosynthetic reactions leading to carbohydrate formation and in the formation of other macromolecules. Since it is hydrolyzed at a rate small enough to permit steady-state levels to exist, it may serve as a kind of measure of biosynthetic or photosynthetic rate, or possibly as a measure of the synthesis of one class of compounds (e.g., carbohydrates) at some particular subcellular site. Operating in conjunction with the as yet unidentified inhibitory factors discussed above, pyrophosphate level could in turn regulate photosynthesis. It is noteworthy that magnesium pyrophosphate complex inhibits the activity of fructose diphosphatase (D-fructose-1,6-diphosphate 1-phosphohydrolase, EC 3.1.3.11).[6] This enzyme is known to be one of the light-dark-regulated enzymes of photosynthesis.[5,7,8]

The stimulation of photosynthesis in isolated chloroplasts[1] by 5 mM PP_i in the absence of any added juice is probably due to the removal of inhibition caused by the inhibitor complex already present in the isolated chloroplasts. From the results in Fig. 2, it is seen that 5 mM PP_i would bring the PP_i/juice ratio well beyond the threshold ratio for any small amounts of inhibitor that might have remained with the isolated chloroplasts.

Although inhibitory regulation, by itself, may not appear to be a "useful" function for

metabolism, it must be remembered that the isolated chloroplasts do not represent the complete metabolic system of the cell. In particular, isolated chloroplasts make only a limited quantity of secondary products. Also, photosynthetic carbon-reduction-cycle intermediates, which diffuse easily from the chloroplasts,[2] are greatly diluted in concentration in the suspending medium, whereas in the intact cell they would be contained in a volume only several times the chloroplast volume. Thus, a change in the activity of a regulated enzyme of the carbon reduction cycle might lead to inhibition in isolated chloroplasts, whereas the same change in vivo could lead to a redistribution of carbon to secondary biosynthetic pathways.

Summary

The rate of photosynthesis by isolated spinach chloroplasts is strongly affected by the presence of clarified juice from spinach leaves. With chloroplasts photosynthesizing under otherwise optimal conditions (which include the presence of 5 mM pyrophosphate) the presence of juice in an amount corresponding to 1/4 of the calculated in vivo ratio of juice/chloroplasts causes a 20% stimulation in the rate, whereas 3/4 of the full calculated amount causes 90% inhibition.

The degree of inhibition or stimulation is a complex function of the ratio of added pyrophosphate to added juice. With a wide range of concentrations of added juice, additions of small amounts of pyrophosphate cause the rate of photosynthesis to decrease, and this inhibition increases with increasing pyrophosphate concentration, becoming and remaining severe until a threshold ratio of pyrophosphate to juice is reached. This threshold ratio is nearly constant over a twelvefold range of added juice. Beyond the threshold ratio, increasing pyrophosphate (at a given level of juice) reverses the inhibition, and with roughly 3 times the threshold ratio, the control rate is surpassed and stimulation is observed.

Gel filtration of the juice produces two well-separated inhibitory fractions. One inhibitory fraction contains a compound of high molecular weight complexed with a small molecule; the second inhibitory fraction contains the unassociated small molecule. The complex is inhibitory only in the presence of pyrophosphate, whereas the small unassociated molecule has the same activity whether pyrophosphate is present or not. The complex is stabilized in the presence of pyrophosphate. Without pyrophosphate present, the complex dissociates almost completely into its constituents. Dialysis of the dissociated complex gives an inactive large molecule in the retentate. The activity of the small molecule is greatly amplified when it is re-added to the inert large molecule.

The inhibitory fractions are found, at least in part, in previously isolated chloroplasts.

These findings and other results described in the text strongly suggest a role for these factors in the in vivo regulation of photosynthesis.

Acknowledgments

This work was supported, in part, by the U. S. Atomic Energy Commission.

R. E. M. was a recipient of a Faculty Appointment for the summer of 1968 by the Associated Western Universities Nuclear Program, cosponsored by the U. S. Atomic Energy Commission.

H. S.-L was a Public Health Service International Postdoctoral Research Fellow (number FO5 TW 1094-01).

We are indebted to Professor Calvin for valuable discussion and helpful suggestions during the course of these studies. We very

much appreciate the help provided by Mrs. Martha Kirk on many phases of our work and are grateful for excellent technical assistance by Mrs. Byrdie Ayres Mann.

We express our special thanks to the Silva Co. and to the Ratto Bros., Bay Farm Island, Alameda, California, for generously allowing us to take spinach from their fields whenever needed for our experiments.

References

1. R. G. Jensen and J. A. Bassham, Proc. Natl. Acad. Sci. U. S. 56, 1095 (1966).
2. J. A. Bassham, Martha Kirk, and R. G. Jensen, Biochim. Biophys. Acta 153, 211 (1968).
3. R. G. Jensen and J. A. Bassham, Biochim. Biophys Acta 153 219 (1968).
4. L. P. Vernon, Anal.Chem. 32, 1144 (1960).
5. T. A. Pedersen, Martha Kirk, and J. A. Bassham, Physiol. Plantarum 19, 219 (1966).
6. I. Morris, Biochim. Biophys. Acta 162, 462 (1968).
7. R. G. Jensen and J. A. Bassham, Biochim. Biophys. Acta 153, 227 (1968).
8. J. A. Bassham and Martha Kirk, in Comparative Biochemistry and Biophysics of Photosynthesis, K. Shibata, A. Takamiya, A. T. Jagendorf, and R. C. Fuller, Eds. (University of Tokyo Press, Tokyo, and University Park Press, State College, Pa., 1968), p. 365.

THE QUANTUM REQUIREMENT OF PHOTOSYNTHESIS IN CHLORELLA*

Kam-sik Ng and J. A. Bassham

The quantum requirement of photosynthesis in Chlorella pyrenoidosa has been reinvestigated. Evolution of oxygen was measured electronically with an instrument that determines the paramagnetism of the gas mixture; carbon dioxide was measured by its infrared absorption. Light measurements were made with a photocell calibrated against a thermopile, using filtered sunlight as a reference beam. Consideration of possible sources of error established the reliability of quantum requirement determinations as ± 6%. Determinations were made only with cultures which exhibited photosynthetic rates exceeding 250 μmoles O_2 evolved per mg chlorophyll per hr. In 16 determinations made over a twofold range of photosynthetic rates, quantum requirements for O_2 varied from 8.8 to 12.4. No correction for respiration was made, and a rationale is given for not making such corrections. Quantum requirements were independent of rate of light absorption over the 2.5-fold range used in this study. A probable cause of error was discovered in previously reported quantum requirements less than 8 which had been determined by a similar method. The measured requirements are consistent with a serial two-light reaction scheme for photoelectron transport and an additional biosynthetic requirement for ATP, generated in part by cyclic photophosphorylation.

*Abstract from Biochim. Biophys. Acta 162, 254 (1968).

INDUCTION OF RESPIRATORY METABOLISM IN ILLUMINATED CHLORELLA PYRENOIDOSA AND ISOLATED SPINACH CHLOROPLASTS BY THE ADDITION OF VITAMIN K_5*

G. H. Krause and J. A. Bassham

The effects on photosynthetic metabolism in Chlorella pyrenoidosa and in isolated spinach chloroplasts of adding vitamin K_5 have been investigated. The most pronounced effect is the induction of the oxidative pentose phosphate cycle in the light, as indicated by the appearance of 6-phosphogluconic acid immediately upon the addition of vitamin K_5. The appearance of 6-phosphogluconic acid in isolated spinach chloroplasts demonstrates the operation of the oxidative pentose phosphate cycle in chloroplasts.

The induction of the oxidative cycle is accompanied by inactivation of two enzymes of the photosynthetic carbon reduction cycle, or the reductive pentose phosphate cycle. These enzymes are fructose diphosphatase and phosphoribulokinase. Some inactivation of ribulose diphosphate carboxylase is also indicated. The inactivation of these enzymes may be related to the normal light-dark regulation of metabolism in vivo.

Although it has been reported that addition of vitamin K stimulates cyclic photophosphorylation in broken chloroplasts, such addition in these experiments caused no increase in the level of ATP in photosynthesizing Chlorella or photosynthesizing intact spinach chloroplasts.

A study of the changes of levels of labeled amino acids and carboxylic acids in photosynthesizing Chlorella pyrenoidosa when inhibitor is added shows an increase in the levels of glutamic and citric acids and a decrease in the levels of aspartic and malic acids. These changes are interpreted as indicating a stimulated increase in the rate of oxidation of pyruvic acid to carbon dioxide and acetyl coenzyme A, which may increase the rate of conversion of oxaloacetic acid to citric acid, leading ultimately to the production of glutamic acid.

*Abstract from Biochim. Biophys. Acta 172, 553 (1969).

PURIFICATION AND SOME CHARACTERISTICS OF THE ENZYME FRUCTOSE-1,6-DIPHOSPHATASE

A. M. El-Badry

Introduction

The enzyme fructose-1,6-diphosphatase isolated from spinach chloroplasts catalyzes the hydrolysis of fructose-1, 6-diphosphate to fructose-6-phosphate and inorganic phosphate:[1-3]

$$\text{fructose-1, 6-diphosphate} \xrightarrow[Mg^{++}]{\text{FDPase}} \text{fructose-6-phosphate} + P_i.$$

The hydrolysis is the reverse of the reaction catalyzed by phosphofructokinase in the glycolytic sequence. These two enzymes (fructose-1,6-diphosphatase and phosphofructokinase) are now recognized as important control points in glycolysis and gluconeogenesis. The inhibition of mammalian and bacterial fructose diphosphatase (FDPase) by

adenosine-5'-phosphate (AMP) suggests allosteric regulation.[4]

Hydrolysis of fructose-1,6-diphosphate (FDP) to fructose-6-phosphate is also an important reaction during the fixation of carbon dioxide in photosynthetic systems.[5] Bassham and his co-workers[6] suggest that the activity of FDPase in photosynthetic Chlorella cells is subject to regulation. That is, although FDPase is active during the photosynthetic fixation of carbon dioxide, its activity appears to decrease markedly when Chlorella cells are transferred to nonphotosynthetic conditions by turning off the light. This suggests light activation of the FDPase enzyme: the activation appears to decay after about 2 min of darkness. Morris[7] found that the activity of FDPase from spinach chloroplasts is inhibited by magnesium pyrophosphate ($MgP_2O_7^{--}$), $MgATP^{--}$, and $MgADP^{--}$ at concentrations of 1 to 3 mM. The degree of inhibition by all these inhibitors decreases with increasing concentrations of Mg^{++} and substrate (FDP). $MgP_2O_7^{--}$ and $MgADP^{--}$ are approximately equally effective as inhibitors; both are less effective than $MgATP^{--}$.

The activity of FDPase follows a sigmoidal saturation curve, and this becomes more pronounced in the presence of the inhibitor. A sigmoidal relationship between activity and substrate concentration is generally interpreted as being indicative of cooperative effects between two or more active sites on the enzyme. Hill plots indicate that the interaction coefficient with respect to substrate increases with increasing inhibitor concentrations. Similar increases in the interaction coefficient with respect to Mg^{++} have also been observed.

The enzyme appears to require Mg^{++} for its activity.[8] However, the enzyme has a wide range of pH optima from 7.5 at a Mg^{++} concentration of 40 μmoles/ml to 8.7 at a Mg^{++} concentration of 5 μmoles/ml. The FDPase is also activated by EDTA, and is more stable in the presence of sulfhydryl reagents such as glutathione, β-mercaptoethanol, or dithiothreitol (DTT); however, DTT has by and large the highest effect of all sulfhydryl reagents tested in protecting FDPase activity and stabilizing the enzyme.

More recently, Buchanan et al.[9] claimed that reduced ferredoxin activates the enzyme. In this report, however, we have conclusive evidence to the contrary. Reduced ferredoxin and glutathione were found to act as protective agents against the oxidation of the enzyme sulfhydryl groups. We have no evidence of direct activation of the enzyme by ferredoxin. The use of illuminated chloroplasts or molecular hydrogen and bacterial hydrogenase proved to give misleading results, due to the high background of inorganic phosphate for illuminated chloroplasts and to high contaminating fructose-1,6-diphosphatase activity in both cases. Our results indicate that chemically reduced ferredoxin showed no significant activation of the enzyme.

Materials and Methods

Isolation of the Enzyme Fructose-1,6-diphosphatase

The enzyme fructose-1,6-diphosphatase (FDPase) was isolated by the following method:

(i) Fifty bunches of commercial spinach were washed thoroughly with water and the blades were separated from the midribs. The blades were then dried between two sponges, chopped, and divided into 50-g batches.

(ii) Each 50-g batch was homogenized for 8 sec in a Waring Blendor with 200 ml of solution A (containing 0.33 M sorbitol, 0.002 M $NaNO_3$, 0.02 M EDTA (dipotassium salt), 0.02 M Na isoascorbate, 0.001 M $MnCl_2$, 0.001 M $MgCl_2$, 0.0005 M KH_2PO_4, 0.05 M [2-(N-morpholino) ethane sulfonic acid] adjusted with NaOH to pH 6.1, and 0.02 M NaCl).

The blendorate was then passed through six layers of cheesecloth to strain out fibrous material.

(iii) The homogenate was centrifuged at 2000×g in the Sorvall centrifuge for 3 min. The supernatant was decanted and each pellet was suspended in 10 ml of 0.05 M tris buffer pH 7.4, 0.002 M glutathione, 0.0002 M EDTA, and 0.001 M $MgCl_2$ (basic buffer).

(iv) The chloroplast suspension was sonicated for 30 sec in batches of 50 ml by use of the Biosonik at 0° C.

(v) The sonicated suspension was centrifuged in the Sorvall centrifuge at 36 000×g for 1 hr and the suspension was saved as the crude enzyme preparation.

(vi) The crude enzyme was acetone-fractionated by adding the acetone to a concentration of 30%. The acetone was precooled in the freezer at -14° C and was added to the crude enzyme solution slowly, with stirring, at 4° C. The crude enzyme in 30% acetone was allowed to stand in the cold room (4° C) for 30 min and the mixture was centrifuged at 13 200×g (in a Sorvall using a GSA 34 rotor at 9000 rpm) for 4 min. The supernatant was collected and the acetone concentration in the supernatant was brought to 75%. The enzyme in 75% acetone was allowed to stand in the freezer at -14° C for 1 to 2 hr. A copious precipitate formed and settled toward the bottom of the container. The upper layer of 75% acetone solution was decanted. The lower layer, containing the precipitated enzyme and some other proteins, was then centrifuged for 1 min at 5000× g and the pellets were collected.

(vii) The greyish-white precipitate was dissolved in the smallest possible volume of basic buffer and was dialyzed against cold water for 4 hr. Then it was twice dialyzed against basic buffer for 8 hr each time.

(viii) The dialyzed mixture was centrifuged in the Sorvall at 36 000×g for 10 min.

(ix) The supernatant was passed through a DEAE-cellulose column which had been preequilibrated with 0.05 M tris-HCl, with a pH of 7.4.

(x) A phosphocellulose column was then poured and equilibrated with basic buffer at pH 8 and the concentrated enzyme solution was applied to the column. The column was washed with four column volumes of basic buffer, which eluted an admixed series of protein peaks. The tubes containing FDPase activity were pooled.

(xi) To avoid loss of activity due to dilution, the enzyme was osmodialyzed by placing the dilute enzyme solution in large dialysis bags and burying these dialysis bags in crystalline sugar for 5 hr. The remaining concentrated enzyme solution was then dialyzed against basic buffer after being transferred to small dialysis tubing.

(xii) The enzyme FDPase was subjected to gel filtration on a G-100 Sephadex column. The column was pre-equilibrated with basic buffer containing 0.05 M tricine pH 7.4, 0.002 M DTT, 0.0002 M EDTA and 0.001 M $MgCl_2$. All fractions that contained significant activity were pooled.

Isolation of Bacterial Hydrogenase

Thirty grams of a frozen cell paste of C. pasteurianum was thawed overnight and suspended in water with the aid of a magnetic stirrer to a final volume of about 200 ml. Small amounts of deoxyribonuclease and ribonuclease were added to obtain a free-flowing suspension. Fifty-ml aliquots of this suspension were subjected to sonication for 10 min by the Biosonik. Cell debris was removed by a 15-min centrifugation at 36 000×g. The supernatant was then heated for 10 min at 60° under hydrogen. The precipitate was centrifugated off, and the supernatant was dialyzed

against tris buffer at pH 7.4. No attempts at further purification were made. The crude enzyme was dialyzed before use to minimize the level of inorganic phosphate present in the enzyme preparation.[10]

Isolation of Spinach Ferredoxin

Spinach ferredoxin was isolated and purified by a procedure which involved acetone extraction, according to San Pietro and Lang,[11] followed by chromatography on DEAE-cellulose based on the method of Lovenberg et al.[12] Its quantitative determination was based on the spectrum of the purified material.

Methods of Reducing Ferredoxin

(a) Reduction by illuminated chloroplasts: Ferredoxin can be reduced in the presence of chloroplast particles and light.[12] The evidence for such reduction was measured spectroscopically at 420 mμ by use of the Cary Model 14 spectrophotometer. Ferredoxin photoreduction by illuminated chloroplasts was stable and the ferredoxin could be largely reoxidized by NADP even after a considerable period in the dark.[13]

(b) Reduction by hydrogen: Tagawa and Arnon[14] showed that molecular hydrogen can reduce ferredoxin in the dark if the enzyme hydrogenase from C. pasteurianum is present. Partially purified hydrogenase was used in experiments presented here. Spectroscopic evidence was the criterion for ferredoxin reduction.

(c) Chemical reduction: Ferredoxin can be reduced by either hydrosulfite or hydrogen and platinum asbestos. Kassner has also shown[15] that ferredoxin can be photoreduced in the presence of a porphyrin and light with an electron donor such as EDTA, glutathione, sodium dithionite, titanous chloride, or ascorbic acid. If ferredoxin was reduced by dithionite, it could be reversibly oxidized to a large extent with oxygen. Bleaching of ferredoxin was also reversible upon exposure to oxygen.

Methods of Enzyme Assay

FDPase was assayed by direct determination of the inorganic phosphate released in the enzymatic reaction, by use of the Fiske-Subbarow method. Alternatively, the enzyme was assayed by the determination of NADPH produced, when the FDPase reaction is coupled with the enzymatic reactions of phosphoglucose isomerase and glucose-6-phosphate dehydrogenase. The latter reaction requires $NADP^+$, and reduced NADPH produced by this reaction is directly proportional to the quantity of fructose-6-phosphate produced by the FDPase reaction. The measurement of change in optical absorption at 340 nm is used to estimate the quantity of NADPH formed in the reaction. Presence or absence of bovine serum albumin in the reaction mixture showed no major change in the resulting kinetic curve. Thus BSA was omitted from the reaction mixture. The assay mixture was adjusted to pH 8.7 at a Mg concentration of 5 μmoles/ml, which constitutes the optimal reaction conditions for the spinach chloroplast FDPase.

Determination of Protein

In the process of enzyme purification, in order to determine the specific activity of the enzyme or to scan the fractions collected from the chromatography column, protein determinations were carried out by using UV absorption at 280 nm for preliminary estimations. The Lowry method of protein determination was used for more precise results. Bovine serum albumin was used as the standard for both methods.

The change of the protecting sulfhydryl reagent in the basic buffer from glutathione to DTT resulted in complications in the assay method. DTT interferes with the Lowry assay at lower concentrations than glutathione. The

use of a two-blank assay, one containing only the Lowry reagents in distilled water and the other containing the Lowry reagents in basic buffer, was the most satisfactory solution to the problem. Dialysis against water or tricine buffer was another way of eliminating the sulfhydryl reagent, but resulted in volume changes and nonquantitative transfer from the dialysis tubing to the test tube, due to foaming and to adsorption on the surface of the dialysis tubing (as evident from protein assays using standard BSA solutions).

One can arrange the three sulfhydryl reagents tested with reference to their interference with the Lowry assay as follows:

β-mercaptoethanol > DTT > gluthathione.

However, none of these reagents exhibits significant interference if its concentration in the assay mixture does not exceed 6 to 7 μmoles per assay tube (3 ml).

Results and Discussion

Stabilizing the Enzyme FDPase

The problem in isolating the enzyme FDPase was the great sensitivity of the enzyme to changes in conditions, and lack of stability of the enzyme, which was a limiting factor in the purification procedure. We found it more important to start by finding the best way to stabilize the enzyme, and the following is a summary of our findings:

Effect of temperature. The enzyme has an optimum stability at 0°. Storage at 0° for 2 months did not result in a significant decrease in activity. Storage of the enzyme at 4° (cold-room temperature) resulted in loss of activity within 96 hr. Temperatures higher than 4° resulted in loss of activity at a faster rate. The enzyme lost its entire activity a after 4 hr at room temperature. The only problem with storing the enzyme at 0° results from bacterial growth, which is believed to be Pseudomonas sp. A study of the best antibiotics or other bactericidal or bacteriostatic chemicals which would have little or no inhibitory effect on the enzyme resulted in the choice of EDTA at a concentration of 0.002 M as the best protective agent. It must, however, be dialyzed out before use of the enzyme.

The enzyme FDPase is apparently stable to storage in frozen form. Freezing the enzyme for as long as 3 months, then thawing it, resulted in active enzyme. However, if the FDPase was frozen once more and then thawed, the result was inactivated enzyme. It may be that the process of thawing (or freezing) has deleterious effects on the enzyme FDPase.

Effect of Mg^{++} on the Stability of FDPase

Mg^{++} is one of the best stabilizing factors for the enzyme FDPase. Preparations with Mg^{++} at 0.001 M were stable at 0° for 2 weeks with nothing else added to the tris buffer (0.05 M).

Effect of EDTA

EDTA is an absolute requirement for prolonged stability of the enzyme (i.e., over a period of months). EDTA at concentrations of 0.0002 M is sufficient by itself to stabilize the enzyme (in tris buffer) for 2 weeks at 0°.

Effect of Sulfhydryl Reagents

Glutathione and DTT were used as stabilizing agents. DTT was found to be much more effective as a stabilizing agent for the activity of FDPase. Use of DTT resulted in enhanced stability of the enzyme not only during storage, but also during the first steps of isolation and on the various chromatographic columns.

Effect of the Substrate

The substrate FDP is a good reagent for stabilizing the enzyme, although we have no evidence it is an absolute requirement. Due to the tight binding of the substrate to the enzyme in the absence of magnesium, FDP is a

selective eluting agent on the chromatographic column. It provides the same stabilizing effect as magnesium in addition to the selectivity in elution. Thus a modified buffer for the elution of the phosphocellulose column was devised. This buffer contains 0.05 M tricine, 0.002 M DTT, 0.0002 M EDTA, and 0.001 M FDP.

Conditions Resulting in the Maximum Stability of FDPase

Mixing experiments with solutions containing the various reagents in tricine buffer at pH 7.4 at 0° showed that maximum stability of the enzyme is achieved in a buffer containing the following components: tricine 0.05 M, Mg^{++} 0.001 M, EDTA 0.0002 M, DTT 0.002 M, FDP 0.001 M. FDPase stored in this buffer was stable at 0° for a period of more than 2 months.

Forms of the Enzyme FDPase

Our experimental results tend to accumulate knowledge pointing toward the existence of two forms of the enzyme FDPase.[4,17] One such piece of evidence is the behavior on the G-100 Sephadex column. The fractionated FDPase comes down as one broad peak of protein; the activity of the enzyme, however, forms two overlapping peaks. The specific activity of the first peak is higher than that of the second.

Elementary studies on the effect of ammonium on the enzyme activity was one other factor leading us to believe that the enzyme has at least two forms, one more active than the other. Although ammonium sulfate failed to separate the enzyme (after acetone fractionation) from other contaminating proteins significantly, it made the enzyme about four times as active as it was if untreated.

Incubation studies with the enzyme fructose-1, 6-diphosphatase at different pH's showed that the enzyme exhibits a lag period before it shows any activity, if the enzyme has been preincubated at pH 9 before its introduction to the assay mixture at pH 8.7. Preincubation at pH 6 resulted in a kinetic curve of a smaller slope than that obtained when the enzyme was preincubated at pH 7.4. All preincubation studies were carried out at the desired pH in tris buffer containing DTT, EDTA, and $MgCl_2$. The substrate FDP was omitted from all preincubation mixtures to avoid complications in interpretation of the results.

We find that FDPase loses its activity upon dilution. The enzyme is very inactive at concentrations below 1 mg/ml. However, if the diluted preparations are concentrated by osmodialysis the specific activity increases nearly twofold.

This might indicate that the enzyme is more active in an aggregated form. More interesting is the fact that diluted enzyme at concentrations between 1 and 3 mg/ml shows a lag period of 20 sec to several minutes. This lag period is unnoticed when the enzyme is at higher concentrations. Moreover, addition of BSA to the assay mixture or the enzyme solution did not eliminate this lag period. Only concentration of the enzyme solution to 3 or more mg/ml resulted in elimination of the lag period--that is, gave a straight-line kinetic curve.

The evidence presented above, in addition to the previously known fact that the enzyme shifts its peak of activity to a lower pH optimum upon the increase of Mg^{++} concentration, suggests a multiplicity of forms of the enzyme. It may be that an equilibrium between forms can be shifted in favor of a more active form in the presence of Mg^{++} or by ammonium sulfate or by incubation at neutral pH.

The Possibility for a Natural Inhibitor in the Chloroplast

Ammonium sulfate fails to activate FDPase if the enzyme is subjected to ammonium sulfate fractionation before the acetone

fractionation. Yet ammonium sulfate precipitation increases the specific activity of FDPase fourfold if carried out after the crude enzyme preparation has been acetone fractionated. This may suggest the presence of an acetone-extractable inhibitor of the enzyme, which either prevents the aggregation by ammonium sulfate to the active form or directly inhibits the enzyme after it has been aggregated to its more active form.

The Specificity of FDPase

The enzyme FDPase in its present state of purification does not hydrolyze sedoheptulose-1, 7-diphosphate, but it does hydrolyze pyrophosphate into inorganic phosphate. One should always run a double control when analyzing for the pyrophosphatase activity of FDPase, since at optimal pH of 8.7 pyrophosphate hydrolyzes slowly. For this same reason, the time of the reaction should be controlled exactly for quantitative data. The pyrophosphatase activity is undoubtedly present in our preparation, but whether it is due to FDPase or to a pyrophosphatase contaminant of the system is a question which must await further purification of the enzyme. If the pyrophosphatase activity is proven characteristic of the enzyme, the activity toward both ATP and ADP should also be tested, since these two compounds in addition to the pyrophosphate are the known inhibitors of FDPase.

Testing for pyrophosphatase activity was carried out by stopping the reaction after 10 min by use of trichloroacetic acid solution, then spinning down the protein and determining the inorganic phosphate formed by the method of Fiske-Subbarow.

Interaction of Ferredoxin with FDPase

The use of illuminated chloroplasts resulted in the reduction of ferredoxin, but this system was not suitable for the assay of FDPase activity. The chloroplast suspension contributed a high background level of inorganic phosphate, and also contained a considerable level of FDPase activity. This interfered with the determination of inorganic phosphate by the Fiske-Subbarow method.

The use of hydrogen reduction catalyzed by bacterial hydrogenase has the drawback of interference due to a high level of bacterial FDPase activity. Because of lack of kinetic and other data on the FDPase from the two sources, spinach chloroplasts and C. pasteurianum, it was not possible to obtain conclusive results.

Table I shows that reduced ferredoxin has a small effect on the activity of the enzyme FDPase. However, the results cannot be considered conclusive, since the crude hydrogenase obviously contains FDPase activity, and the interaction between the enzyme obtained from the bacterial source and that obtained from spinach chloroplasts is not known.

Now we are left with one possibility, the use of chemicals to reduce ferredoxin. Photochemical methods were not used, in order to avoid possible light activation of the enzyme. Reduction by dithionite was the only chemical method tried, and it has proven to be the most efficient of all the methods we tried for reducing ferredoxin. Unfortunately, the presence of the hydrosulfite ion interfered with the activity of FDPase. Therefore a method was devised to achieve reduction of ferredoxin and eliminate the excess hydrosulfite ion and its oxidation products from the medium. Ferredoxin was mixed with sodium dithionite under nitrogen in a closed system. The resulting reduced ferredoxin was then transferred to a dialysis tubing and dialysis was carried out under nitrogen with change of the dialysis buffer (0.05 M tris) every 3 hr, for a total of four changes. The dialysis was done at 0°C. Reduced ferredoxin was introduced into the assay mixture just

prior to the introduction of FDPase. The reaction was allowed to proceed for 10 min, then was stopped by adding 0.1 ml of 50% trichloroacetic acid. The precipitate was centrifuged out, and the inorganic phosphate produced in the enzymatic reaction was determined by the Fiske-Subbarow method. Failure to centrifuge out the precipitate results in delay of the color formation and gives misleading color densities.

Table I. Comparative effect of glutathione and ferredoxin reduced by molecular hydrogen and bacterial hydrogenase on the activity of the enzyme fructose-1,6-diphosphatase.

	Inorganic phosphate liberated mg of protein per 10 min (μmoles)
Complete[a]	1.30
- FDPase	1.32
- Ferredoxin	1.12
- Glutathione	1.00
- Hydrogenase	0.36
- Hydrogen	0.86
- FDP	0.07

a. 50 μmoles of tris-HCl, 5 μmoles of FDP, 5 μmoles of $MgCl_2$, 2 μmoles of EDTA, 200 μg of ferredoxin, 5 μmoles of glutathione, 100 μliters of the hydrogenase, and 1 mg of FDPase in a total volume of 1 ml.
The enzyme was dialyzed for 16 hr against the basic buffer containing tris-HCl, glutathione, $MgCl_2$, and EDTA at pH 7.4.

From Tables II and III we conclude that reduced ferredoxin has no significant effect on the activity of the enzyme FDPase. The small increase in activity can be explained by the protective effect of reduced ferredoxin on the enzyme. Reduced ferredoxin can act, like any sulfhydryl reagent, as an antioxidant for the enzyme--that is, reduced ferredoxin prevents the oxidation of the sulfhydryl groups of the enzyme FDPase. This is clear if we compare the effect of reduced ferredoxin with that of glutathione.

Table II. The activation of FDPase by chemically reduced ferredoxin, sulfhydryl reagents, Mg^{++}, and EDTA, at pH 7.5 and 40 μmoles of Mg^{++} and at pH 8.7 and 5 μmoles of Mg^{++}.

	Inorganic phosphate liberated per mg of protein per 10 min (μmoles)	
	At pH 8.7 and 5 μmoles of Mg^{++}	At pH 7.5 and 40 μmoles of Mg^{++}
Complete[a]	0.26	0.31
- Ferredoxin	0.25	0.29
- $MgCl_2$	0.24	0.22
- $MgCl_2$, ferredoxin, and EDTA	0.24	0.25
- $MgCl_2$, glutathione, and EDTA	0.25	0.24
- Ferredoxin, glutathione, and EDTA	0.23	
- Ferredoxin, Glutathione, and $MgCl_2$	0.20	0.21
- FDPase	0.01	0.01

a. 50 μmoles of tris-HCl, 5 μmoles of FDP, 5 and 40 μmoles of $MgCl_2$, 2 μmoles of EDTA, 200 μg of reduced ferredoxin, 5 μmoles of glutathione (reduced) in 1 ml final volume at pH 7.5 and 8.7.
The enzyme was dialyzed against tris-HCl buffer at pH 7.4 for 16 hr.

Table III. The activation of FDPase by chemically reduced ferredoxin and glutathione.

	Inorganic phosphate liberated per mg of protein per 10 min (μmoles)
Complete[a]	1.26
- Ferredoxin	1.15
- Glutathione	1.17
- FDPase	0.06
- FDP	0.06

a. 50 μmoles of tris-HCl, 5 μmoles of FDP μmoles of $MgCl_2$, 5 μmoles of EDTA, 200 μg of reduced ferredoxin, 5 μmoles of glutathione (reduced), and 1 mg FDPase, in 1 ml final volume, pH 8.7.
The enzyme was dialyzed for 16 hr against the basic buffer at pH 7.4.

Effect of Sulfhydryl Reagents

Glutathione was selected as the sulfhydryl reagent in this experiment. As seen from the data in Tables I, II, and III, sulfhydryl reagents have a slight effect on the activity of the enzyme. This effect is comparable to that of ferredoxin, which shows that both reagents merely protect the reduced sulfhydryl group of the enzyme from oxidation. We can also see that ferredoxin and glutathione have an additive effect.

Effect of Magnesium Chloride

The data provided by this study are in agreement with previously reported results, which show that magnesium is needed for FDPase activity. The enzyme shifts its pH optimum as the magnesium ion concentration changes. At magnesium ion concentration of 40 μmoles/ml, the optimum is 7.5, and at 5 μmoles/ml, the optimum pH is 8.7. Also, the activity of the enzyme is much higher at pH 7.5 and 40 μmoles/ml of Mg^{++} than at pH 8.7 and 5 μmoles/ml of Mg^{++}.

Effect of EDTA

Ethylene diamine tetraacetic acid also has some activating effect on FDPase; this may of course be due to its protecting the enzyme from being inhibited by metal.

Some of the pH Effects on the Enzyme FDPase

Incubation of the enzyme FDPase at pH 9 before the assays resulted in a lag period followed by an increase in enzyme activity with time. The pH of the assay mixture is 8.7, and one might not expect such a lag period upon preincubation at pH 9. If the enzyme is incubated at pH 7.4 before its introduction into the assay mixture of pH 8.7, the kinetic curve showed no lag period. These results might indicate some sort of association-dissociation equilibrium which is connected with the activity of the enzyme, and which is influenced by changes in hydrogen ion concentration.

References

1. S. Pontremoli, E. Grazi, and A. Accorsi, Biochemistry 7, 1955 (1968).
2. S. Pontremoli, B. Luppis, S. Traniello, and A. Bargellesi, Arch. Biochem. Biophys. 114, 24 (1966).
3. S. Pontremoli, S. Traniello, B. Luppis, and W. A. Wood, J. Biol. Chem. 240, 3459 (1965).
4. E. S. Vessell, Ann. N. Y. Acad. Sci. 151, Art. 1 (1968).
5. E. Racker and E. A. R. Schroeder, Arch. Biochem. Biophys. 74, 326 (1958).
6. R. G. Jensen and J. A. Bassham, Proc. Natl. Acad. Sci. U. S. 56, 1095 (1966).
7. I. Morris, Biochim. Biophys. Acta 162, 462 (1968).
8. J. Preiss, M. L. Biggs, and E. Greenberg, J. Biol. Chem. 242, 2292 (1967).
9. B. B. Buchanan, P. P. Kalberer, and D. I. Arnon, Biochem. Biophys. Res. Commun. 29, 74 (1967).

10. R. Bachosen, B. B. Buchanan, and D. I. Arnon, Proc. Natl. Acad. Sci. U. S. 51, 690 (1964).
11. A. San Pietro and H. M. Lang, J. Biol. Chem. 231, 211 (1958).
12. W. Lovenberg, B. B. Buchanan, and J. C. Rabinowitz, J. Biol. Chem. 238, 3899 (1963).
13. M. Shin, K. Tagawa, and D. I. Arnon, Biochem. Z. 338, 84 (1963).
14. K. Tagawa and D. I. Arnon, Nature 195, 537 (1962).
15. R. J. Kassner and M. D. Kamen, Proc. Natl. Acad. Sci. U. S. 58, 2445 (1967).
16. K. Taketa and B. M. Pagell, J. Biol. Chem. 240, 651 (1965).
17. F. Wróblewski, Ann. N. Y. Acad. Sci. 94, Art. 3 (1961).

THE SYNTHESIS OF 1,4-SUBSTITUTED IMIDAZOLES*

Preston K. Martin, H. Randall Matthews, Henry Rapoport, and G. Thyagarajan

A specific and unambiguous synthesis of 1,4-substituted imidazoles is described. α-Amino-β-methylaminopropionic acid was cyclized in triethyl orthoformate with a catalytic amount of hydrochloric acid to 1-methyl-2-imidazoline-4-carboxylic acid, which was esterified and dehydrogenated, with use of active manganese dioxide, to methyl 1-methyl-4-imidazolecarboxylate. This ester was further converted into several other 1,4-substituted imidazoles. The same procedure has been used to synthesize 1,5-substituted imidazoles; e.g., α-methylamino-β-aminopropionic acid was cyclized, esterified, and dehydrogenated under conditions similar to those for methyl 1-methyl-5-imidazolecarboxylate.

*Abstract of paper published in J. Org. Chem. 33, 3758 (1968).

STEREOCHEMIE DER UMWANDLUNG VON DIHYDROTHEBAIN IN THEBAIN SYNTHESE VON MARKIERTEN THEBAINEN*

U. Eppenberger, M. E. Warren, and H. Rapoport

The complete stereochemistry of the Δ^6-dihydrothebaine → 7-bromodihydrocodeinone dimethyl ketal → codeinone dimethyl ketal → thebaine sequence of transformations has been elucidated by NMR studies of the isotopically labeled compounds prepared by using diimide-d_2, methyl hypobromite-[^{14}C], and methyl hypobromite-d_3. Final elimination of methanol from codeinone dimethyl ketal proceeds in a stereospecific manner: cis under acid catalysis with $POCl_3$, and trans under alkaline catalysis with EtO^-. As a result of these reactions, variously isotopically labeled thebaines can be prepared.

*Abstract of paper published in Helv. Chim. Acta 51, 381 (1968).

Animal and Bacterial Biochemistry

COMPETITIVE HYBRIDIZATION TO DETECT RNA SPECIES IN BRAIN INDUCED THROUGH TRAINING

Kern von Hungen

There is now considerable circumstantial evidence to implicate protein[1-3] and RNA[4,5] synthesis in memory consolidation, and one is encouraged to assume the working hypothesis that neurons operate during learning by the same basic cellular mechanisms as are believed to be involved in cellular development and differentiation. That is, electrical stimuli reaching the brain act through inducer substances to derepress genes, giving rise to messenger RNA molecules which effect the synthesis of proteins which, acting as enzymes or structural units, alter the electrical circuitry of the brain. Such a derepression model has been advocated by Bonner,[6] who suggested that testing it should be relatively simple. Since these new RNA molecules would be gene products and present in learning animals, but not in nonlearning animals, it should be possible to pulse label them and detect them by competitive hybridization experiments.

Messenger RNA molecules are synthesized in cell nuclei on DNA so that they have base sequences complementary to those of the DNA segments coding for those RNA molecules. Hybridization refers to the in vitro recombination of isolated nucleic acids with complementary base sequences.

The extent of RNA-DNA hybridization is usually measured by radioactive labeling of the RNA and determination of the fraction of the radioactivity that becomes attached to the DNA when the two are incubated together. In competitive hybridization, nonlabeled RNA is added to the labeled RNA, or hybridized with the DNA before the labeled RNA, and the amount of base sequence identity between the RNA's is estimated by the extent to which the nonlabeled RNA competes for the sites to which the labeled RNA would hybridize.

The "detection of an RNA species unique to a behavioral task" by competitive hybridization has recently been reported by Machlus and Gaito.[7,8] In their experiment, they isolated DNA and RNA from the brains of trained and naive rats. They divided brains in half, and used one portion for DNA isolation and the other for RNA isolation. For labeled RNA, animals were sacrificed 90 minutes after intracranial injection of 200 μCi of ^{3}H-orotic acid. Animals to be trained were placed in a training box 60 min after injection (unlabeled animals were injected with unlabeled orotic acid). After 15 minutes of adaptation to the training apparatus, they were given 15 minutes of shock avoidance training. Fifty μg of DNA was hybridized for 12 hours with 50 μg of competitor RNA and then 12 hours with 50 μg of labeled testor RNA. Hybridization was carried out by the method of Gillespie and Spiegelman.[9] The essential data are the following:

	Labeled RNA hybridized (%)
DNA_L - RNA^*_L	3.10 ± 0.24
DNA_L - RNA_{NL} - RNA^*_L	1.40 ± 0.21
DNA_L - RNA_L - RNA^*_{NL}	0 ± 0

Subscripts L and NL refer to DNA or RNA from learning and nonlearning animals respectively; * means RNA is labeled.

Preincubation of DNA with RNA from nonlearning animals inhibited hybridization of the DNA with labeled RNA from learning animals 55%, while preincubation with RNA from learning animals inhibited hybridization with labeled RNA from nonlearning animals 100%. Since RNA_{NL} did not mask all the DNA sites for hybridization with complementary RNA^*_L, it was inferred that new species of RNA were present in the RNA from the trained animals. The fact that RNA from learning animals (RNA_L) masked all the sites for RNA from nonlearning animals (RNA^*_{NL}) was considered additional support for this view.

Most researchers interested in molecular mechanisms in the brain as related to learning are not experienced with the technique of competitive hybridization, and may have some difficulty in evaluating these results. Because of the fundamental importance of this type of experiment to our understanding of molecular brain mechanisms, I have attempted to reproduce these results, and provide further controls on the method. The discussion section refers to a number of other articles relevant to the interpretation of competitive hybridization data.

Methods

Labeling

Sprague-Dawley male rats, 200 to 250 grams, were used in all experiments. The rats were injected intraventricularly with 40 μCi ^{3}H-uridine in physiological saline, 20 μl on each side. Unlabeled animals were injected with the same volume of physiological saline.

Training

Rats were put in the training apparatus 60 min after injection, and, after 15 min of adaptation to the apparatus, were trained for 15 min. Shock avoidance training consisted of teaching the rats to run from a dark box (for which they have a natural preference) through an opening into a lighted box. If the animal did not escape to the lighted box within 10 sec of being placed in the dark box, a bell was sounded for 2 sec followed by a shock for 2 sec; the bell and shock were repeated every 10 sec until the animal escaped to the lighted box, where it was allowed to remain until the next trial. For each trial the animal was returned to the dark box, and the escape latency recorded. All trained animals received 15 trials in 15 min. Rats were sacrificed, immediately after training, by decapitation.

Nucleic Acid Isolation

DNA was isolated by the method of Marmur[10] from a crude nuclear fraction from rat liver. The rats were starved for 24 hr before sacrifice for DNA isolation, and a pronase step was included in the procedure immediately following the RNase step.

The standard procedure used for RNA isolation was as follows: A 10% homogenate of total brain, including cerebellum and olfactory bulbs, was made in cold 0.5% naphthalene disulfonate containing bentonite. (Less than 1 min elapsed between decapitation and homogenization.) This was extracted immediately with an equal volume of phenol II (phenol, water, m-cresol, and 8-hydroxyquinoline, 500:55:70:0.5) at 60 °C for 15 min. The solution was rapidly and thoroughly chilled on ice and centrifuged in the Spinco SW-25 rotor at 20 000 rpm for 5 min. The aqueous layer was added to 1/10 volume of 1% sodium dodecylsulfate (SDS) plus bentonite. The mixture was reextracted at room temperature for 5 min and chilled and centrifuged as before, once with phenol II and once with chloroform. SDS and bentonite were added to each aqueous

layer except the last. The final aqueous layer was made 0.1 M NaCl, 2 volumes of ethanol were added, and the RNA was precipitated overnight at -20°C. The RNA was collected by centrifuging at 1 000 g for 10 min, dissolved in water, and reprecipitated with NaCl and ethanol. The typical yield of RNA was approximately 2.0 mg per brain, based on the optical density at 260 mμ (1 mg = 25 OD units).

Hybridization

Hybridization was carried out by the method of Gillespie and Spiegelman.[9] DNA was immobilized on nitrocellulose membranes which, after being dried, were incubated with RNA in 1 ml of 6× SSC (1 × SSC = 0.15 M sodium chloride, 0.015 M sodium citrate, pH 7.0) at 66°C in scintillation vials. In competition experiments membranes were hybridized for 12 hr with competitor RNA, after which time testor RNA was added and the hybridization continued for another 12 hr. For determination of total hybrid, membranes at the conclusion of hybridization were rinsed in three washes of 2 × SSC, dried, and the radioactivity remaining on the membranes determined by scintillation counting. For the determination of RNase-resistant hybrid, membranes were incubated with pancreatic RNase (previously heated to 95°C for 10 min) for 1 hr at room temperature at a concentration of 20 μg/ml. The activity on membranes containing no DNA that were incubated with labeled RNA and then washed as usual was indistinguishable from background. Input activities were determined by applying 50 μg of RNA directly onto a membrane, drying the membrane, and counting.

Results

Learning is clearly evident with the training procedure used in these experiments. Figure 1 shows that the rats on the average learn to escape without receiving a shock

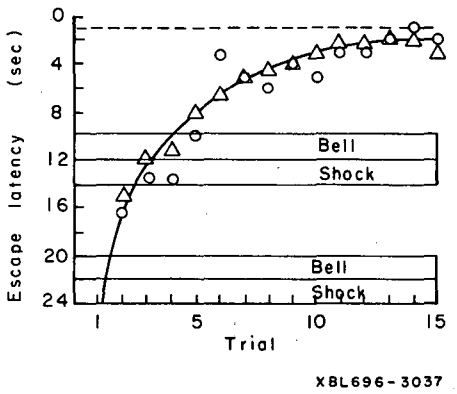

Fig. 1. Learning curves for trained rats. Escape latency is the time taken for the animal on each trial to run into the lighted box after being placed in the dark box. Average of four unlabeled rats, o ; average of six labeled rats, Δ .

after about five trials. After about 10 trials they run immediately from the dark box to the lighted box.

All possible combinations of competitor and testor are represented in Table I. Naive and trained RNA can be compared as competitor, A versus B, or as testor, A versus C. In the first case, competition should be greater in B than in A if induction has taken place, since the trained competitor in B will have species in common with the testor which are absent in A. In the second case, competition should be greater in C than A, since in C, as in B, the composition of the competitor and testor should be identical. C and

Table I. Possible combinations of competitor and testor RNA.

	Competitor	Testor	Examined
A	naive	trained	M & G; here; Table II
B	trained	trained	here: Table II, Fig. 2
C	naive	naive	here: Table II
D	trained	naive	M & G; here: Fig. 2

D need not be compared, since in both of these the competitor should contain all the species present in the testor.

Machlus and Gaito have looked at A and D. From the lack of complete competition in A, they inferred that new RNA species were present in the RNA from the brains of the trained animals. They did not look at B or (what would have been preferable) C as a control. Our data with B and C, and the data of others to be discussed later, indicate that complete competition should not have been expected. With D they observed complete competition, no activity on the membranes after hybridization with testor. We observe with D--using the same amounts of DNA, competitor RNA, and testor RNA as Machlus and Gaito used--the same level of competition as we do in A, B, and C, about 35%.

The results of our experiments comparing RNA from trained and naive rats as competitor and testor are shown in Table II. In the first three pairs of data, we see the results when various amounts of RNA, prepared individually from four trained and four naive rats, are tested for their effectiveness as competitor in the hybridization of pooled, labeled RNA from four trained rats. The figures for percent inhibition are the average of four determinations, using competitor RNA from four different rats. Percent inhibition, which indicates the extent of

Table II. Comparison of RNA from trained and naive rats as competitor and testor.

	Competitor		Testor	Inhibition ± S. D. (%)
A	$RNA_{N_{1,2,3,4}}$ (10 μg)	-	$RNA^{*}_{T_{4P}}$ (50 μg)	28.2 ± 2.4
B	$RNA_{T_{1,2,3,4}}$ (10 μg)	-	$RNA^{*}_{T_{4P}}$ (50 μg)	18.2 ± 12.6
A	$RNA_{N_{1,2,3,4}}$ (50 μg)	-	$RNA^{*}_{T_{4P}}$ (50 μg)	35.8 ± 4.8
B	$RNA_{T_{1,2,3,4}}$ (50 μg)	-	$RNA^{*}_{T_{4P}}$ (50 μg)	38.0 ± 2.3
A	$RNA_{N_{1,2,3,4}}$ (200 μg)	-	$RNA^{*}_{T_{4P}}$ (50 μg)	54.0 ± 8.3
B	$RNA_{T_{1,2,3,4}}$ (200 μg)	-	$RNA^{*}_{T_{4P}}$ (50 μg)	58.5 ± 3.4
A	$RNA_{N_{1,2,3,4}}$ (50 μg)	-	$RNA^{*}_{T_{1,2,3,4}}$ (50 μg)	32.7 ± 4.9
C	$RNA_{N_{1,2,3,4}}$ (50 μg)	-	$RNA^{*}_{N_{1,2,3,4}}$ (50 μg)	36.8 ± 3.1

The first three pairs compare 10, 50, and 200 μg of competitor from trained and naive rats for their efficiencies in inhibiting subsequent hybridization with testor RNA from trained rats. The numerical subscripts on the competitor refer to RNA from individual rats. The testor is RNA pooled from four trained rats; label is indicated by *. Each percent inhibition is the average of four with its standard deviation. The fourth pair compares trained and naive testor after hybridization with naive competitor. Each percent inhibition is from 16 determinations.

competition, is calculated from the level of hybridization of testor when no competitor was present during the preincubation period. The specific activity of testor RNA was about 30 cpm/μg, and the level of hybridization without competitor was about 2.5% for total hybrid and 1.0% for RNase-resistant hybrid. The inhibition levels in Table II were calculated from total hybrid, because the activity in RNase-resistant hybrid was so low. No statistically significant difference between the trained and naive RNA is observed. In the case in which only 10 μg of competitor was used, in which the difference was the largest, it was both not significant and in the wrong direction. It should be noted that even with 200 μg of competitor only about 55% inhibition was observed.

In the fourth pair of data in Table II, trained and naive RNA are compared as testor. New RNA was prepared for this experiment. Competitor RNA from each of four naive rats was tested against testor from each of four trained and four naive rats, so that each entry for percent inhibition is the average of 16 determinations. In this experiment, as in the first experiment, no difference between trained and naive RNA was observed. The competition levels were the same as in that part of the first experiment in which the same amount of competitor was used.

The basic conflict between our data and those of Machlus and Gaito is in the extent of competition exhibited by RNA from trained rats, D in Table I. To examine further the question of how much competition should be expected, a third experiment was performed using various amounts of trained competitor and a fixed amount of testor. Figure 2 shows the results of this experiment. Each point is the average of duplicate determinations. Fluctuation in the data is considerable, but it is clear that there is only about 50% inhibition with 200 μg of competitor. The figure also shows that inhibition levels can be calculated equally well from total or RNase-resistant hybrid. The inhibition levels in this experiment are comparable to those in the table, although the inhibition with small amounts of competitor is a little less here.

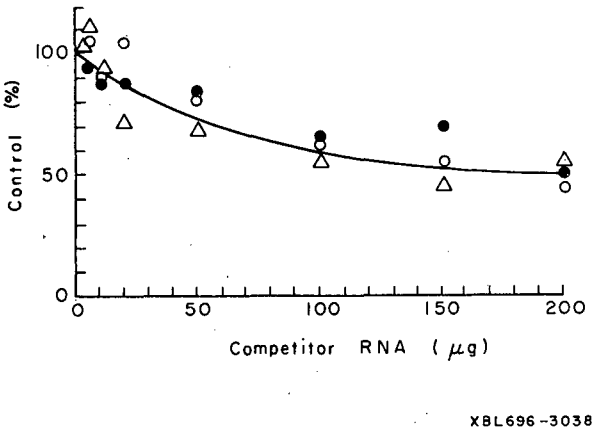

Fig. 2. Nitrocellulose membranes loaded with 50 μg of DNA were hybridized for 12 hr with various amounts of unlabeled competitor RNA, after which 50 μg of labeled testor RNA was added and the hybridization continued for 12 hr more. The results are expressed as percent of control, the level of hybridization of testor when no competitor was added. In the first experiment, in which RNase-resistant hybrid was measured, the competitor was pooled RNA from the brains of four trained rats, and the testor was pooled RNA from the brains of four naive rats, △. In the second experiment both RNase-resistant, ●, and total, o, hybrid were determined; the competitor was the same as in the first experiment, and the testor was pooled RNA from the brains of four trained rats.

Two of the factors which help explain why complete inhibition is not achieved can be appreciated from the data in Figs. 3 and 4. Increasing amounts of labeled RNA were hybridized for 12 hours with 50 μg of DNA. In the region of 50 to 200 μg of RNA there is a nearly linear increase in the amount of hybrid formed (Fig. 3). This means that in this region the DNA sites complementary to the labeled RNA are not saturated, and hence complete inhibition in the competition experiments could not be expected. Figure 4 shows the effect of increasing the duration of the hybridization. There is an increase in the extent of hybridization when the incubation is extended to 24 and 36 hr, indicating that the reaction had not gone to completion after 12 hr, and, again, saturation was not achieved with the 12-hr incubation. In all these experiments RNase-resistant hybrid was about 40% of the total hybrid.

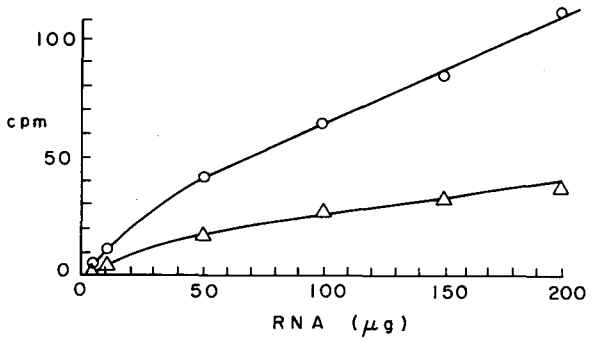

XBL696-3039

Fig. 3. The relationship between the amount of labeled RNA input and the amount of RNase-resistant, Δ, and total, o, hybrid formed after 12 hr of hybridization. The specific activity of the RNA was 30 cpm/μg. Membranes were loaded with 50 μg of DNA.

Discussion

The results in this report have failed to show any differences between the hybridization characteristics of RNA extracted from the brains of trained and naive rats. This

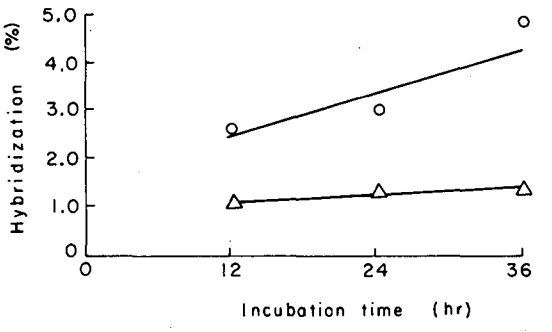

XBL696-3040

Fig. 4. The effect of the duration of hybridization on the percentage of input forming RNase-resistant, Δ, and total, o, hybrid. The input was 50 μg of RNA, 30 cpm/μg. Membranes were loaded with 50 μg of DNA.

does not mean, of course, that new RNA species are not synthesized in the brain as a result of training; it means only that the method used could not detect such species if they exist. We should not discard the idea that learning may be associated with the induction of RNA synthesis. In fact, we know that prolonged exposure of rats to an enriched environment results in "growth" in certain areas of the brain.[11] While this is probably not directly related to learning, it does demonstrate an environmental (or behavioral) stimulation of macromolecular synthesis in the brain.

Let us look at the systems in which hybridization has been used to detect induction or differences in RNA populations, and then examine in more detail the characteristics of various hybridization systems in order to evaluate the potential use of this technique for studying the relationship between learning and macromolecular metabolism in the brain.

In the early days of the messenger RNA theory, hybridization was used in elegant experiments by Attardi et al.[12] and Hayashi et al.[13] to demonstrate the induction of

specific messenger RNA's by inducer substances. Special techniques were used in these bacterial systems to increase greatly the sensitivity of the method. For instance, "nonrelevant" m-RNA was removed by hybridization with DNA from mutants lacking the genes under study, and the relative concentration of the DNA segment carrying the genes under study was increased by using DNA from transducing phages such as λdg in which specific bacterial genes were incorporated into the episome by recombination. Also in this work very high specific activities were used. These special techniques cannot be used with higher organisms.

It has, however, been possible to demonstrate differences in the RNA's synthesized by animal cells during periods of major alteration of structure or function. Competitive hybridization has been used by Denis[14, 15] to study the release of genetic information during amphibian development. He found that some DNA sites which were active in RNA synthesis at the gastrula stage continued to be active during later development, whereas others seemed to be no longer active. As the embryo developed, stable molecules formed an increasing portion of the total population of messenger RNA. Similar studies were conducted by Church and McCarthy[16, 17] on regenerating and embryonic mouse liver. Liver regeneration appeared to be partly mediated by short-lived RNA molecules, the synthesis of which commences rapidly after partial hepatectomy and ceases at various times during the regenerative process. The new species of RNA which appeared in response to partial hepatectomy were compared with those associated with rapid cell proliferation in embryonic liver. Since embryonic liver RNA was an efficient competitor for early regenerating liver RNA, it was concluded that much of the characteristic regenerating liver RNA was the result of reactivation of genes active in liver development but repressed in adult liver.

Drews and Brawerman[18] have reported that cortisol (hydrocortone) causes the appearance of new species of messenger RNA both in normal and in regenerating rat liver. The administration of cortisol led to a two- to threefold increase in the labeling of nuclear RNA, and affected ribosomal and messenger RNA to about the same extent. The methods in that work were similar to those used in the work presented here. The hybridization of 20 μg of DNA with 20 μg of nuclear RNA testor from normal animals was inhibited 90% when conducted in the presence of 200 μg of nuclear RNA from normal animals, but only about 60% inhibition was observed when the testor was from cortisol-treated animals. Competitor from cortisol-stimulated rats inhibited hybridization with testor from normal and cortisol-stimulated animals to the same extent, about 75%. No differences were observed between normal and regenerating liver 24 hr after partial hepatectomy. The 200 μg of nuclear RNA competitor is effectively 10 times as much RNA as our 200 μg of total cellular RNA, since only about 5% of the latter is nuclear RNA. Later, using the same method, those authors were unable to find any such effects with growth hormone.[19] From similar studies, Gupta and Talwar[20] also concluded that although growth hormone stimulates the rate of RNA synthesis in the liver of hypophysectomized rats, it does not induce the synthesis of new RNA species to an extent detectable by their methods. Wyatt and Tata[21] reported that growth hormone and tri-iodothyronine stimulated nonhybridizing RNA more than hybridizing RNA. This was interpreted as reflecting preferential synthesis of ribosomal RNA in response to these hormones.

Competitive hybridization has also been used by Neiman and Henry[22] to demonstrate the presence, in human chronic lymphocytic leukemia lymphocytes, of RNA species not present in normal lymphocytes.

The articles referred to above are the major reports of the detection of altered populations of cellular RNA by competitive hybridization. Now let us look at some of the details of hybridization. One should recognize the following as important questions about a hybridization system: What kinds of RNA hybridize and to what extent? What kinds of RNA are labeled and to what extent? What levels of hybridization should one thus expect? How much RNA is required to saturate DNA gene sites? What is the difference between preincubating competitor with DNA and adding it simultaneously with the testor? How specific is hybridization?

It has been shown by McCarthy and Hoyer[23] that, as far as can be determined by hybridization, DNA from different tissues of an animal is identical. The base composition and amount of DNA per diploid nucleus from different tissues is also identical. One can thus use DNA from brain, liver, or kidney equally well for studying the hybridization characteristics of brain RNA. Virtually all RNA in animal cells is synthesized in the nuclei; a small amount is synthesized in mitochondria. A short time after pulse labeling, incorporated activity is localized in the nuclei. Thereafter, messenger, ribosomal, and transfer RNA migrate out into the cytoplasm. Not all the RNA is transferred to the cytoplasm, however. Shearer and McCarthy[24] have found that approximately 80% of the RNA synthesized in the nucleus never leaves the nucleus; this RNA turns over very rapidly. The extent to which RNA species are labeled with a pulse label depends on their turnover rates. For example, only a small fraction of the ribosomal RNA molecules, which constitute 70 or 80% of the cellular RNA and have a half-life of about 12 days in brain,[25,26] would be labeled shortly after a pulse, whereas the specific activity of specific messenger RNA's with a much shorter half-life and constituting very small populations of molecules would be much higher. Those familiar with the kinetics of brain RNA metabolism will realize that RNA isolated after 90 min incorporation (as in the experiments presented here) has most of the activity in ribosomal and transfer RNA; this can be seen from the similarity of the optical density and activity profiles when the RNA is run on sucrose density gradients. In spite of this, these species contribute negligibly to the observed hybridization, because of their low specific activity and genome representation. Other types of RNA, namely cytoplasmic messenger and nuclear RNA, although perhaps containing less of the total activity, are responsible for almost all the observed hybrid, because of their greater genome representation and the higher specific activities of some of their species. The greater genome representation of these types of RNA is reflected by their DNA-like base composition. The level of hybridization one can obtain depends on what fraction of the input label is in RNA species that hybridize efficiently. With long labeling times most of the activity will be in ribosomal and transfer RNA and only very low levels of hybridization will be observed. In various cellular systems with short incorporation times, hybridization levels from 1 to 5% for RNase-resistant hybrid are typically observed;[18,20-22] levels for total hybrid are consistently 2 to 3 times those for RNase-resistant hybrid.[21,27,28] McCarthy[24] and Bondy,[29] among others, do not use the RNase treatment. Some of the variation between levels of hybridization reported by different

groups can be attributed to differences in the way the input activity is determined; other experimental variables, of course, also contribute to this variation. Most workers have found that under the usual conditions of incubation the maximum level of hybridization is reached after about 18 hr,[16,29,30] although others find longer incubation times necessary.[28] Lowering the RNA/DNA ratio increases the percentage of the labeled input that hybridizes, but this requires high specific activities of RNA for the detection of the hybrid. Virtually complete hybridization can be obtained in bacterial systems at very low RNA/DNA ratios.[31,32] Ribosomal RNA from rat brain has been found by Stevenin et al.[30] to saturate the DNA sites coding for it at a RNA/DNA of about 1/5. The sites for messenger RNA began to become saturated at a RNA/DNA ratio of about 25/1. The higher levels of hybridization at low RNA/DNA ratios is due to the more complete hybridization of ribosomal RNA and other RNA's with relatively low genome representation, some of which may be messenger RNA species. Other workers have failed to obtain saturation plateaus with nuclear RNA at RNA/DNA ratios as high as 200/1.[21,28] The data of Stevenin et al. indicate that 0.15% of the DNA genome codes for ribosomal RNA; this amounts to about 6 000 cistrons. About 1.2% of the genome codes for messenger RNA in adult rat brain, or 50 000 to 500 000 cistrons. One can avoid the problem of differential labeling of RNA species with different turnover rates by labeling all species of RNA equally, either by chronic application of label or by labeling the isolated RNA with labeled dimethyl sulfate,[33] but usually one is interested in having labeled only the molecules synthesized during a given short period of time.

It is becoming generally recognized among workers using hybridization that the formation of hybrids does not require absolute complementarity of base sequence by the two participating strands.[22,34] From detailed analysis of the kinetics of DNA-DNA hybrid formation, Britten and Kohne[35] have shown that there are hundreds of thousands of copies of DNA sequences in the genome of higher animals. There appears to be some mechanism which from time to time extensively reduplicates certain segments of DNA. During evolution the repeated DNA sequences apparently change slowly and thus diverge from each other, resulting in many families of nearly identical sequences in the genome. It is estimated that these families comprise more than 30% of the base sequences in mammalian DNA. This may explain the relatively low levels of hybridization obtained with mammalian RNA. It may be that only the products of these families of cistrons hybridize to an appreciable extent. How nearly identical sequences have to be to form hybrids is difficult to evaluate, and varies with the experimental conditions. Church and McCarthy[34] suggest that the hybridization assay with mammalian nucleic acids might better be viewed as a chromatographic system in which there are a great number of different adsorption sites than as one in which specific cistrons are titrated with their own gene products. The specificity of adsorption is limited, and and similar but different RNA molecules may well be indistinguishable. Thus, in competition experiments, observed differences must reflect real differences, although failure to discriminate does not prove identity.

The specificity of competition has also been questioned by Birnboim et al.[28] They reported that they were unable to obtain competition when DNA-loaded membranes were

prehybridized with large amounts of competitor and then hybridized with testor in another vial after the membranes had been washed. If testor was added to the competitor after prehybridization, the same amount of competition was observed as when the two were added together without any prehybridization. Riggsby and Merriam[36] found, however, that competition could be demonstrated by the prehybridization method if saturating amounts of testor were used. In simultaneous incubation competition studies, Neiman and Henry[22] found that large amounts of heterologous animal cell RNA interrupted hybrid formation in excess of the probable sequence similarity of the competing polyribonucleotides. They suggested that this nonspecific interference may have led to overestimates of the degree of similarity of the competing RNA's in some studies.

These considerations should make it clear that it is not simple to test whether induction is involved in learning by using competitive hybridization. Only a relatively small number of brain cells need be involved in learning any particular task or fact, and the same RNA species induced in these cells could be present and turning over in large numbers in other cells which are simply maintaining their induced state. We should not expect a large effect in the hybridizability of the total cellular RNA even if induction does take place. One should be cautious in accepting the results of Machlus and Gaito as demonstrating the induction of an RNA species unique to a behavioral task; the data in the report presented here and those of others cast doubt upon their observed level of competition by total cellular brain RNA from trained animals. This discussion should not be construed as arguing that it will be impossible to detect new species of RNA induced through training by competitive hybridization. A reproducible, demonstrable difference in the RNA populations in the brains of trained and naive animals would be highly significant, and the sensitivity of the technique could be increased over that in this work in various ways, such as using only RNA from specific brain regions, using fractionated RNA, using larger amounts of competitor and testor, etc. This discussion should, however, have clarified some of the limitations of the method.

Other possible macromolecular control mechanisms besides induction could be operative in memory consolidation. Protein synthesis could be regulated at the level of translation. The fact that so much RNA synthesized in the nucleus is broken down without leaving the nucleus has suggested to several workers another control mechanism.[34, 37, 38] This may be potential messenger, which is expressed only if it can escape into the cytoplasm. It should be stressed that one cannot equate rapidly labeled, DNA-like RNA with functional messenger RNA, as many have done in the past. Brain messenger RNA can be isolated from polysomes,[39] and hybridization experiments with this RNA hold more promise than those using total cellular RNA. In spite of the conviction of most biochemists who have considered the question, it is also possible that RNA and protein biosynthesis have nothing directly to do with learning.

Summary

An attempt is made to reproduce the results of a report in the literature of the detection by competitive hybridization of an RNA species unique to a behavioral task. The data from attempts to replicate this experiment and from experiments to characterize further the hybridization system suggest that the method is not sufficiently sensitive to detect such species if they exist. Hybridization of mammalian RNA in general is discussed.

Bibliography

1. B. W. Agranoff, R. E. Davis, and J. J. Brink, Proc. Natl. Acad. Sci. U. S. 54, 788 (1965).
2. L. B. Flexner, J. B. Flexner, and R. B. Roberts, Science 155, 1377 (1967).
3. S. H. Barondes and H. D. Cohen, Science 160, 556 (1968).
4. J. W. Zemp, J. E. Wilson, K. Schlesinger, W. O. Boggan, and E. Glasman, Proc. Natl. Acad. Sci. U. S. 55, 1423 (1966).
5. H. Hydén, Behavior, Neural Function, and RNA; Progr. Nucleic Acid Res. Mol. Biol. 6, 186 (1967).
6. J. Bonner, Molecular Biological Approaches to the Study of Memory, in Macromolecules and Behavior, John Gaito, ed. (Appleton-Century-Crofts, Inc., New York, 1966.
7. B. Machlus and J. Gaito, Psychonomic Sci. 10, 253 (1968).
8. B. Machlus and J. Gaito, Psychonomic Sci. 12, 111 (1968).
9. D. Gillespie and S. Spiegelman, J. Mol. Biol. 12, 829 (1965).
10. J. Marmur, J. Mol. Biol. 3, 208 (1961).
11. E. L. Bennett, M. C. Diamond, D. Krech, and M. R. Rosenzweig, Science 146, 610 (1964).
12. M. Hayashi, S. Spiegelman, N. C. Franklin, and S. E. Luria, Proc. Natl. Acad. Sci. U. S. 49, 729 (1963).
13. G. Attardi, S. Naono, J. Rouvière, F. Jacob, and F. Gros, in Cold Spring Harbor Symposium, 1963.
14. H. Denis, J. Mol. Biol. 22, 269 (1966).
15. H. Denis, J. Mol. Biol. 22, 285 (1966).
16. R. B. Church and B. J. McCarthy, J. Mol. Biol. 23, 459 (1967).
17. R. B. Church and B. J. McCarthy, J. Mol. Biol. 23, 477 (1967).
18. J. Drews and G. Brawerman, J. Biol. Chem. 242, 801 (1967).
19. J. Drews and G. Brawerman, Science 156, 1385 (1967).
20. S. L. Gupta and G. P. Talwar, Biochem. J. 110, 401 (1968).
21. G. R. Wyatt and J. R. Tata, Biochem. J. 109, 253 (1968).
22. P. E. Neiman and P. H. Henry, Biochemistry 8, 275 (1969).
23. B. J. McCarthy and B. H. Hoyer, Proc. Natl. Acad. Sci. U. S. 52, 915 (1964).
24. R. W. Shearer and B. J. McCarthy, Biochemistry 6, 283 (1967).
25. S. C. Bondy, J. Neurochem. 13, 955 (1966).
26. K. von Hungen, H. R. Mahler, and W. J. Moore, J. Biol. Chem. 243, 1415 (1968).
27. I. Merits, W. Schultze, and L. R. Overby, Arch. Biochem. Biophys. 115, 197 (1966).
28. H. C. Birnboim, J. J. Pene, and J. E. Darnell, Proc. Natl. Acad. Sci. U.S. 58, 320 (1967).
29. S. C. Bondy and S. Roberts, Biochem. J. 109, 533 (1968).
30. J. Stevenin, J. Samec, M. Jacob, and P. Mandel, J. Mol. Biol. 33, 777 (1968).
31. D. Kennell and A. Kotoulas, J. Mol. Biol. 34, 71 (1968).
32. D. Kennell, J. Mol. Biol. 34, 85 (1968).
33. K. D. Smith, J. L. Armstrong, and B. J. McCarthy, Biochim. Biophys. Acta 142, 323 (1967).
34. R. B. Church and B. J. McCarthy, Proc. Natl. Acad. Sci. U.S. 58, 1548 (1967).
35. R. J. Britten and D. E. Kohne, Science 161, 529 (1968).
36. W. S. Riggsby and V. Merriam, Science 161, 570 (1968).
37. J. Drews, G. Brawerman, and H. P.

Morris, Eur. J. Biochem. 3, 284 (1968).
38. D. T. Sullivan, Proc. Natl. Acad. Sci. U. S. 59, 846 (1968).
39. M. R. V. Murthy, Biochim. Biophys. Acta 166, 115 (1968).

PRELIMINARY INVESTIGATION OF PARAMETERS FOR USE OF SOME ANTIBIOTICS IN INHIBITION OF PROTEIN SYNTHESIS

Ann E. Orme and Edward L. Bennett

Several investigators have used antibiotics to inhibit various steps in protein synthesis to see what effects this inhibition may have in learning or memory or both. Barondes and Cohen found that a dose of cycloheximide or acetoxycycloheximide which inhibited 90% of cerebral protein synthesis did not impair the mouse's ability to learn either a shock-escape task or a water-reinforcement task when given before or shortly after the learning task.[1, 2] In addition, the mice "remembered" their training if tested 3 hr later, but showed definite loss of memory if tested at 64 hr, 24 hr, or 7 days. Other workers have used different drugs. Agranoff et al. used puromycin to produce memory loss in a shock avoidance task in goldfish.[3]

Experiments using specific inhibitors of protein synthesis could add significant information to the study of brain biochemistry, so preliminary work was begun this past summer by Shapiro and Bennett[4] to test the training and testing criteria that have been reported by Barondes and Cohen.[1] Since that time acetoxycycloheximide has become unavailable, so we hoped to find other commerically available antibiotics that would be as successful as acetoxycycloheximide.

The work reported here was done to determine the parameters of dose and time to produce a high degree of protein synthesis inhibition using cycloheximide and pactamycin.

Materials and Methods

Male Swiss albino mice, estimated weight 30 g, and Sprague-Dawley rats, approximately 150 to 200 g, were obtained from Bio-Sciences Laboratories, Oakland; DBA/2J mice were obtained from Jackson Laboratories, Bar Harbor, Maine. A sample of pactamycin was obtained as a gift from Upjohn Co. Cycloheximide was purchased from Cal Biochem under the trade name of Acti-dione. A small sample of acetoxycycloheximide remained from previous experiments. L-Valine-U-^{14}C was purchased from Cal Biochem (sp. act. 175 mCi/mmole)and from New England Nuclear (sp. act. 199 mCi/mmole).

We attempted to replicate, at least in part, the methods described by Barondes and Cohen.[1, 5] Both drug and valine-^{14}C (either 4 or 5 μCi per animal) were injected subcutaneously on the back of the animal. At an appropriate time the animal was decapitated. The cortex was removed, weighed, frozen on dry ice, and stored in deep freezer for further work-up. The subcortex and liver were treated in a similar way. Each sample was homogenized in sufficient 0.1 N NaOH to give a concentration of 15 mg wet tissue/ml for liver and

20 mg/ml for the brain sections. (In later experiments with rats, the liver was put through a press and about 1 g of the paste weighed and homogenized.) Six ml of 12% trichloroacetic acid (TCA) was added to a 2-ml aliquot to precipitate the protein. Two further washes, resuspensions, and centrifugations were used to remove free valine. One ml of Biosolv BSS-3 solubilizer (Beckman Instruments, Inc.) was added to the TCA precipitate, which was mixed and allowed to dissolve for at least 30 min. This mixture was then quantitatively transferred to scintillation counting vials with repeated aliquots of either dioxane-Fluor II scintillation fluid or Toluene-Fluor II scintillation fluid. One-ml aliquots of the first TCA supernatants were also counted by use of Dioxane-Fluor II scintillation fluid.

Definition of Terms

Graphs and tables are in terms of total drug time, which is the duration from injection of the drug to decapitation. In most experiments the valine-^{14}C incorporation time has been standardized to 30 min. For example, in a "total cycloheximide time" of 240 min, the drug was injected at "0" time, valine was injected at 210 min, and decapitation was at 240 min.

The degree of incorporation was calculated by determining for each section the ratio of valine-^{14}C incorporated into the precipitate to the total activity of valine-^{14}C found in the sample--that is,

$$\%P/P+S = \frac{\text{precipitate dpm (P)}}{\text{precipitate (P) dpm} + \text{supernatant (S) dpm}} \times 100.$$

Values obtained from two control animals injected with valine-^{14}C were averaged and represent 100% incorporation.

$$\text{"\% inhibition"} = 100 \times \left(1 - \frac{\text{experimental incorporation } \%P/P+S}{\text{ave. control incorporation } \%P/P+S}\right).$$

Results

In the first series of experiments, the effect of pactamycin, acetoxycycloheximide, and cycloheximide on protein synthesis was measured in mouse cortex. Table I shows the results.

Table I. Effects of various substances on protein synthesis in mouse cortex.

Drug[a]	Dose (mg/mouse)	Inhibition (%)
Acetoxycycloheximide	0.25	94
Cycloheximide	0.72	85
Pactamycin	0.125	63
Pactamycin	0.0625	35

[a] Total drug time is 50 min. Five μ Ci valine-^{14}C incorporation time is 40 min.

The 94% inhibition obtained by use of acetoxycycloheximide indicated that the procedures followed were satisfactory. In subsequent experiments, using pactamycin, we could not repeat inhibition levels of 63%. At best we found only 40% in the brain sections, with most values around 10%. In addition, we could not show increasing inhibition with increasing doses to a maximum of 0.375 mg/mouse. Liver sections in these same mice did show increasing inhibition with dosage up to a maximum inhibition of 70%.

Table II shows a compilation of four experiments on mice; there were variables of both time and dose/mouse. From these data it can be seen that there is a rapid loss of inhibition with time in all three tissues. The degrees of inhibition for longer times after administration of 2.5 mg/mouse are shown in Fig. 1. Increasing the dosage of cycloheximide has only a moderate effect on the duration of maximum inhibition, which lasts about 60 min with doses varying from 2.5 to 5 mg/mouse. In general, the degree of inhibition is similar for liver and brain. The inhibition through 90 min in DBA/2J mice injected with 4 mg of cyclo-

heximide is similar to that obtained with Swiss mice.

In another experiment with Swiss mice, the degree of inhibition of protein synthesis obtained by multiple injections of 1 to 2 mg/mouse, at 90-min intervals, was compared with that obtained by a single dosage. The multiple injections were found to be no more effective. For example, after 6 hr, 65% inhibition was found when four injections of 2.1 mg had been given at 90-min intervals, whereas a single injection of 8.5 mg produced 75% inhibition.

Table III is a similar compilation of our data from experiments in which Sprague-Dawley rats were used. The same loss in inhibition with time is noted in these animals, again with the same general pattern for all three tissues. One major difference between the two species is that the mouse is considerably more tolerant of cycloheximide, and a dose of 2.5 mg/mouse or 8.3 mg/100 g is required to produce maximum inhibition, whereas only 0.3mg/rat or 0.15 mg/100 g will produce greater than 90% inhibition in the rat. Other experiments[8] have shown that doses greater than 1.0 mg will kill rats of 150-200 g size within 24-48 hr.

Discussion

Barondes and Cohen,[2,6] using the same strain of mice that we use, found in cortical tissue a loss of inhibition with time similar to that which we have noted. They have used this observation to set up experiments to separate "long term" memory from "short term" memory. We found that liver sections also followed this same loss pattern. However, Traketellis et al.[7] observed a different pattern in C3H/HeJ mouse liver. The results from the three laboratories have been recalculated to the same scale, and are presented in Fig. 1. We did not observe the long-term inhibition reported by Traketellis et al.

In the initial experiments with pactamycin, the dose given was severely limited by its low solubility in H_2O at pH 7. However, pactamycin is very soluble in ethanol, and additional experiments are planned with higher dosages of pactamycin. Some preliminary data indicate that pactamycin is an effective inhibitor of liver protein synthesis in the rat and mouse, but it appears to be less effective in brain. This contrasts with the data for cycloheximide, which inhibits equally in brain and liver. The pactamycin may enter the brain less readily than cycloheximide.

Experiments are planned to test the effectiveness of cycloheximide and other inhibitors of protein synthesis in altering learning and memory in a number of behavioral tests.

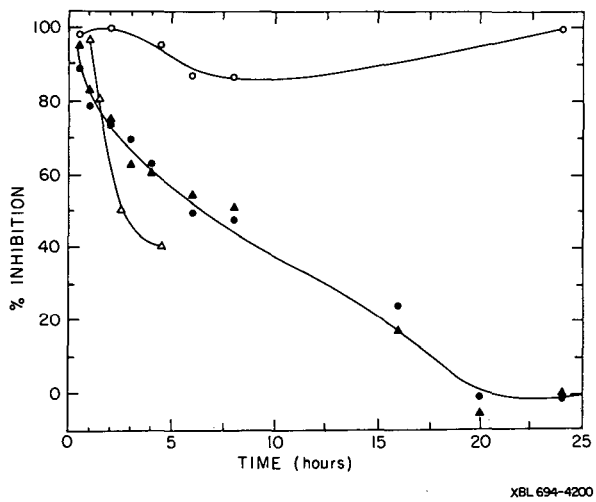

Fig. 1. Comparison of cycloheximide-initiated inhibition of protein synthesis from three laboratories. Subcutaneous injection in all cases.
O–O Recalculated data from Traketellis C3H/HeJ Mouse liver. Dose of 2.7 mg/mouse.
●–● Orme-Bennett data using Swiss albino mouse liver. Dose of 2.5 mg/mouse.
▲–▲ Orme-Bennett data using Swiss albino mouse brain. Dose of 2.5 mg/mouse.
△–△ Barondes-Cohen data from Swiss albino mouse cortex. Dose of 5.0 mg/mouse.

Table II. Effect of cycloheximide on inhibition of proten synthesis as a function of time and dose in Swiss albino mice. Heavy line denotes duration of maximum inhibition.

Total cycloheximide time (min)	Cycloheximide (mg/mouse) 0.5	1.0	2.0	2.5	4.0	5.0	6.0	8.0
% Inhibition in cortex								
30				95		93		
45	63	75	72	94	92		93	93
60				84		87		
90				91				
120				78	84	77		
150					67		74	88
240				65		80		
					58		61	64
% Inhibition in subcortex								
30				95		94		
45	61	72	70	95	70		91	93
60				84		88		
90				90				
120				76	83	68		
150					68		76	87
240				80		62		
					60		59	65
% Inhibition in liver								
30				89		80		
45	31	55			87		88	91
60				68		72		
90					79			
120					68		72	86
150				56				
240					64		53	62

Table III. Effect of cycloheximide on inhibition of protein synthesis as a function of time and dose in Sprague-Dawley rats. Heavy line denotes duration of maximum inhibition.

Total cycloheximide time (min)	Cycloheximide (mg/rat) 0.05	0.10	0.30	0.50	1.00	1.50	2.00
% Inhibition in cortex							
30					94		
45	62	71 77	91	93	95	94	92
60			89	90	93		
90			83	74	92		
120			77	87			
180			75	66			
240				45			
% Inhibition in subcortex							
30					92		
45	63	70 74	90	94 88	95	94	93
60		76	88	88	95		
90			80	84	94		
120			76	84			
180			73	45			
240				52			
% Inhibition in liver							
30					89		
45	49	72 72	91	92	94	94	94
60		74	90	84	94		
90			88	85	94		
120			80	82			
180			78	76			
240				67			

References

1. S. H. Barondes and H. D. Cohen, Proc. Natl. Acad. Sci. U.S. 58, 157 (1967).
2. H. D. Cohen and S. H. Barondes, Commun. Behav. Biol., Part A, 1, 337 (1968).
3. B. W. Agranoff, R. E. Davis, and J. J. Brink, Brain Res. 1, 303 (1966).
4. I. Shapiro and E. L. Bennett, Laboratory of Chemical Biodynamics Quarterly 19, 10 (1968).
5. S. H. Barondes and H. D. Cohen, Science 160, 556 (1968).
6. S. H. Barondes and H. D. Cohen, Proc. Natl. Acad. Sci. U.S. 61, 923 (1968).
7. A. C. Traketellis, M. Montjar, and A. E. Axelrod, Biochem. 10, 2065 (1965).
8. Ann Hughes (Lawrence Radiation Laboratory), personal communication.

ISOLEUCYL RNA SYNTHETASE FROM E. COLI

Joyce Yueh Hsu

A current, generalized picture of protein synthesis consists of the following steps:

(a) activation of amino acids and formation of amino acyl-tRNA molecules,
(b) formation of a competent complex between ribosomes and mRNA,
(c) binding of amino acyl-tRNA to this complex,
(d) formation of peptide bonds in the complex,
(e) release of completed chains from the complex.

An activating enzyme (amino acyl-RNA synthetase) is responsible for the specific activation (reaction 1) and transfer (reaction 2) of one of the 20 amino acids with the formation of the amino acyl-tRNA molecule:

$$\text{Enz} + \text{ATP} + \text{AA}_1 = \text{Enz-AA}_1\text{-AMP} + \text{PP}_i \,,$$

$$\text{Enz-AA}_1\text{-AMP} + \text{tRNA}^1 = \text{AA}_1\text{-tRNA}^1 + \text{Enz} + \text{AMP}.$$

The overall picture.

$$\text{Enz} + \text{ATP} + \text{AA}_1 + \text{tRNA}^1 = \text{AA}_1\text{-tRNA}^1 + \text{Enz} + \text{PP}_i + \text{AMP}.$$

This is a crucial step during protein synthesis, for as Chapeville et al.[1] have shown, once the appropriate amino acyl-tRNA has been formed, the only operative code is the anticodon on tRNA -- i.e., there are no additional safeguards assuring the rejection of the wrong amino acids. Therefore the consequence of any mistake made by the amino acyl-RNA synthetase would result in an amino acids being placed on an incorrect tRNA, and synthesis of a mutant protein would be inevitable.

Procedures for the purification and some of the proper ties of a number of amino acyl-RNA synthetases have appeared. In general, all these enzymes have a molecular weight of around 100 000. Aside from the reaction of L-valine with the isoleucyl-RNA synthetase, and L-threonine with the valyl-RNA synthetase, all the enzymes so far isolated either from Escherichia coli or from yeast show high specficity for a single amino acid.

Berg et al.[2] demonstrated that the isoleucyl-RNA synthetase could activate valine but did not successfully transfer it to tRNA.

Similar results were also found by Arca et al.[3] when they worked with preparations from a thermophilic organism, Bacillus stearothermophilus, at 50°. However, when they increased the temperature to 70° they found that the isoleucyl-tRNA formation underwent a rapid decline, and that there was almost no formation at 80°. On the other hand, while there was little or no formation of valyl-tRNA at from 50° to 60°, its formation increased sharply between 65° and 80° (Fig. 1). They suggested that above 70° some conformational change takes place in the tRNA or in the enzyme, resulting in loss of ability to to transfer isoleucine and gain of ability to transfer valine.

On the basis of this previous knowledge, it would seem interesting to investigate the question whether isoleucyl-RNA synthetase from E. coli could undergo a directional change in specificity under various environmental conditions -- e.g., temperature, pH, and concentration of potassium ion, sodium ion, magnesium ion, calcium ion, etc.

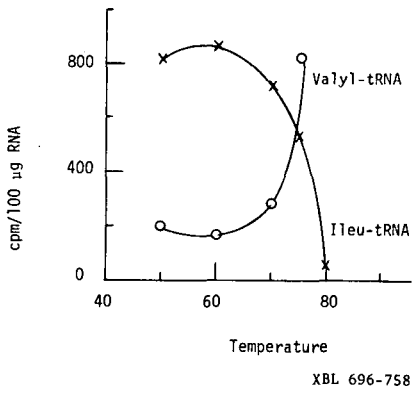

Fig. 1. Effect of temperature on the formation of ^{14}C-valyl-tRNA (o - o) and ^{14}C-isoleucyl-tRNA (× - ×) by purified isoleucyl-tRNA synthetase from B. stearothermophilus (Ref. 3).

Assay Methods

Two assay methods were used:

(a) based on the activation of the amino acid, an amino-acid-dependent ATP-$P^{32}P_i$ exchange reaction,

$$Enz + ATP + AA_1 = Enz\text{-}AA_1\text{-}AMP + PP_i;$$

one unit of activity is defined as the incorporation of 1 µmole of $P^{32}P_i$ into ATP in 15 min at 37°.

(b) Based on the rate of formation of aminoacyl-C^{14} tRNA,

$$Enz + ATP + AA_1 + tRNA^1 = AA_1\text{-}tRNA^1 + Enz + PP_i + AMP;$$

one unit of enzyme is equivalent to the formation of 1 mµmole of aminoacyl-tRNA in 10 min at 37°.

Isolation Procedure

The purification procedure included six major steps:

Crude extract. E. coli B late log cells were softened in phosphate buffer and homogenized by blending in a Waring Blendor with glass beads (200 µ diameter).

Autolysis. The crude extract was incubated at 37°C for 6–8 hr in order to promote the autodigestion of the bulk of the nucleic acid in the extract.

Ammonium sulfate fractionation. 27% w/v of enzyme grade ammonium sulfate was added to the autolysate. After the mixture was centrifuged for 20 min at 12 000 × g the precipitate was discarded, and 15% w/v of ammonium sulfate was added to the supernatant. After the second mixture was centrifuged, the supernatant was discarded and the precipitate was immediately dissolved in 0.02 M sodium succinate buffer, pH 6.0, and dialyzed against the same buffer.

Adsorption and elution from alumina Cγ gel. A suspension of alumina Cγ gel (15–20 mg dry weight per ml) was added to the protein solution to give a gel/protein ratio of 0.75. The adsorbed protein in the gel was then released by washing the gel successively with phospate buffers of increasing basicity and molarity, (a) 0.05 M, pH 6.5; (b) 0.05 M, pH 7.0; (c) 0.05 M, pH 7.5; (d) 0.1 M, pH 7.5, (e) 0.2 M, pH 7.5; (f) 0.5 M, pH 7.5 Fractions (a)—(f) were assayed for enzyme activity and protein content (by Lowry) and those that showed high specific activity were pooled and dialyzed.

DEAE-Cellulose chromatography. Around 1 g of protein was adsorbed onto a DEAE column packed to a volume of 375 ml. The protein was then eluted with a linear gradient of phosphate buffer. The mixing chamber contains 2 liters of 0.02 M potassium phosphate, pH 7.5, and the reservoir contains 2 liters of 0.1 M potassium phosphate, pH 7.5. The column was run at a flow rate of 120 ml/hr. Fractions containing enzyme activity were pooled and dialyzed.

Hydroxylapatite chromatography. A hydroxylapatite column was packed (100 ml in a column 2.4 cm × 20 cm for 250 mg protein), and protein sample was applied to the column. A linear gradient produced with 400 ml of 0.05 M

potassium phosphate, pH 7.5, to 400 ml of 0.3 M potassium phosphate, pH 7.5, was employed. The flow rate was maintained at 10–20 ml/hr. The isoleucyl-RNA synthetase was eluted between 0.20 M and 0.25 M phosphate and was the last protein peak to be eluted. The pooled enzyme fractions were concentrated by vacuum dialysis.

Characteristics of the Isolated Enzyme

The purification procedure, starting with 250 g of E. coli B cells, is summarized in Table I. The overall yield of enzyme is about 10% and the purification achieved is approximately 260-fold.

By the criteria of acrylamide gel electrophoresis, the enzyme appeared to be homogeneous. The electrophoresis patterns of various fractions across the enzyme peak are shown below the hydroxylapatite chromatography elution pattern (Fig. 2).

The enzyme shows a single symmetric boundary by velocity sedimentation, with a sedimentation coefficient of 5.6 S. This value is very close to the 5.8 S that Holde & Baldwin[4] have found.

By using assay method (a), the ratio of isoleucyl-dependent activity vs. valyl-dependent activity is found to be 1:0.5, which agrees with what Berg et al.[2] have found. In the presence of the other 15 naturally occurring amino acids, the enzyme shows almost no activity.

By using assay method (b), a more stringent assay, the enzyme forms the acid-insoluble AA-tRNA only with isoleucine, and not with valine.

Temperature Effect on the Enzyme

A temperature test was carried out for the E. coli enzyme, using the assay method (b). The result is shown in Fig. 3. The enzyme activity curve in transferring isoleucine appeared to be a normal bell shape with its maximum at 37°. Valine did not get transferred through the temperature range from 25° to 70°.

Table I. Purification of isoleucyl-RNA synthetase from E. coli.

Fraction	Total Protein (mg)	Total Units	Yield (%)	Specific Activity (units/mg of protein)
Crude extract	18 000	36 000		2
Autolysate	13 500	30 000	84	2.2
Ammonium sulfate	6 300	23 000	64	3.6
Alumina C_γ gel	1 700	12 320	34	7.2
DEAE	170	11 000	30	65
Hydroxylapatite	7.5	4 000	10	535

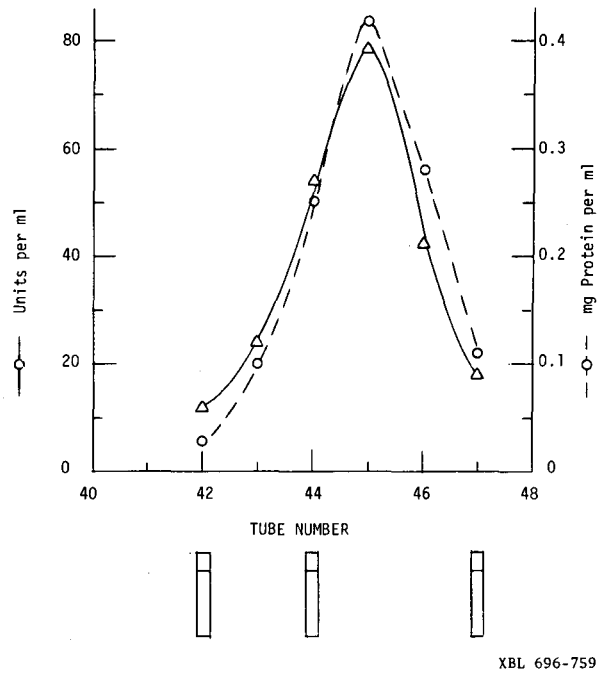

Fig. 2. Chromatography of purified isoleucyl-RNA synthetase on hydroxylapatite (10 ml/tube). Acrylamide gel electrophoresis patterns are shown below the corresponding fractions from the column.

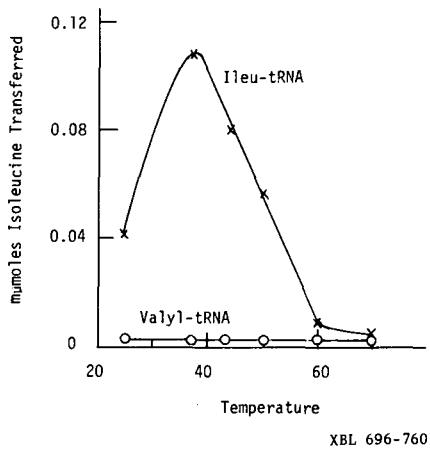

Fig. 3. Effect of temperature on the formation of ^{14}C-valyl-tRNA (o - o) and ^{14}C-isoleucyl-tRNA (× - ×) by purified isoleucyl-tRNA synthetase from E. coli B.

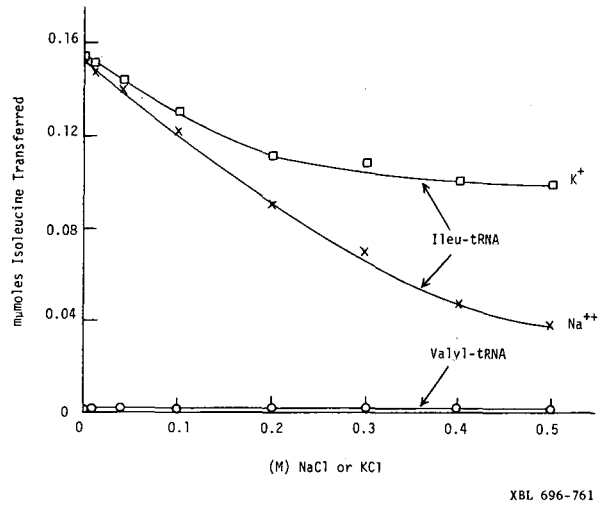

Fig. 4. Effect of K^+ and Na^+ on the formation of ^{14}C-valyl-tRNA (o - o). Effect of K^+ (□ - □) and Na^+ (× - ×) on the formation of ^{14}C-isoleucyl-tRNA.

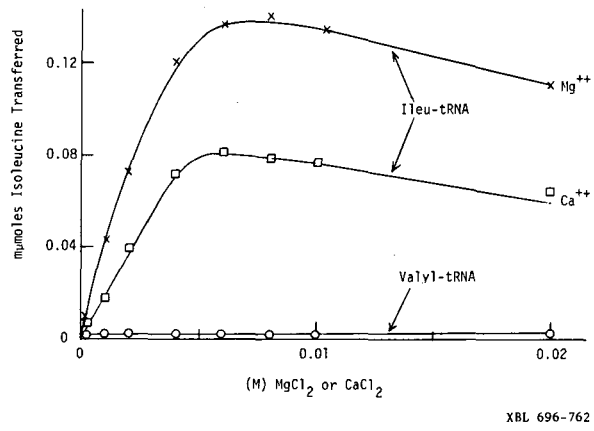

Fig. 5. Effect of Mg^{++} and Ca^{++} on the formation of ^{14}C-valyl-tRNA (o - o). Effect of Mg^{++} (× - ×) and Ca^{++} (□ - □) on the formation of ^{14}C-isoleucyl-tRNA.

Ion Effect on the Enzyme

K^+ and Na^+ effect. The formation of isoleucyl-tRNA declined gradually with the increase of either K^+ ion concentration or Na^+ ion concentration in the assay mixture. Valyl-tRNA was not formed through the ion concentration from 10^{-5} M to 1 M. Results are shown in Fig. 4.

Mg^{++} and Ca^{++} effect. Both Mg^{++} and Ca^{++} served as activators to the enzyme, Mg^{++} being the more effective one (Fig. 5). Again, no valyl-tRNA was formed while the ion concentration changed.

References

1. F. Chapeville, F. Lipmann, G. Von Ehrensteen, B. Weisblum, W. J. Ray, and S. Benzer, Proc. Natl. Acad. Sci. U. S. 48, 1086 (1952).
2. F. H. Bergman, P. Berg, and M. Dieckmann, J. Biol. Chem. 236, 1735 (1961).
3. M. Arca, L. Frontali, and G. Tecce, Biochim. Biophys. Acta 108, 326 (1965).
4. K. Van Holde and R. L. Baldwin, J. Phys. Chem. 62, 734 (1958).

DEVELOPMENT OF SPECIFIC CHROMATOGRAPHIC MATERIALS FOR AMINOACYL-tRNA SYNTHETASE PURIFICATION

Brian C. Myhr

The class of enzymes known as the aminoacyl-tRNA synthetases have the crucially important function of attaching an amino acid to the particular tRNA molecules containing an anticodon specific for that amino acid.[1] This translation of amino acid identities into specific trinucleotide sequences must operate flawlessly to produce functional proteins. Once an amino acid has been attached to a tRNA molecule, it is placed into protein according to the base-pairing recognition between the tRNA and mRNA on the ribosomal complex. Clearly, there must exist at least one specific synthetase and cognate tRNA chain for each of the 20 amino acids, and the aminoacylation process must operate with high fidelity.

Within the cell the synthetases are probably saturated at all times with their respective tRNAs, but in vitro experiments have established that aminoacylation can occur in two distinct steps.[1] The first step (reaction 1) is the activation of a specific amino acid with ATP to form the aminoacyl adenylate, which remains bound to the enzyme. In the absence of tRNA, the Enz^1-AA_1-AMP complex can be isolated by removing the pyrophosphate formed, thereby preventing the reversal of reaction 1.[2] But in the presence of tRNA species recognized by the enzyme, transaminoacylation occurs (reaction 2), producing a charged tRNA molecule, free enzyme, and AMP. This two-step mechanism seems well suited to the elimination of errors. For example, valine can be activated by the isoleucine-specific enzyme of E. coli, but the conformation of the resulting complex is apparently altered to such an extent that the complex breaks down when reacted with tRNA containing isoleucyl-specific chains,[3,4]

$$Enz^1 + ATP + AA_1 \overset{Mg^{++}}{\rightleftharpoons} Enz^1\text{-}AA_1\text{-}AMP + PP_i, \qquad (1)$$

$$Enz^1\text{-}AA_1\text{-}AMP + tRNA^1 \rightleftharpoons AA_1\text{-}tRNA^1 + Enz^1 + AMP. \quad (2)$$

At present virtually nothing is known about how the structures of the synthetases are related to their functions. The chemical groups important for the activation and binding of amino acid are unknown, and no information exists on how the enzyme selectively interacts with only one rRNA (or several iso-accepting species) from among the many other similar nucleic acids. A major reason for this lack of knowledge on the structure-function relationship is the lack of sufficient quantities of highly purified enzyme. Optical techniques of studying conformational changes, for example, often require milligram quantities. To obtain such large quantities of enzyme by the conventional biochemical procedures is a difficult task. The various steps involved are time-consuming and subject to frequent failure, and usually give very poor overall yields. Furthermore, different procedures must be devised for each synthetase and for each source, such as E. coli, yeast, or mammalian tissues, of a given enzyme. Accordingly, we have been led to investigate the possibility of preparing a chromatographic material that would exhibit a high specificity for the enzyme of interest. With such a material the above-mentioned difficulties may be largely circumvented.

Recognition Chromatography

The impetus for this attempt came from a report by Calendar and Berg[5] that certain tyrosine analogs are good competitive inhibitors of tyrosine activation, as measured by the $PP_i \rightleftharpoons ATP$ exchange in reaction 1. If the tyrosine carboxyl group is amidated, esterified (methyl or ethyl esters), reduced to the alcohol, or absent (tyramine), the resulting compounds still strongly bind to the enzyme, in spite of the fact that they cannot react with ATP to form the adenylate. On the other hand, the N-acetyl and N-glycl derivatives of L-tyrosine did not function as inhibitors (or activators). Apparently, the amino group is involved in the binding of the amino acid to the enzyme, whereas the carboxyl group is of little importance in this respect. This suggested to us that the amino acid might be attached to an insoluble support through its carboxyl group without entirely destroying its capacity to function as substrate for the enzyme. Such a chromato graphic support would exhibit a selectivity toward the enzyme of interest.

The theory of operation of such a column was envisioned as follows: The crude enzyme solution is placed on top of a column containing, for example, isoleucyl side chains. If the cross-linking of the gel is sufficiently high, undesired protein and other synthetases will quickly pass through in the void volume. But because the isoleucine-activating enzyme would recognize and bind to the isoleucyl side chains, its travel would be sufficiently retarded to effect its separation from the other macromolecular components. In the event that the enzyme became tightly bound to the column, it was expected to be eluted with free isoleucine, ATP, and Mg^{++}. Excess free isoleucine should effectively compete with the column-bound isoleucine to form the $Enz^1\text{-}AA_1\text{-}AMP$ complex (reaction 1), which would then be immediately eluted.

Before a column material specific for the isoleucyl-tRNA synthetase could be prepared it was necessary to determine if a derivative of the carboxyl group would still bind to the enzyme. With the help of H. Ottenheym, the ethyl ester was prepared from absolute ethanol by the thionyl chloride method and then recrystallized from ether-ethanol. Its ability to inhibit the enzyme was tested qualitatively by placing in the reaction mixture used to assay the enzyme

($P^{32}P \rightleftharpoons AT^{32}P$ exchange) a 50-fold excess of the ester over the isoleucine present. Since enough isoleucine is present for zero-order kinetics, this is not a very sensitive test for inhibition. Nevertheless, the apparent number of units in an enzyme sample was reduced by more than one-half in the presence of the ester, showing that the ester does interact strongly with the enzyme. A Lineweaver-Burk plot and determination of K_I remain to be done.

Recently, Cuatrecasas et al.[6] described a chromatographic method for the purification of staphylococcal nuclease, α-chymotrypsin, and carboxypeptidase A that is based upon the same principle envisioned for the purification of the synthetases. In each case a competitive inhibitor was attached covalently to Sepharose 4B, a highly porous, cross-linked dextran. When the inhibitor groups were located at a sufficient distance from the solid matrix to minimize steric interference, the crude enzyme solutions could be purified rapidly and completely in a single step. The enzymes were selectively adsorbed on the inhibitor-gel and could be eluted by the addition of competitive inhibitors in solution or by changing the salt concentration or pH.

Our efforts to prepare an inhibitor-gel for the purification of isoleucyl-tRNA synthetase from E. coli are described below. The first attempt was to prepare a Sephadex gel to which L-isoleucine would be attached through an amide linkage between its carboxyl group and an aminoethyl ether side chain (Ile-E-Seph). After the appearance of the paper by Cuatrecasas et al.,[6] the cyanogen bromide activation method was employed to prepare a gel with the L-isoleucine attached by an ester bond to a n-hexyl side chain (Ile-H-Seph).

Isoleucyl Ethyl-Sephadex

Preparation

Sephadex G-50 was chosen for the chromatographic support because of its immediate availability and the presence of many secondary hydroxyl groups to which aminoethyl side chains may be attached. The reaction sequence followed is given below.

$$\text{Seph-OH} + HO_3SOCH_2CH_2NH_2 \xrightarrow[110\,^\circ C]{NaOH}$$

$$\text{Seph-O-}CH_2CH_2NH_2 \quad \text{(AE-Seph)}, \qquad (3)$$

$$\text{Seph-O-}CH_2CH_2NH_2 + \text{tBOC-Ile} \xrightarrow[\text{dioxane}]{DCC}$$

$$\text{Seph-O}CH_2CH_2NHC(=O)CH(R)NH\text{-tBOC}$$

$$\xrightarrow[1.5\text{ hrs}]{1\text{ N HCl}} \text{Seph-O}CH_2CH_2NHC(=O)CH(R)NH_2$$

$$\text{(Ile-E-Seph)}. \qquad (4)$$

Abbreviations used:

Seph	=	glucosidic backbone of Sephadex
DCC	=	dicyclohexylcarbodiimide
tBOC	=	tertiary butyloxycarbonyl (protective group for the isoleucine amino group)
Ile	=	L-isoleucine
AE-Seph	=	aminoethyl Sephadex

The actual synthetic procedure used to obtain the Ile-Seph gel used in the enzyme experiments is described here. Variations leading to difficulties are described in the section on synthesis problems.

Aminoethyl sulfate was not available at the beginning of this work, and was prepared by the reaction

$$BrCH_2CH_2NH_2HBr + Ag_2SO_4 \xrightarrow{\Delta}$$

$$NH_2CH_2CH_2OSO_3H + 2\,AgBr\downarrow \; . \qquad (5)$$

A small excess of Ag_2SO_4 was used, which

was removed by the addition of HCl and filtration of the resultant AgCl. After the final evaporation to a crystal mass, the aminoethyl sulfate was recrystallized from water. The yield was 3.9 g (83% of theoretical).

The preparation of AE-Seph (reaction 3) was performed according to Eldjarn and Jellum.[7] Five g of G-50 Sephadex (fine) was stirred rapidly into 12 ml of water containing 4.6 g NaOH and 1.5 g of aminoethyl sulfate. The gel immediately absorbed the solution and swelled remarkably. After stirring for 5 min, the gel was spread out on a large watch glass and dried at 110°C for 4 hr. This treatment yielded a yellow, crusted material, which was rehydrated and washed by repeated filtration until the filtrate was colorless and at pH 7. Virtually all the color seems to wash out of the gel.

A nitrogen analysis by the method of Lang[8] (essentially a Kjeldahl followed by Nesslerization and absorption readings at 420 nm) revealed 0.6% N content by weight. This corresponds to 0.45 mmole of AE-groups per gram of dry gel. Approximately 2.4% of the available hydroxyl groups were substituted. Eldjarn and Jellum also obtained 0.3-0.5% N yields.

The gel was qualitatively titrated with 0.1 N HCl and shown to contain titratable groups with a pK near 8. For comparison, $NH_2CH_2CH_2COOCH_2CH_3$ has a pK near 7.5.

Attempts to carry out reaction 4 in aqueous solution with a water-soluble carbodiimide resulted in a gel with about three times the N content of the AE-Seph and essentially no titratable groups. Therefore, the AE-Seph was dried with 95% ethanol, followed by absolute ethanol, then 12 hr at 70°C. Then 0.53 g of dry AE-Seph was stirred into a solution of 0.29 g tBOC-Ile in a small volume of dioxane. No swelling was obvious. This mixture was cooled with ice to just above the slush temperature and 1 g of DCC, dissolved in a small volume of dioxane, was added slowly and with stirring. After 1.5 hr with intermittent stirring at this temperature, the mixture was suction filtered and washed with dioxane. Then 1 N HCl was added to the gel. After 1.5 hr at room temperature with frequent stirring, the acid suspension was filtered and washed well with water.

A single N analysis of the Ile-E-Seph yielded 1.3% N by weight, which represents a doubling within experimental error over the AE-Seph N content. Thus, the Ile-E-Seph contains about 9.8 mmole of isoleucyl chains per g of dry gel. A quantitative titration with 0.1 N HCl revealed the presence of titratable groups with a pK near 9; an estimated 0.24 meq was used in the titration and 0.21 meq was found.

Enzyme Experiments

Several initial batchwise experiments showed that the enzyme was either bound or denatured by the Ile-E-Seph. In 0.02 M potassium phosphate buffer, pH 7.5, containing 0.01 M β-mercaptoethanol, considerable protein was also bound, but this could be eluted by using 0.3 M buffer. In contrast, the bound enzyme was not eluted, nor could it be eluted with 0.1 M isoleucine. Always included in the buffers and washes "for good measure" were 2.5×10^{-3} M $MgCl_2$ and 2.5×10^{-4} M ATP. It was later shown in the column experiments that one or both of these compounds are required for enzyme binding or denaturation by the gel. Sephadex G-50 itself was run as a control and never exhibited any binding of enzyme or protein.

The remainder of the Ile-E-Seph preparation was used to prepare a column (0.9×13.5 cm) containing 8.6 ml of gel and enough capacity to bind 14×10^6 units, if each isoleucyl sidechain was available to interact with the enzyme. The column was

equilibrated in 0.3 M potassium phosphate buffer, pH 7.5, 0.01 M β-mercaptoethanol, 2×10^{-3} M ATP, and 5×10^{-3} M $MgCl_2$. Then 1.0 ml of a crude enzyme solution, obtained after the alumina gel step in the purification procedure, was placed on the column and eluted with the above buffer system. The recovery of enzyme and protein are shown in Table I, along with the results of a second trial performed in exactly the same manner but at a later date. The enzyme was assayed by the $P^{32}P \rightleftharpoons AT^{32}P$ exchange, and protein was determined by the Lowry method.

Table I. Enzyme and protein recovery from an Ile-E-Seph column in the presence of ATP and Mg^{++}.

	Trial 1*	Recovery (%)	Trial 2	Recovery (%)
Enzyme placed in the column	44 μ		45.6 μ	
Protein placed on the column	8.14 mg		14.1 mg	
Enzyme collected	7.3 μ	17*	31.8 μ	70
Protein collected	7.62 mg	93*	14.4 mg	100

*A portion of the peak was not collected in Trial 1. Probably 100% of the protein was eluted, making the estimated enzyme recovery about 24%.

Both enzyme and protein peaks emerged in the same volume, suggesting that the enzyme losses were due to tight binding to the gel or a denaturing process. In view of the great excess of isoleucyl side chain present over the small number of units used, neither alternative is very understandable. The flow rates were small, always being less than 2 ml per hour, so that nearly complete binding or denaturation might have been expected. The much larger recovery of enzyme in the second run strongly indicates that sites were occupied or expended in the first trial. Perhaps, as suggested later, these sites are not the isoleucyl side chains, but a very small number of uncharacterized groups introduced during the gel synthesis.

After the first trial, two attempts were made to elute any bound enzyme. In the first case, 0.2 M isoleucine was added to the buffer system given above. Secondly, the pH was increased by using 0.3 M tris-HCl, pH 9, containing 0.1 M isoleucine and the ATP, Mg^{++}, and β-mercaptoethanol concentrations given above. Neither attempt resulted in the collection of any active enzyme. A third elution attempt was made after the second column run by using 0.1 M pyrophosphate in 0.3 M potassium phosphate, pH 7.5, and 0.01 M β-mercaptoethanol. Because pyrophospate causes the breakdown of the enz-AA-AMP complex by reversal of reaction 1, it was thought an analogous breakdown of the enz-column complex might occur in the presence of pyrophosphate. However, again no active enzyme was eluted.

Two enzyme samples were also applied to the column in the absence of ATP and Mg^{++} between the two runs given in Table I. In both cases, all the applied enzyme was recovered in the eluant at the same position where all the protein was eluted; 94 units were placed on the column and 107 units and 99 units were recovered in the two trials.

Finally, after all the above experiments, the Ile-E-Seph was removed from the column and incubated in 20 ml of the reaction mixture used to assay for the enzyme. The lack of formation of any $AT^{32}P$ showed that if any enzyme was bound to the gel, it was bound in an inactive state. Possibly, the enzyme is bound at the amino acid activation site.

To summarize, it seems that a very small percentage of the isoleucyl side chains or a few unknown groups produced in the synthesis of Ile-E-Seph are capable of interaction with isoleucyl-tRNA synthetase, but

only in the presence of ATP and Mg^{++}. It is not known whether the enzyme becomes tightly bound to the gel or whether it is inactivated and passes through. In either case the gel sites are expended. If the enzyme is indeed bound, the ATP requirement suggests the possibility of a covalent bond formation, which would be consistent with the failure of attempts to elute the enzyme with isoleucine or pyrophosphate. Furthermore, any bound enzyme is incapable of activating isoleucine.

Synthesis Problems

For the synthesis of additional batches of AE-Seph, commercial aminoethyl sulfate (Eastman, practical grade) was used after three recrystallizations from water. The crystals were white and the final mother liquor colorless.

The second batch of AE-Seph was prepared as already described, except the reaction at 110°C was carried out under moist conditions for 4 hours and then allowed to dry out. This produced a very crusted and brownish-yellow material. After washing and subsequent drying with ethanol and heat, the gel was nearly colorless, but only 34% of the starting gel weight was recovered. Obviously, much of the gel had been decomposed and solubilized. The N content of the remaining gel was 0.22% by weight. This gel did not, however, condense with tBOC-Ile under exactly the same reaction conditions described earlier, since the N content did not change. No further chemical characterization was carried out.

A column (0.9 cm×15 cm) of this AE-Seph was prepared to test its interaction with the enzyme in the absence of ATP and Mg^{++}. Only 0.3 M potassium phosphate, pH 7.5, plus 0.01 M β-mercaptoethanol was used to equilibrate the column and elute the same enzyme solution used in the previous experiments. Because some of the eluant was lost in the peak region, only 91% of the applied protein was recovered. The enzyme eluted in the same position, and if 10% is added to the amount recovered, the yield would be 73% of the applied sample of 43 units. This result contrasts with the Ile-E-Seph behavior (no loss of enzyme). It also underscores the possibility that gel decomposition in the AE-Seph synthesis may usually lead to the production of other reactive groups, such as aldehydes, that may denature the enzyme.

A third batch of AE-Seph (25 g) was prepared from G-25 Sephadex (coarse, bead form) instead of G-50. The reaction conditions were exactly as in the first case, producing light yellow beads. The color was removed by washing and 100% of the gel was recovered. Its N content is 0.53%. A qualitative nitrous acid test was definitely positive for primary amino groups. However, after an attempt was made to form the peptide bond in reaction 4 under the conditions already described, the N content did not change (0.55%). An IR spectrum of the DCC showed that it had not decomposed significantly. Perhaps the higher degree of cross-linking of the G-25 Sephadex is not amenable to amide formation via reaction 4. This AE-Seph preparation has not yet been tested with the enzyme.

It was learned recently that Bio-Rad markets an aminoethyl-cellulose powder, and a quantity of this material was obtained. If the enzyme is not denatured by this preparation, it should be possible to prepare an Ile-E-cellulose (according to reaction 4) that may exhibit a selective affinity for the enzyme.

Isoleucyl Hexyl-Sephadex

A much milder way of attaching side chains to Sephadex was described by Axén, Porath, and Ernback[9,10] and used by Cuatrecasas et al.[6] to prepare their successful chromatographic materials. This procedure involves a gel activation step by

treatment with aqueous cyanogen bromide for a short time period, followed by a coupling reaction with an added primary amine in a slightly alkaline aqueous suspension. The reaction is a complex one that has not been well characterized yet, but available evidence suggests that the chief active intermediate and the final coupled product are both imino carbonic acid esters. The primary reaction sequence, then, can probably be written as follows:

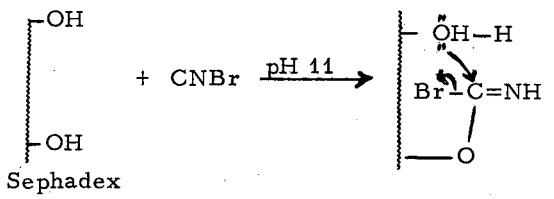

Sephadex

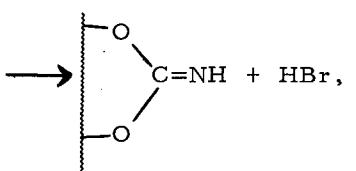

(6)

"Activated" Sephadex

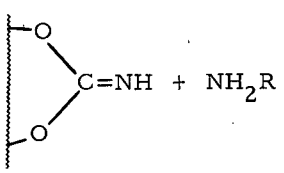

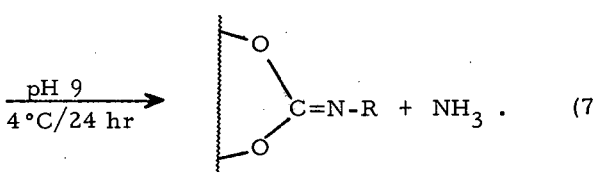

(7)

The activated Sephadex contains no bromine and the coupling reaction produces no change in the nitrogen content; ammonia is released. Activation also appears to cause an increase in the cross-linking (swelling capacity reduced), which is consistent with the formation of imino carbonic acid esters. An infrared absorption band at 5.8 μ, corresponding to the -C=N- system, was found for the activated product, as well as another band at 5.6 μ, attributed to the C=0 stretching frequency of a carbonic acid ester. Upon acid hydrolysis the 5.8-μ band decreases while the 5.6-μ band increases. On the other hand, the coupled product appears to be quite stable over a wide pH range. Glycylleucine-Sephadex was stable in acid down to the limit of stability of Sephadex; exposure for 24 hours to 0.1 M NaOH caused release of 25% of the chains. There was no detectable loss with 10^{-3} M NaOH.

Experimental Procedure

Attempts were made to adapt the above procedure to produce a gel with L-isoleucine attached through a hexyl chain to the matrix. 6-Amino-1-hexanol was used as the amine in reaction 7. Then, with the use of dicyclohexyl carbodiimide, the N-blocked isoleucine was to be attached to the alcohol side chain by esterification, assuming that this reaction would be much faster than esterification with the gel secondary hydroxyl groups. In fact, an earlier effort to attach carbobenzoxy-^{14}C-phenylalanine directly to G-50 Sephadex by the DCC method failed within the limits of detection of the radioactive label. The proposed reaction sequence for preparing Ile-H-Seph is:

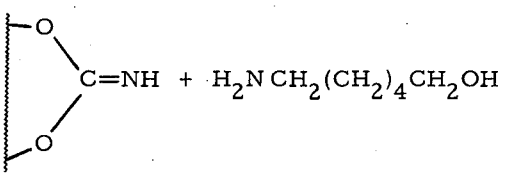

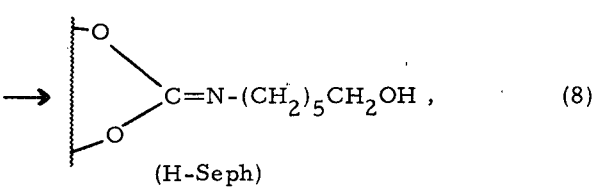

(8)

(H-Seph)

H-Seph + tBOC-Ile

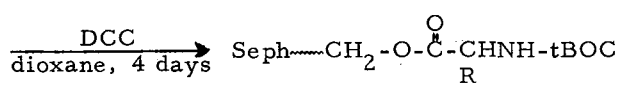

(9)

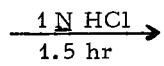

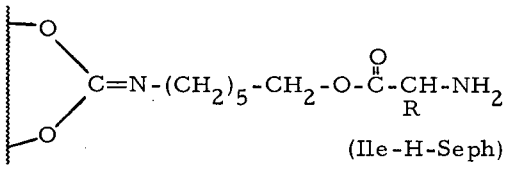

(Ile-H-Seph). (10)

A successful synthesis of Ile-H-Seph has not yet been accomplished because the esterification of reaction 9 has not proceeded to any significant extent. This may be due, in part, to steric hindrance problems with DCC, but more likely is the result of attempting this reaction at low concentrations of the reactants (less than 10^{-2} molar). Coupling reactions described in the literature with DCC or carbonyldiimidazole[11] are typically run at concentrations above 0.2 M. The dioxane solvent was not purified before use, so it is conceivable that many competing side reactions are consuming much of the reactants. Therefore, attention is now being directed toward preparing the complete side chain before carrying out the coupling to G-50 Sephadex (reaction 8). Any unreacted ester could be recovered from the gel wash. Furthermore, with the planned uses of ^{14}C-tBOC-Ile and tBOC-C^{14}-Ile, analysis of the reactions and modified gels will be considerably simplified.

References

1. G. D. Novelli, Ann. Rev. Biochem. 36, 449 (1967).
2. A. T. Norris and P. Berg, Proc. Natl. Acad. Sci. U. S. 52, 330 (1964).
3. A. N. Baldwin and P. Berg, J. Biol. Chem. 241, 839 (1966).
4. M. Yarus and P. Berg, J. Mol. Biol. 28, 479 (1967).
5. R. Calendar and P. Berg, Biochem. 5, 1690 (1966).
6. P. Cuatrecasas, M. Wilchek, and C. B. Anfinsen, Proc. Natl. Acad. Sci. U. S. 61, 636 (1968).
7. L. Eldjarn and E. Jellum, Acta Chem. Scand. 17, 2610 (1963).
8. C. A. Lang, Anal. Chem. 30, 1692 (1959).
9. R. Axén, J. Porath, and S. Ernback, Nature 214, 1302 (1967).
10. J. Porath, R. Axén, and S. Ernback, Nature 215, 1491 (1967).
11. H. A. Staab, Angew. Chem., intern. Edit. 1, 351 (1962).

BRAIN CHEMISTRY AND ANATOMY: IMPLICATIONS FOR THEORIES OF LEARNING AND MEMORY*

Edward L. Bennett and Mark R. Rosenzweig

A combined approach to learning and memory involving both neurochemistry and neuroanatomy is essential to relate brain to behavior (or mind). Our research, which began chiefly as a neurochemical study, has become progressively more neuroanatomical.

We have found that rats raised in an enriched environment develop brains that differ both chemically and anatomically from those of isolated littermates. The enriched-experience animals show greater total activity of AChE and especially of ChE. Anatomically, the enriched-experience animals show heavier and thicker cortices, more glial cells, and perhaps greater branching of dendrites. This additional growth of cortex must have its counterpart in terms of increased ribonucleic acid, protein, and lipid synthesis and of altered levels of activity of synthetic enzymes. One month of differential experience is sufficient to bring about reliable changes in the brain, indicating a high degree of plasticity.

We have obtained evidence in 10 strains of rats that problem-solving ability is related to the "corticalization" (the cortical/subcortical ratio of brain weight). This correlation has been obtained within as well as between strains of rats. Attempts to obtain within-strain correlation of problem-solving efficiency with the activity of two important enzymes in brain—AChE and ChE—gave less consistent results than correlations between problem-solving and weights. These correlation studies are being continued in the hope of finding chemical correlates of problem-solving ability in addition to the anatomical correlates that we have obtained.

*Abstract from Mind as a Tissue, Charles Rupp, ed. (Hoeber Medical Division, Harper and Row, New York, 1968), p. 63.

DEUTERIUM OXIDE EFFECT ON SPERMATOGENESIS IN THE MOUSE*

E. F. Oakberg and Ann M. Hughes

Drinking water containing 30% D_2O by volume was given to young adult S and C57 black mice. Quantitative histological study of the testes at weekly intervals indicated a progressive decline in number of spermatogonia to about 60% of control by the end of the 7-week experimental period. Number of degenerating mononuclear giant cells, abnormal clumps of spermatids, and frequency of tubules with missing cell layers were more frequent in D_2O-treated mice. The normality of spermatogenesis was surprising in view of the known effect of D_2O on fertility of C57 male mice, and investigations on both number and functional capacity of spermatozoa of these males are indicated.

*Abstract from Exptl. Cell Res. 50, 306 (1968).

EFFECTS OF A FEW HOURS A DAY OF ENRICHED EXPERIENCE ON BRAIN CHEMISTRY AND BRAIN WEIGHTS*

Mark R. Rosenzweig, William Love, and Edward L. Bennett

Instead of exposing rats to environmental complexity (EC) for 24 hr a day as in previous experiments, we exposed some groups to EC for either 2, 2.5, or 4.5 hr a day. In five experiments, brain values of the various EC groups were compared with those of littermates kept continuously in the isolated condition (IC) for the duration of the experiment. A few hours a day of EC were found to produce significant changes in activities of acetylcholinesterase and cholinesterase and in weights of brain samples; these changes were quite similar to those produced by 24 hr a day. In Experiments I and II, 2.5-hr and 4.5-hr groups were in standard colony (SC) conditions when they were not in EC. Each of these experiments also included a 24-hr EC group, and the experiments lasted for 8 weeks. Experiment III included a 2-hr EC group and an SC group; the main differences from IC were found to be due to EC and not to SC. In Experiments IV and V, the enriched-experience groups spent 2 hr a day in EC and 22 hr in IC, and the experiments lasted only 1 month. Two hr a day removal from IC to EC over a 30-day period produced significant cerebral effects.

*Abstract from Physiol. Behav. 3, 819 (1968).

EVIDENCE FOR THE NONSPECIFICITY OF THE INTERACTION BETWEEN 5-HYDROXYTRYPTAMINE AND BOTULINUM TOXIN*

Lance L. Simpson

A comparison of the effects of the drugs 5-hydroxytryptamine and pargyline on intoxication by botulinum toxin and nereistoxin has been made. Results indicate that the former can be a non-specific antagonizer of poisoning; the latter, a non-specific augmenter of poisoning. Histamine is shown to be without effect on intoxication by either poison. The effect of 5-hydroxytryptamine appears to be a function of the interval between its injection and injection of a toxin. If given before a toxin, 5-hydroxytryptamine will antagonize it; if given at the same time as a toxin, 5-HT will augment it. 5-HT is impotent when administered after a toxin. The actions of both 5-HT and pargyline are suggested as being mediated through their effects on the circulatory system.

*Abstract from Toxicon 5, 239 (1968).

EXAMINATION OF THE POSSIBLE PATHOPHYSIOLOGY OF THE CENTRAL NERVOUS SYSTEM DURING BOTULINAL POISONING*

Lance L. Simpson, Daniel A. Boroff, and Ursula Fleck

The effects of α and β components of type A botulinum toxin were tested for their ability to affect the central nervous system of cats, rabbits, and guinea pigs. Components α and β, when administered in lethal doses into the circulatory system of cats and rabbits, do not alter the ongoing electroencephalographic activity. Furthermore, α intoxication of guinea pigs does not result in changes in the brain concentration of acetylcholine or norepinephrine. Ingestion by mice of organs from intoxicated rats causes death only in those instances of organs that are well perfused with blood. The diaphragm and brain, both cholinergic sites, proved not to be toxic.

*Abstract from Exptl. Neurol. 22, 85 (1968).

THE INTERACTION BETWEEN 5-HYDROXYTRYPTAMINE AND BOTULINUM TOXIN TYPE A*

Lance L. Simpson

5-Hydroxytryptamine (5-HT) is shown to be active in antagonizing botulinal poisoning. L-5-Hydroxytryptophan is also active, the effect apparently being mediated through the synthesis of 5-HT. Neither 5-hydroxyindoleacetic acid (5-HIAA) nor D-5-hydroxytryptophan is capable of offsetting intoxication. Pargyline, a monoamine oxidase inhibitor, is shown to augment the onset of toxin-induced death. 5-HT, but not 5-HIAA, counters the pargyline effect. p-Chlorophenylalanine, an inhibitor of 5-HT synthesis, does not facilitate intoxication. Both time-course and dose-response studies with 5-HT suggest that it is not engaged in a competitive antagonism with botulinum toxin. Work with isolated nerve-muscle preparations showed the synaptic junction not to be the site of the 5-HT-toxin interaction. Data permit the assumption that the hydroxyindole may act to slow the movement of the toxin toward the synapse.

*Abstract from Toxicol. Appl. Pharmacol. 12, 249 (1968).

SOLUBLE PROTEIN PROFILES IN ESCHERICHIA COLI

V. Moses and D. G. Wild

It is known that bacterial cells cultured on a variety of media have different protein compositions. The content of ribosomes, and therefore the relative amount of ribosomal protein, is directly proportional to the growth rate,[1] and the formation of many known inducible and repressible enzymes depends on the presence or absence of specific effectors in the medium. Together, however, these components probably account for only a small proportion of the total cellular protein. We thought it of interest to survey briefly the overall profiles of soluble protein in Escherichia coli, both in a number of strains cultured in the same medium, and also in one strain grown in a number of different media. The data to be presented compare these parameters in a semi-quantitative manner; no investigation has been made at this stage of the relative amounts of soluble, ribosomal, and insoluble protein in the various cultures.

For comparison of the soluble protein profiles of the different strains (four derivatives of K12, and one each of B and ML), the cells were grown exponentially at 37°C in minimal medium 63,[2] supplemented with glucose (0.2%) and thiamine (1 mg/liter). In studies of cells grown in different media, strain 3000 was grown in minimal medium 63 supplemented with succinate, lactate, glycerol, or glucose (each at 0.2%), Difco nutrient broth (0.8%), or nutrient broth (0.8%) plus glucose (0.2%).

Flasks containing 1 liter of medium were inoculated with 50 ml of an overnight culture of the organism in the same medium. Growth was allowed to proceed exponentially for at least three generations, and the cells were then harvested when there was about 110 μg of bacterial protein/ml (extinction of 0.5 in a 1-cm cell at 650 mμ). The pellet was resuspended in 5 ml of buffer (10 mM tris, 10 mM Mg acetate, 100 mM KCl, pH 7.4) and the cells were disrupted with a French pressure cell. After the addition of a minute crystal of DNA'ase the preparation was centrifuged for 90 min at 100 000 × g(max) to sediment ribosomes and other insoluble material.

Aliquots (10-15 μl) of the supernatant liquid were subjected to electrophoresis in slabs of polyacrylamide gel for 90 min at an initial current of 90 mA (270V). The gels were made from 7.5% Cyanogum-41 and 0.07% N,N,N',N'-tetramethylethylenediamine in tris (25 mM)-glycine (190 mM) buffer, pH 8.3, and were polymerized by the addition of ammonium persulfate (0.1%). The same buffer was used in the electrode vessels. Extracts from the six different strains were subjected to electrophoresis in parallel slots in the same gel. Similarly, the extracts of strain 3000 grown in the six different media were also run together. The protein bands were stained by immersing the slab of gel for 15 min in a solution (0.1%) of naphthalene black 12B in acetic acid–methanol–water (2:5:13 by vol); excess stain was removed by washing with frequent changes of 7.5% acetic acid. The gels were scanned in a Joyce-Loebl Chromoscan. More bands could be seen by eye than were clearly resolved by the densitometer, and their locations are indicated on the diagrams. However, use of this instrument permitted semiquantitative estimate of the various components, and the original traces have been redrawn so that the total areas under the curves for all six parts of Fig. 1 are approximately equal. The curves in Fig. 2 were similarly normalized. Some fine detail has been lost in redrawing these curves.

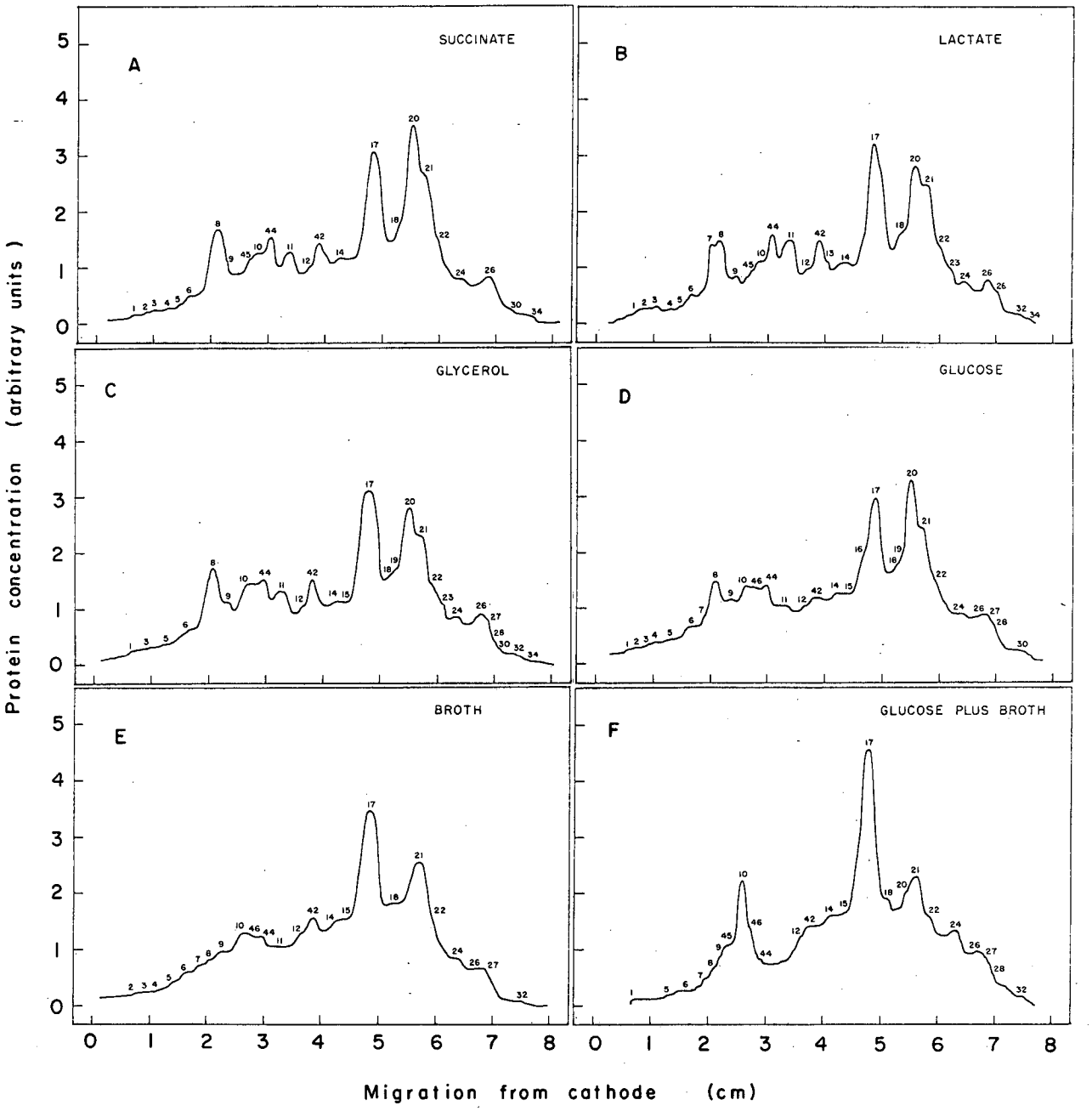

Fig. 1. Soluble protein profiles of different strains, all grown on glucose-minimal medium. Ordinates, protein conc. (arbitrary units); abscissae, distance of migration from cathode (cm). Strain numbers are indicated for each profile.

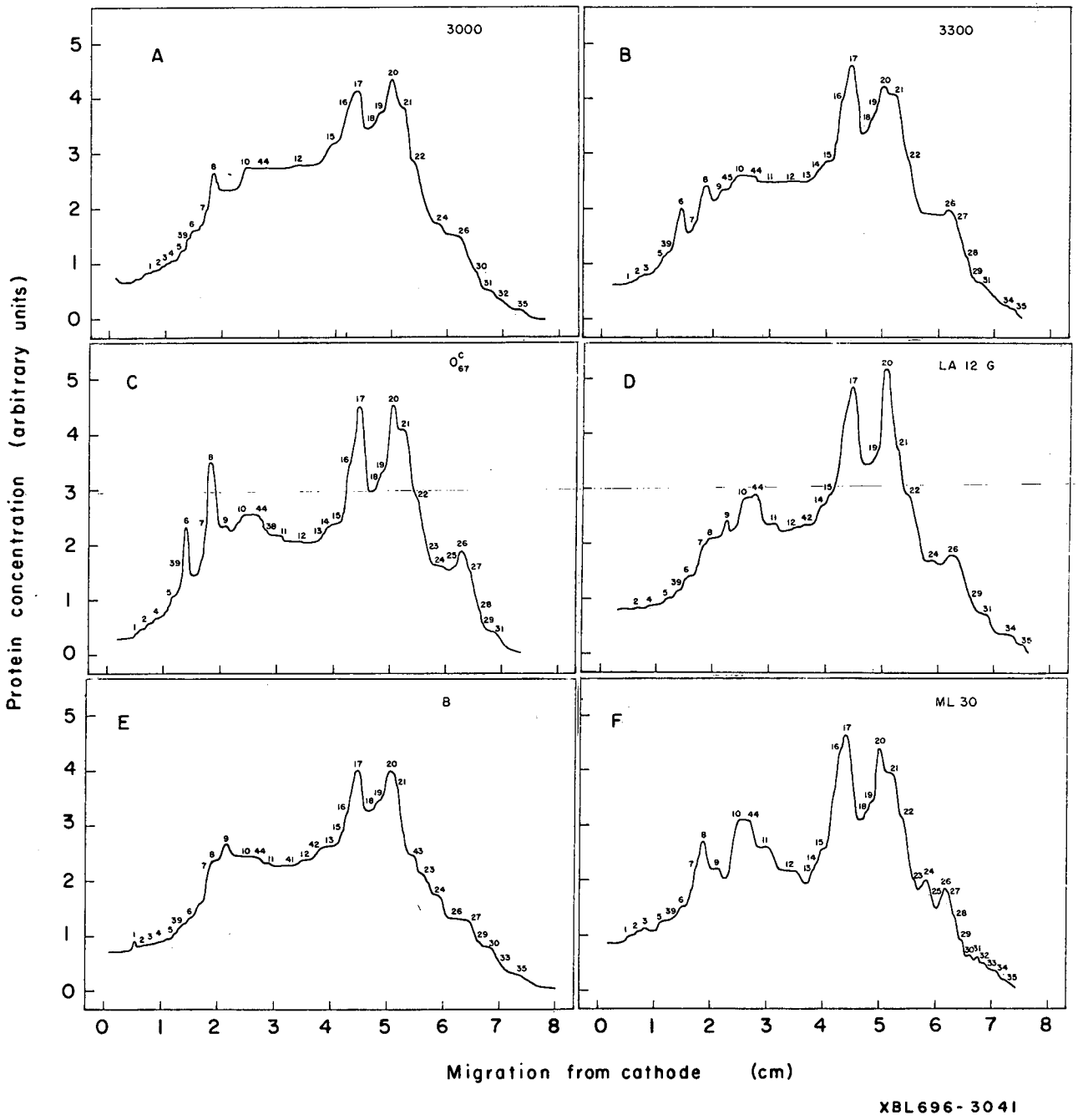

Fig. 2. Soluble protein profiles of strain 3000 grown on different media. Ordinates, protein conc. (arbitrary units); abscissae, distance of migration from cathode (cm). Carbon sources are indicated for each profile.

Figure 1 shows that differences were observed even among very closely related strains. With strain 3000 used as the standard, 3300 (a lac i^- derivative of 3000) showed differences in bands 6, 9, 10, 20, 26, and 44, with minor variations in other peaks. Strain o^c_{67} (a lac i^- o^c derivative of 3000) was similar to strain 3300, though peak 8 was particularly prominent in o^c_{67} and peak 20 resembled that found in strain 3000 rather than that in strain 3300. Strains 3300 and o^c_{67} are constitutive for the lactose enzymes, while strain 3000 is inducible, so that peak 6, prominent in the constitutive strains but not in the inducible one, may represent β-galactosidase.

Strain LA12G, derived from strain 3000 but carrying the CR^- genotype[3] was intermediate between strains 3000 and o^c_{67}, except for peak 8, which was almost entirely absent. Peak 9 was more prominent than in strain 3000, and peak 6 was virtually absent, as would be expected for β-galactosidase in this inducible strain.

The two other organisms examined are not derivatives of K12. Strain B resembled strain 3000 except for peaks 1, 8, 9, and 21 and minor differences in other peaks. ML30 showed rather more differences from 3000, of which those affecting peaks 3, 9, 10, 12, 13, 24, 26, and 44 were the most prominent.

Appreciable differences thus exist in the relative proportions of the soluble proteins in the six strains. Replicate electrophoretic analyses have shown that these are not adventitious effects of the analytical techniques. We have, however, found it to be essential to make comparisons on one gel slab, as the degree of resolution of these complex patterns varies from one electrophoresis run to another. The closely related K12 derivatives (3000, 3300, o^c_{67}, and LA12G) showed appreciable variation among themselves; one is thus led to conclude that although these four strains were originally isolated on the basis of single or few genetic differences, their prolonged maintenance as distinct lines has resulted in other changes in overall phenotype beyond those to be expected solely from their known genotypic differences.

Figure 2 shows the profiles of parallel cultures of strain 3000 grown in different media. Three of the four mineral media (succinate, lactate, and glycerol) gave similar but not identical patterns. When cells grown on succinate were used as the standard, lactate-grown cells showed distinct differences in peaks 7, 9, 11, 20, and 24. The most pronounced change concerned peak 7, which was prominent only in cells grown on lactate, and may represent lactic dehydrogenase. Glycerol-grown cells differed from those grown in succinate mostly in the relative prominence of peaks 10, 17, and 20. The prominence of peak 10 in glycerol-grown cells is probably not specifically related to the metabolism of glycerol, as it was also well marked in cells grown on glucose or broth. The overall similarity of the patterns with succinate-, lactate- and glycerol-grown cells suggests that the balance of metabolic activity in these organisms differs but little, and probably involves to a high degree the reactions of the tricarboxylic acid cycle. These three substrates are among those which characteristically fail to evoke catabolite repression in growing cells. Glycerol, unlike glucose, appears not to be extensively metabolized through the pentose phosphate cycle,[4] and is probably utilized mostly via glycolysis to produce a metabolic pattern similar to those found with succinate and lactate.

More differences were visible with glucose-grown cells; these may be related to the more rapid growth on this substrate, as well as to the difference in metabolic pattern which results in the high degree of catabolite repression. Peaks 8, 11, 42, and 44 were

much reduced in relative prominence.

Rich media produced the greatest alteration in the profiles. In broth-grown cells, peaks 8, 11, 20, and 44, so prominent in succinate-grown cells, were nearly or entirely absent, while the presence of both glucose and broth in the medium resulted in effects more extensive than caused by either alone. Peaks 21 and 42, already relatively small in broth-grown cells, were reduced in size still further when glucose was also present, while peak 10 (and, to a lesser extent, peak 24) was much larger than with either glucose or broth alone.

As shown by these studies, the phenotypic character of a bacterial cell is altered in a number of ways by the nature of the growth medium. Generally, the differences shown by cells grown in minimal medium containing alternative carbon sources were not extensive, and such variations as could be seen may result from the synthesis of specific enzymes for the initial metabolism of the various substrates. The more pronounced effects of glucose are consistent with the widespread action that this carbon source is known to exert on many enzymes through catabolite repression. Growth in a rich broth medium did produce extensive changes and is known to cause repression of enzymes responsible for the synthesis of amino acids, nucleotides, and other cellular constituents. The further addition of glucose to broth medium enhanced the repressive effect seen in either glucose or broth alone, but also profoundly increased the size of peak 10, which was present to a smaller extent in cells grown in all the minimal media but not in those grown in broth devoid of a supplementary carbon source.

The results complement those of Raunio and Sarimo,[5] who found changes in the protein composition of E. coli during the active phase of growth in glucose-minimal medium. They reported that growth of a batch culture resulted in changes in the soluble protein profile as the culture developed. Presumably this was the consequence of changes in the medium with time, and may be compared with the differences we have found in cells harvested at constant density from different media. From a practical viewpoint, these results show that the preparation of cells of constant composition requires rigorous control of the growth conditions. They also illustrate the complexity of the regulatory factors which interact to produce the bacterial phenotype, and suggest that the alteration of the enzyme balance to accommodate the metabolism of a different substrate is likely to have widespread effects on the relative quantitative distribution of proteins, many of which may not be closely involved in substrate metabolism

We are grateful to Dr. R. E. MacDonald for the loan of the electrophoresis cell.

References

1. O. Maaløe and N. O. Kjeldgaard, in Control of Macromolecular Synthesis (W. A. Benjamin Inc., New York and Amsterdam, 1966), p. 90.
2. A. B. Pardee and L. S. Prestidge, The Initial Kinetics of Enzyme Induction, Biochim. Biophys. Acta 49, 77 (1961).
3. W. F. Loomis, Jr., and B. Magasanik, Genetic Control of Catabolite Repression of the Lac Operon in Escherichia coli, Biochem. Biophys. Res. Commun. 20, 230 (1965).
4. C. Prevost and V. Moses, Pool Sizes of Metabolic Intermediates and their Relation to Glucose Repression of β-Galactosidase Synthesis in Escherichia coli, Biochem. J. 103, 349 (1967).
5. R. Raunio and S. Sarimo, Changes in Protein Composition of Escherichia coli during the Active Growth Phase, Acta Chem. Scand. 19, 2428 (1965).

Radiation Chemistry, Photochemistry, Chemical Evolution

ROLE OF TRAPPED ELECTRONS IN THE RADIOLYSIS OF CHOLINE CHLORIDE

A. Nath, L. Marton, R. Agarwal, V. Subramanyan, and R. M. Lemmon

Earlier workers[1] have shown that choline chloride is a remarkably radiation-sensitive compound. They observed that the radiation damage could be deferred indefinitely by storing the irradiated samples at -196°. At room temperature damage develops gradually over several hours, and much faster at elevated temperatures. However, at temperatures above 70°, choline chloride undergoes phase transformation, and the phase stable at higher temperatures was shown to be radiation resistant,[2] unlike the crystal form stable at lower temperatures.

Since the radiolysis does not proceed at lower temperatures, it was felt that the thermal activation could be responsible for either diffusion of radicals or release of trapped electrons from sites that are populated with electrons during γ irradiation. The following experiments were conducted to decide between these two alternatives, which in turn will permit an insight into the mechanism of radiolysis.

We placed in a sealed, evacuated tube one sample of pure, labeled choline chloride, $[(^{14}CH_3)_3NCH_2CH_2OH]^+Cl^-$, and in three similar tubes (separately) this compound mixed with about ten times its weight of (a) the electron acceptor ortho-chloranil, (b) the electron acceptor tetracyanoethylene, and (c) the electron donor Brilliant Green (a triphenylmethane dye). The samples were irradiated at liquid nitrogen temperature in a cobalt-60 γ-ray source for an hour, receiving a dose of about 2×10^6 rads. The samples, after the heat treatment (if any), were dissolved in an aqueous solution containing trimethylamine carrier and slightly acidified with HCl and made to 1 ml volume. Aliquots were pipetted out and spotted on Whatman No. 1 paper. A solution consisting of butanol, HCl, and water in the ratio 8:1:1 was used for chromatographic development, giving clean separations between trimethylamine hydrochloride and choline chloride. The two fractions are located on the paper by radioautography and cut apart accordingly. The pieces of paper are immersed in a liquid scintillator (toluene containing PPO and POPOP) and counted. The activity as trimethylamine represents the fraction of choline chloride having undergone radiolysis. The results are given in Table I. The values in the first row represent the amount of radiolysis (% decomposition) as a result of irradiation at -196°. The values for % radiolysis after heating the samples for 2 hr at 50° are given in the second row. These are average values.

It is apparent from the data that the electron acceptors orthochloranil and TCNE retard the radiolysis whereas the electron donor, Brilliant Green, enhances the radiolysis. It appears that a free electron triggers the chain leading to radiolysis. The major sources of these electrons are the "donors" in the choline chloride. They are presumably formed during irradiation, as indicated by a few preliminary measurements on thermoluminescence. The trapped electrons in them are released during thermal treatment. The acceptors compete for these electrons and thereby retard the reaction, whereas the donors increase the

Table I. Effect of electron donors and acceptors on radiolysis of choline chloride (% decomposition)

	Compounds added to finely divided choline chloride			
	Pure choline chloride	Ortho-chloranil	TCNE	Brilliant Green
No heating after irradiation	0.28	0.28	0.20	0.26
Heated for 2 hr at 50°C	8.7 ± 0.1	7.4 ± 0.1	7.5 ± 0.1	9.3 ± 0.1

Table II. Effect of thermal treatment for different times at different temperatures on the radiolysis of pure choline chloride and of a mixture with o-chloranil.

		Pure choline chloride	Choline chloride mixed with o-chloranil
Without thermal treatment		0.38	0.43
With thermal treatment			
Temp. 50°			
Time (min)	5	2.9	2.5
	10	4.6	4.0
	20	6.6	6.0
	120	8.5	7.8
Temp. 60°			
Time (min)	5	4.6	4.0
	10	6.1	4.6
	20	7.5	4.9
	120	8.2	5.1
Temp. 90°			
Time (min)	5	2.4	--
	10	2.2	--
	20	2.3	--

density of free electrons and so enhance the radiolysis.

It was mentioned earlier that choline chloride undergoes phase transformation above 70° into an enantiomorph which is not radiation sensitive. This is clearly shown in our data In Table II. Choline chloride undergoes a greater extent of radiolysis at 50° and 60° than at 90°. As a matter of fact, what is significant is the radiolysis that proceeds before the sample undergoes phase transformation at 90°. This is apparent from the observation that no further radiolysis occurs beyond 2 min heating at 90°.

The above results indicate a role for trapped electrons in the chain radiolysis process, and this possibility has been pursued in the following kinds of investigations.

Addition of Gaseous Ambients

We have determined the effects of the presence of three gaseous ambients (O_2, SF_6, and N_2O--all electron acceptors) on the radiolysis. The results, obtained on finely divided (rapidly precipitated) choline chloride are shown in Table III. The only purpose of the heating at 50° is to speed up the radiolysis.

Table III. Influence of gaseous ambients (% radiolysis)

Ambient (at 70 cm pressure)	Without heating	Time of heating at 50° 20 min	120 min
Vacuum	0.2	8.4 ± 0.2	12.1 ± 0.2
O_2	0.2	7.9 ± 0.2	11.1 ± 0.2
SF_6	0.2	8.0 ± 0.2	10.7 ± 0.2
N_2O	0.2	8.0 ± 0.2	10.9 ± 0.2

These results appear to confirm the earlier data that electron acceptors retard the radiolysis.

Phototransfer of Electrons

We tested the effect of the presence of the photoemitting dye, Brilliant Green, a triphenylmethane derivative with the formula

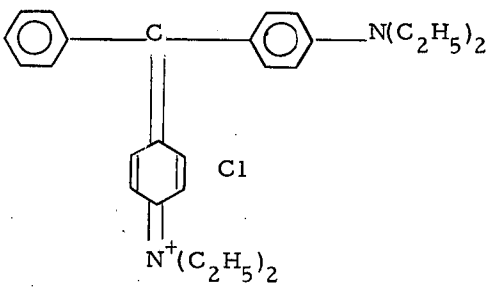

This compound is reasonably inert (so that "chemical" reaction with choline chloride was not a problem), and has a quantum yield of charge carriers at the surface much higher than other dyes.[3] Brilliant Green absorbs strongly in the region 500–800 nm, and its photoexcited behavior has been interpreted as the migration of excitons to the crystal surface, where they form holes and electrons. It was our expectation that electron transfers at the interface of Brilliant Green–choline chloride crystals would effect the choline's radiolysis. Consequently, samples of finely crystalline choline chloride were γ-irradiated (-196°, 10^6 rads) and then mixed (under dry N_2) with powdered Brilliant Green in a 1:1 ratio of the two compounds. The mixture was then illuminated with a G. E. A-H6 high-pressure mercury lamp, at a distance of about 7 in. The samples were kept at dry ice and room temperatures respectively. The results are shown in Table IV.

These results indicate that the illuminated Brilliant Green is providing electrons to the irradiated choline chloride, and that these electrons are enhancing the radiolysis.

Effect of Prior Thermal Treatment

It is reasonable to assume that crystal imperfections in choline chloride constitute potential electron traps and that these traps are populated with electrons during γ irradiation. Such imperfections would be likely to

Table IV. Effect of phototransfer of electrons

Treatment of γ-irradiated choline chloride plus Brilliant Green	Radiolysis (%)
At -70°	
Blank	0.8 ± 0.2
Illuminated for 4 hr	2.7 ± 0.2
At room temperature	
Stored for 4 hr	5.7 ± 0.2
Illuminated for 4 hr	12.3 ± 0.2

be annealed out by thermal treatment of the crystals. Consequently, we subjected crystalline choline chloride to a "prior thermal treatment" at 150° before γ irradiation. The data of Table V indicate that such treatment does indeed considerably reduce the choline's susceptibility to radiation damage, a probable result of a diminished density of electron traps.

Table V. Effect of thermal treatment of choline chloride prior to irradiation.

	Postirradiation thermal treatment at 50°	
	20 min	120 min
No prior thermal treatment at 150°	8.2%	12.2 %
Prior thermal treatment at 150° for 48 hr	6.5%	8.6%

Repeated Irradiation Cycles

Crystals have a finite number of traps. In choline chloride, after all these are electron-populated during γ irradiation, continued irradiation may have little further effect in promoting the radiolysis. On the other hand, if only a buildup of free radicals is important for the radiolysis, continued irradiation would continue to cause radiolysis. We therefore tested interrupted versus noninterrupted radiation effects, as follows: A sample of choline chloride was irradiated at liquid N_2 temperature for 1 hr followed by thermal treatment for 2 hr at 50°. It was again irradiated for another hour followed by the same thermal treatment. This cycle was repeated again, viz., a total of three cycles. The sample showed a radiolysis of 24.5%. This is to be compared with a sample of choline chloride which was irradiated for an uninterrupted 3 hr and subsequently heated for 6 hr at 50°. It was only 13.6% decomposed. A reasonable interpretation of these data is that upon recycling we are repopulating the depleted donors with electrons, thereby enhancing the radiolysis.

Effect of Compression

Compression of finely divided material is known to enhance the density of defects. Irradiated samples of choline chloride were compressed in a dye chilled in solid CO_2 to 2 tons/in.^{2}. Two of the pellets, analyzed immediately after their formation, showed a radiolysis of 0.25%. On thermal treatment of the pellets for 2 hr at 50° the radiolysis increased to 0.8%. Compared with the usual amount of 12% in non-pelleted material; the radiolysis is drastically inhibited by compression.

Concomitant ESR observations indicated that there was no change, on compression, of the concentration of radicals. We interpret these results to mean that, during compression, a large number of defects are created, and that these defects compete very favorably for free electrons during the subsequent thermal treatment. The electrons, which otherwise would react with an ion or radical and start the chain mechanism, are trapped in the high density of defects produced by the compression.

References

1. R. O. Lindblom, R. M. Lemmon, and M. Calvin, J. Am. Chem. Soc. 83, 2484 (1961).
2. P. Shanley and R. L. Collin, Rad. Res. 16, 674 (1962).
3. V. A. Benderskii, B. Ya. Kogan, Yu. Yu. Abramov, and L. E. Kapranova, Doklady Akad. Nauk SSSR 156, 897 (1964).

ATTEMPTS TOWARD IDENTIFICATION OF THE UNKNOWN COMPOUND "U-2" FROM THE $^{14}C^{+}$ - BENZENE REACTION

T. - H. Lin, Helmut Pohlit, Wallace Erwin, and R. M. Lemmon

Introduction

We have made further investigations on the chemistry of the interesting, yet structurally unknown compound, "U-2," from our $^{14}C^{+}$ irradiations of benzene. U-2 has a retention time in gas-liquid chromatography (CW 20M) approximately corresponding to those of both n-hexylbenzene and indene, it reacts with bromine, and it gives toluene and methylcyclohexane upon hydrogenation. The formation of toluene indicates the presence in the molecule of a phenyl group or a group that gives the benzene ring in the process of hydrogenation. Toluene and methylcyclohexane could be formed from different parts of the U-2 molecule. In such a case, U-2 would contain at least 13 or 14 carbons. However, the circumstances that (a) it has much shorter retention time than any known 13-carbon compound and (b) fragmentation of a hydrocarbon on hydrogenolysis seems most unlikely may be taken as indication that U-2 possesses only 7 carbons. This conclusion is supported by the essentially identical ^{14}C ring-methyl distribution for toluene and methylcyclohexane (indicative of the same precursor for the two compounds). Thus, U-2 may possibly be a C_7 compound which gives toluene and methylcyclohexane when attacked by hydrogen at different sites of the molecule. A similar and more important reaction of this unsaturated U-2 molecule will be hydrohalogenation; such a reaction will probably give isomers of halotoluenes or benzylhalide. However, our attempted hydrobrominations were not successful.

A close examination of the radioactivity trace of the gas-liquid chromatogram reveals that, in the U-2 peak, a small shoulder precedes the major peak. U-2, therefore, may actually be a combination of two compounds that give toluene and methylcyclohexane respectively upon hydrogenation. A preliminary attempt to separate this possible mixture on gas-liquid chromatography (Carbowax) was not successful.

A routine procedure for the determination of an organic compound may require an elemental analysis, some spectroscopic data (such as uv, ir, NMR, and mass spectra), and subsequent confirmation of the result by carrying out suitable chemical reactions. Unfortunately, since we cannot obtain a macro amount of product from our $^{14}C^{+}$ irradiation, a possible "carrier" compound must be found before any investigation can be made. Earlier efforts were made to match the retention times of known

compounds with that of U-2. Among the compounds checked were bicyclo-(2, 2, 1)-heptadiene, cyclooctatetraene, styrene, phenylacetylene, and benzocyclopropene. None corresponded with U-2.

In this report we describe efforts toward the identification of U-2 made under the assumption that U-2 is a 7-carbon compound.

$CH_2 + C_6H_6$

The insertion of carbene into one of the three kinds of bonds in the benzene molecule (C-H, C-C, and C=C) would give the following compounds:

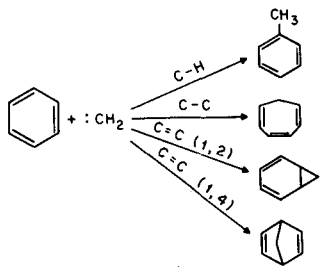

All these have, of course, too short a retention time to be U-2. It is also possible that the hot C_1 species may excite the benzene molecule, leading to the structural isomerization prior to the insertions:

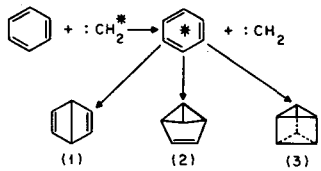

The reaction of carbene toward bicyclo-(2, 2, 0)-hexadine (Dewar benzene) (1), benzvalene (2), and prismane (3) would give compounds (4) through (18):

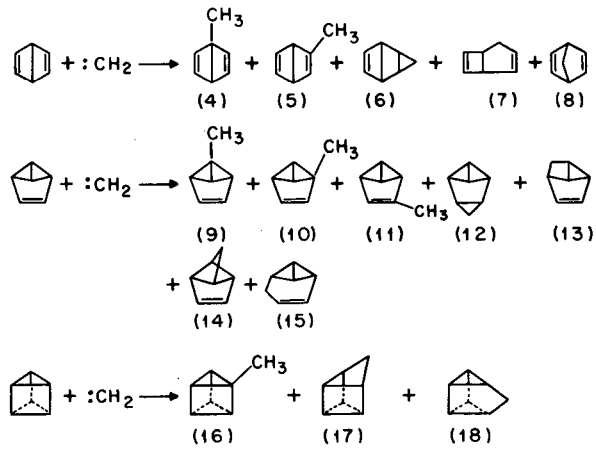

It is not known whether these compounds give toluene on hydrogenation. However, as in the case of U-2, even if toluene appeared it might not be a hydrogenation product, but an isomerization product induced by PtO_2 catalysis. In order to check the possibility of the formation of U-2 from the reaction of carbene and benzene, the Simmons-Smith reagent[2] was refluxed in benzene solution and irradiated with uv. No U-2 was found. It is known that the reactive species in the Simmons-Smith reaction is a carbenoid instead of a free carbene; therefore the validity of the above results should be suspected unless a free carbene is used.

$C + C_6H_6$

The formation of diphenylmethane and phenylcycloheptatriene in our reaction shows beyond any doubt that the major reaction species in the system is indeed a free carbon. Thus, the study of the reaction of carbon with benzene could be pertinent to our problem. The insertion of a carbon atom into C-H, C-C, and C=C linkages of benzene would give phenylcarbene (19), cycloheptatrienylidene (20), norcaradienylidene (21), and bicyclo-(2, 2, 1)-heptadienylidene (22):

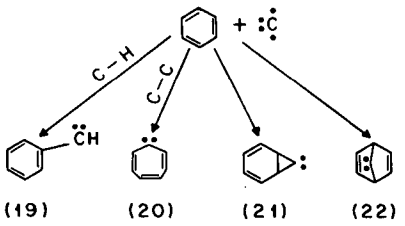

The carbenes (19) - (22) may then undergo intramolecular insertions to give compounds (23) - (35):

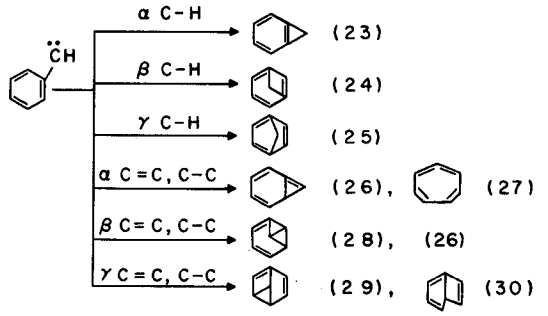

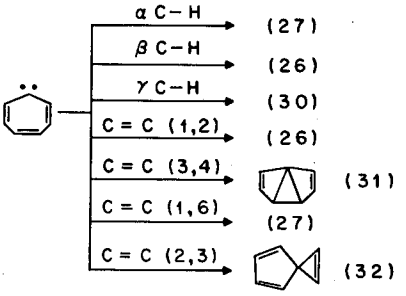

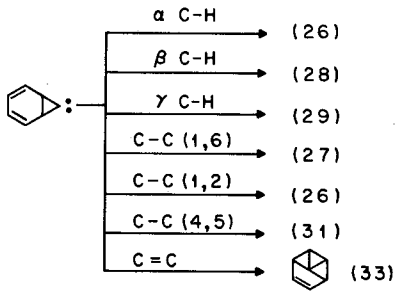

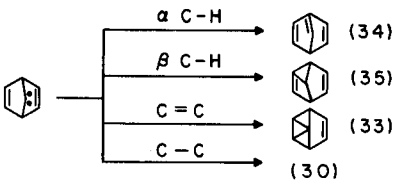

If the isomers of benzene, (1), (2), and (3), were to be considered here, an enormous number (more than a hundred) of these structures could be drawn. There are skeletal resemblances between most compounds shown above. Perhaps they are in fact a resonance hybrid that can be represented by 

Benzocyclopropene (23) is one of the above isomers that was available to us; that it was not U-2 was shown by comparison of retention times on gas-liquid chromatography.

The unknown compounds (24), (25), (34), and  (36) are also attractive possibilities for U-2. Since they are dehydrobicyclo-(2, 2, 1)-heptadienes, the dehydrogenation of bicyclo-(2, 2, 1)-heptadiene, in vapor phase over Pd-C (250°), was carried out. No U-2 was found. The disproportionation of bicyclo-(2, 2, 1)-heptadiene using PtO_2 as catalyst was also unsuccessful.

Our next attempts were the dehydrobromination and debromination respectively of mono- and dibromo-bicyclo-(2, 2, 1)-heptadiene. The reaction schemes are as below:

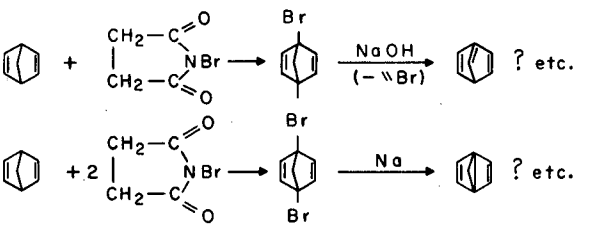

No U-2 was obtained from debromination. In the case of the -HBr route, bromobicycloheptadiene was prepared by refluxing a 0.1 M carbon tetrachloride solution of bicycloheptadiene with 1 mole equivalent of N-bromosuccinimide for 2 hr. After the filtration of the resulting succinimide, the solution was stirred with NaOH for 2 days. About 0.1% of a U-2-like (GLC) compound was obtained. When this compound was purified by gas chromatography

and hydrogenated, the formation of toluene in one run and methylcyclohexane in the other was observed (they did not appear in the same hydrogenation). The mass spectrum of this compound showed a parent ion of mass 92 and abundant tropylium ions at 91. No further study was done on this compound.

In order to simulate the C-benzene reaction in which phenylcarbene is conceivably involved, phenylcarbene was generated in benzene solution. The uv irradiation of stilbene oxide was first employed:[3]

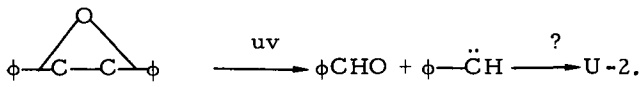

A 0.1 M benzene solution of stilbene oxide was irradiated in a Vycor flask with a high-pressure mercury vapor lamp (A-H6) for 4 days, at a distance of approx 10 in. The gas-liquid chromatography of the resulting mixture indicated the presence of about 1% toluene, 4% U-2-like compound, and 3% of phenylcycloheptatriene. When this U-2-like compound was hydrogenated, a major peak which had a retention time longer than the parent compound was found, and only small amounts (1-5%) of toluene and methylcyclohexane were observed. The major part of this peak was later found (by mass spectrometry) to be benzaldehyde. In order to isolate any possible U-2 that might have been masked by the bulk of the benzaldehyde, the reaction mixture was then extracted thoroughly with saturated $NaHSO_3$ solution. We could not detect any of the compound that had previously given toluene and methylcyclohexane.

Since benzaldehyde has a retention time exactly the same as U-2 and, consequently, interferes with its isolation, phenylcarbene was then generated via the photolysis of phenyldiazomethane:[4]

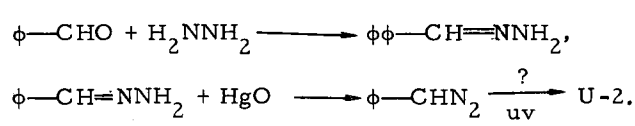

A 125-ml Erlenmeyer flask containing 9 g of benzaldehyde hydrazone and 100 ml of benzene was immersed in an ice-water bath; with stirring, 15 g of yellow mercurous oxide was added in portions (during 10 min). The solution was allowed to react for 1 hr. The red-brown solution was then decanted and dried over KOH pellets. The phenylcarbene thus obtained was then illuminated with a photo DXB lamp for 2 days. About 5% of a U-2-like compound was obtained (no benzaldehyde was present). The nature of this compound will be investigated.

References

1. W. v. Doering and L. H. Knox, J. Am. Chem. Soc. 76, 3202 (1954).
2. H. E. Simmons and R. D. Smith, J. Am. Chem. Soc. 81, 4256 (1959).
3. H. Kristinsson and G. W. Griffin, J. Am. Chem. Soc. 88, 1579 (1966).
4. C. D. Gutsche, G. L. Bachman, and R. S. Coffey, Tetrahedron 18, 617 (1962).

PHOTODEOXYGENATION OF α, α, N-TRIPHENYLNITRONE

Janet Splitter

The deoxygenation of α, α, N-Triphenylnitrone is a competitive reaction in the irradiation of the nitrone to oxaziridine with short-wavelength light under helium (Hanovia 450-watt type L medium-pressure mercury vapor lamp, no Pyrex filter):

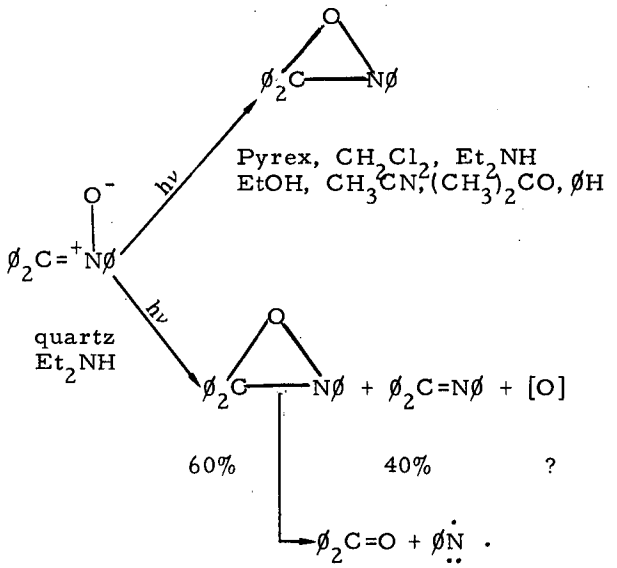

In order to obtain the optimum conditions for the photo-deoxygenation, light of wavelengths longer than 2800 Å was eliminated by using the Rayonet low-pressure mercury vapor lamps (mainly 2537 Å light) with a KI_3 solution filter.[1] Under these conditions, with Et_2NH as solvent, all the light was absorbed by the solvent. The yield of imine was increased to about 80%. The resulting solution showed a correspondingly high active oxygen content. The conditions under which the potassium iodide was oxidized were similar to those employed with hydrogen peroxide (no heat required). It is possible that the agent responsible for the active oxygen is hydrogen peroxide. Diethylamine is known to photolyze with production of hydrogen atoms:[2]

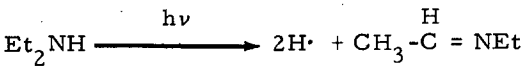

No diethylhydroxylamine was detected. The yield of imine was much less when irradiation was done under air instead of helium. When solvent was used that did not absorb at 2537 Å, such as ethanol, the yield of imine was low. However, the yield appeared to increase as the amount of photofragmentation of the oxaziridine increased:

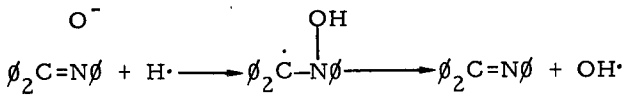

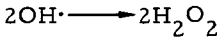

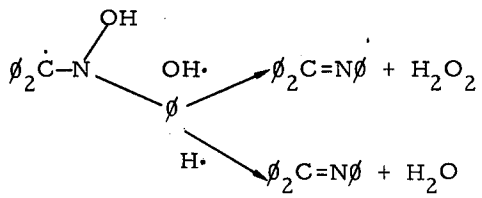

This suggested that the resulting benzophenone was acting as a triplet sensitizer[3] or as a hydrogen atom transfer agent.[4] When the nitrone was irradiated at 2537Å in ethanol with added benzophenone, which absorbed 93% of the light, the yield of imine was greatly increased. The time of irradiation to give 50% nitrone disappearance was 10 min, compared with about 3 min when no benzophenone was added, indicating that benzophenone also was acting as an internal filter. An experiment was done with the same added benzophenone solution irradiated for 6 min under helium; one tube was opened to air immediately after irradiation and the other was kept in the dark and opened 2 days later. The first tube showed 30% disappearance of nitrone after irradiation, and the second one showed 72% disappearance of nitrone. The first tube after 2 days' standing in the dark showed 45% disappearance of nitrone. Both showed high yields of imine by GLC, but the one unopened for 2 days gave a somewhat higher yield. It appeared that a similar thermal reaction was taking place in the injection port of the gas chromatograph, inasmuch as the amount of nitrone present before injection could not be accounted for except by a conversion to imine that took place differently from that of unirradiated nitrone. Benzophenone is known to form an intermediate when irradiated in isopropanol,[5] which slowly reacts over a period of days with benzophenone to form ketyl radicals:

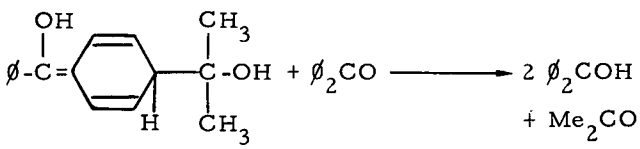

In the presence of oxygen this intermediate was found[5] to regenerate benzophenone over a period of hours. Either the ketyl radicals or the intermediate must be reacting with the nitrone to give a new intermediate, which may be $\phi_2\dot{C}\text{-}\overset{OH}{N}\text{-}\phi$ and which may further react as above. The resulting solution was found to have some active oxygen content, which may be hydrogen peroxide or its addition compound with acetaldehyde. Acetaldehyde is formed in the irradiation of benzophenone in ethanol.

Further work needs to be done to substantiate this mechanism, in particular to account for the active oxygen content observed. Also, a triplet sensitizer whose triplet does not abstract hydrogen atoms from the solvent, such as m-methoxyacetophenone,[4] should be used in place of benzophenone.

Nitrones, in general, deoxygenate readily in the gas chromatograph injection port (300°) and under electron impact in the mass spectrometer. A recent report tells of using a nitrone as a radical trap.[6]

References

1. J. G. Calvert and J. N. Pitts, Jr., Photochemistry (John Wiley & Sons, New York, 1966), p. 729.
2. Ibid., p. 455; L. T. Allan and G. A. Swan, J. Chem. Soc. 4822 (1965).
3. Ibid., p. 349.
4. B. M. Monroe and S. A. Weiner, J. Am. Chem. Soc. 91, 450 (1969).
5. N. Filipescu and F. L. Minn, J. Am. Chem. Soc. 90, 1544 (1968).
6. E. G. Janzen and B. J. Blackburn, J. Am. Chem. Soc. 90, 5909 (1968).

ON THE PHOTOREDUCTION OF BENZOPHENONE IN ISOPROPYL ALCOHOL

Janet Splitter

Recently,[1] the structure of the intermediate (In) in the photoreduction of benzophenone in isopropyl alcohol has been postulated as

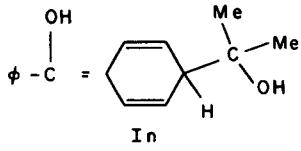

In

In the absence of air, the following series of reactions was proposed:

$$\phi_2CO \xrightarrow{h\nu} {}^1\phi_2CO \longrightarrow {}^3\phi_2CO,$$

$${}^3\phi_2CO + Me_2CHOH \longrightarrow \phi_2\dot{C}OH + Me_2\dot{C}OH,$$

$$\phi_2\dot{C}OH + Me_2\dot{C}OH \longrightarrow In,$$

$$In + \phi_2CO \longrightarrow 2\phi_2\dot{C}OH + Me_2CO,$$

$$2\phi_2\dot{C}OH \longrightarrow \phi_2\text{—}\overset{OH}{\overset{|}{C}}\text{—}\overset{OH}{\overset{|}{C}}\text{—}\phi_2.$$

In the presence of air, samples that contained almost exclusively In were reported to slowly regenerate benzophenone.

In our studies on photochemical reactions involving benzophenone as a product (partially irradiated) a new product was obtained which was not benzpinacol or benzhydrol. It had a longer retention time than benzophenone, benzhydrol, or benzpinacol in GLC and was thermally stable. The benzpinacol, of course, was converted to benzophenone and benzhydrol in the injection port. The $\lambda_{max, EtOH}$ of the product was 250 nm. The spectrum was very similar to that of benzhydrol except that it was shifted about 10 nm to shorter wavelengths. Its infrared absorption spectrum indicated the presence of hydroxy and alkyl groups as well as the aromatic ring. No carbonyl absorption was detected.

The NMR showed the presence of two kinds of aromatic protons at approximately 7.3 δ (5H) and 7.6 δ (3 or 4H), hydroxy protons at 2.2 δ (2H), and alkyl protons at 1.33 δ (7H). The NMR needs to be repeated with a purer sample, and with less background noise. In the following structure, which could fit the data, the benzylic proton was not found where expected. However, it may not have been seen because of the noise.

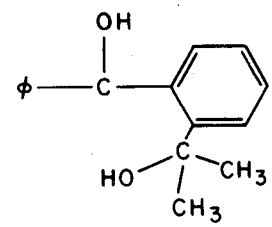

This product could arise from an In that is ortho-substituted in addition to the para-substituted In that was postulated.[1] The following reaction, involving an allylic shift, would be expected to take place readily, the driving

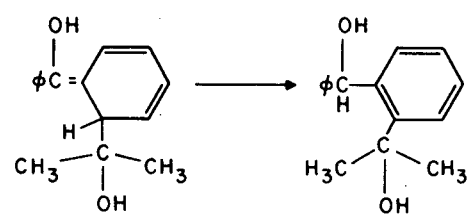

force being the formation of the aromatic ring. The para-substituted In would not be expected to undergo this rearrangement and may regenerate benzophenone as reported.[1]

The mass spectrum of the product at three different electron voltages is given in Table I. In Chart I is a possible scheme for the fragmentation of the product under electron impact.

Further studies need to be done on determining the conditions for the formation of this product in contrast to the conditions for forming benzpinacol.

Reference

1. N. Filipescu and F. L. Minn, J. Am. Chem. Soc. 90, 1544 (1968).

Table I. Mass spectra (MS-12) of new product from irradiation of benzophenone in isopropanol.

	Intensity (%)		
m/e	14 eV	20 eV	70 eV
242	0.1		
241	0.2		
240	1		
224	2		
208	12	11	12
193	2	2	5
185	21	16	5
184	100 (off scale)	100	34
183	39	68	30
182	8	16	20
181	2	6	15
166	3	6	
165		5	15
105	19	84	100
91			9
78	5	10	15
77		6	65
59	6	24	20
51			25
43		6	25

Chart I. Mass spectral fragmentations of new product.

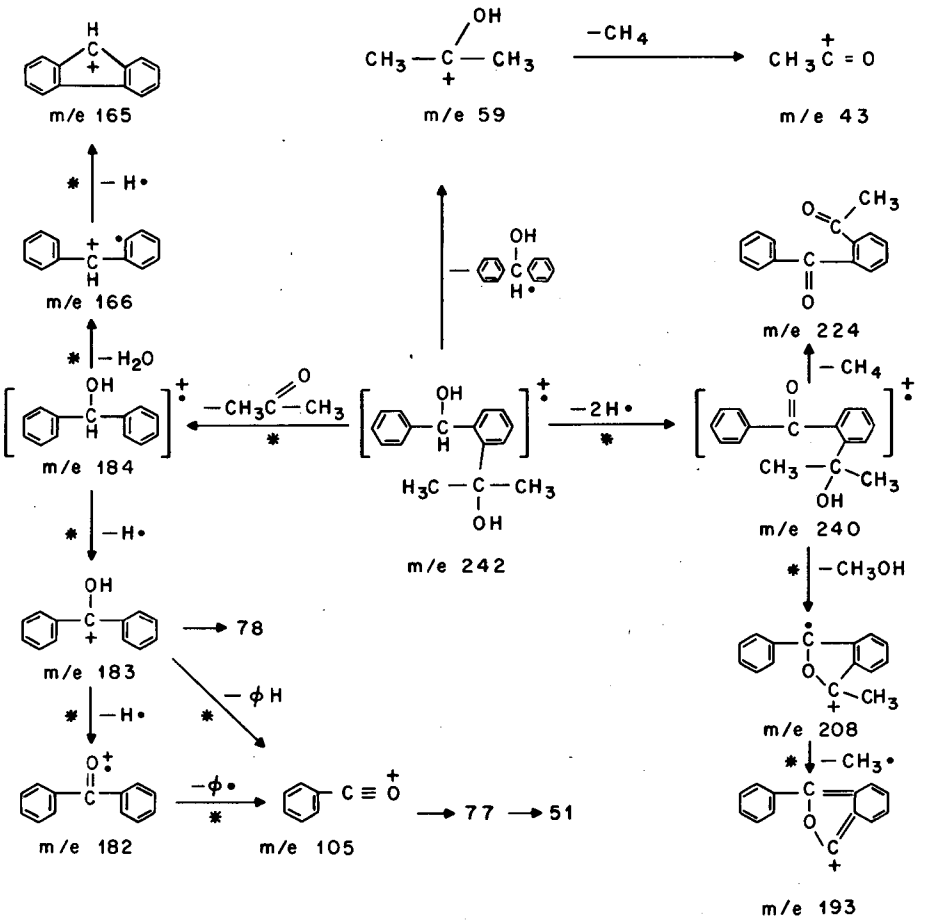

XBL696-3063

OCCURRENCE OF $C_{22} - C_{25}$ ISOPRENOIDS IN BELL CREEK CRUDE OIL

Jerry Han and Melvin Calvin

Introduction

Compounds can be classed as biological markers if they possess all the following characteristic structural skeleton, reasonable stability against degradation over long periods of geological time, structural specificity derived from known biological sequences, and low probability of formation by any nonbiological means. Of all the biological markers, the lipids have probably received most attention. The presence among the lipids of a series of hydrocarbons, whose structures consist of C_5H_8 isoprene units, has been cited as evidence for the biological origin of petroleum.

Isoprenoid compounds ranging from C_{14} (2, 6, 10-trimethylundecane) to C_{21} (2, 6, 10, 14-tetramethylheptadecane) have been isolated from petroleum by Bendoraitis.[1,2] Other authors[3-7] have reported similar isoprenoid hydrocarbons from oil shales and ancient rocks. The isoprenoid hydrocarbons containing 22 or more carbons have not been isolated.

We now report the isolation and identification of C_{22} to C_{25} saturated hydrocarbons in the Bell Creek Crude Oil (Lower Cretaceous, 135×10^6 years old) in Powder River County, Montana.

Experimental Procedure

An alumina column (3 ft × 0.5 in.) was prepared from 150 g of activated neutral aluminum oxide and washed with 200 ml of n-heptane. Two g of crude oil was mixed with 100 g aluminum oxide and transferred to the top of the column, after which it was eluted with 150 ml of n-heptane. The "total hydrocarbons" represented in this fraction show minimal ultraviolet absorption at 270 mμ. The alkanes were separated from alkenes by preparative thin-layer chromatography on a 10% silver nitrate–silica gel plate by use of n-hexane as solvent. After the "total alkanes" were extracted from the silver nitrate–silica gel cut with dry isooctane, the normal alkanes were separated from branched-cyclic alkanes with a 5-Å molecular sieve.[8] A 50:1 weight ratio of sieve to sample was used. The sieve and sample were placed in a round-bottomed flask and refluxed in dry isooctane for 2 days. After centrifugation, the solution containing the branched-cyclic fraction was removed. The sieve was thoroughly extracted with hot isooctane for several hours and the washings were added to the branched-cyclic fraction. The isooctane-washed sieve, which contained the normal paraffins, was treated with a mixture of 20% HF and benzene for 1 hour. After separation of the layers, the benzene solution of n-alkanes was filtered and the solvent was evaporated.

All fractions were analyzed on an Aerograph Model 204 gas chromatograph equipped with a capillary column which had been coated in this Laboratory. The gas chromatograms of "total aliphatic hydrocarbons," "normal alkanes," and "branched-cyclic alkanes" are shown in Figs. 1, 2, and 3 respectively. Three different columns, 100 ft × 0.01 in. Apiezon L, 100 ft × 0.01 in. Polysev, and 150 ft × 0.01 in.

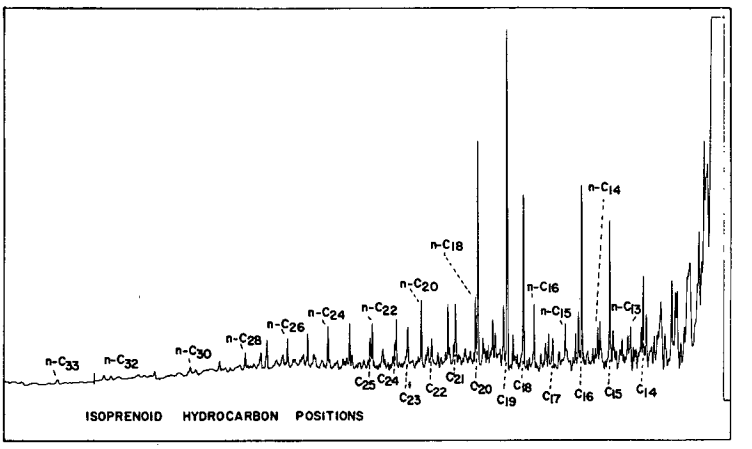

XBL6811-6689

Fig. 1. Gas chromatogram of total aliphatic hydrocarbons of Bell Creek Crude Oil. A 100 ft × 0.01 in. i.d. stainless steel column coated with Apiezon L was used. Helium pressure, 20 psi; flow rate, 2.5 ml/min. An Aerograph 204 apparatus equipped with a flame ionization detector was used. Temperature was programmed at 2°C/min from 90°C to 300°C and was held isothermally at 300°C.

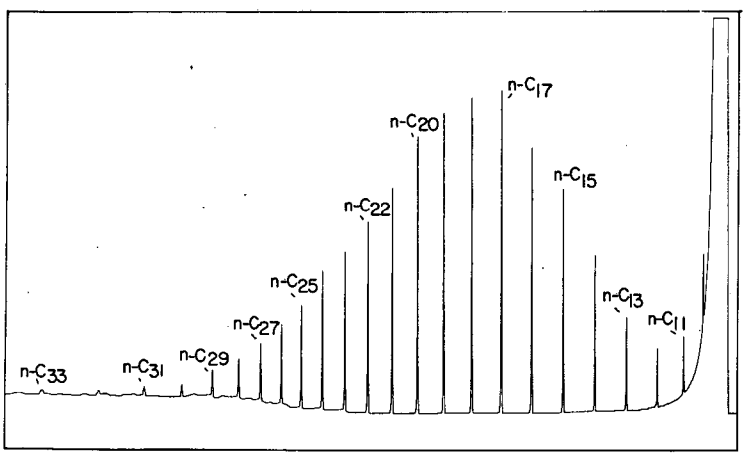

XBL6811-6691

Fig. 2. Gas chromatogram of normal hydrocarbon fraction of Bell Creek Crude Oil. All conditions are the same as for Fig. 1.

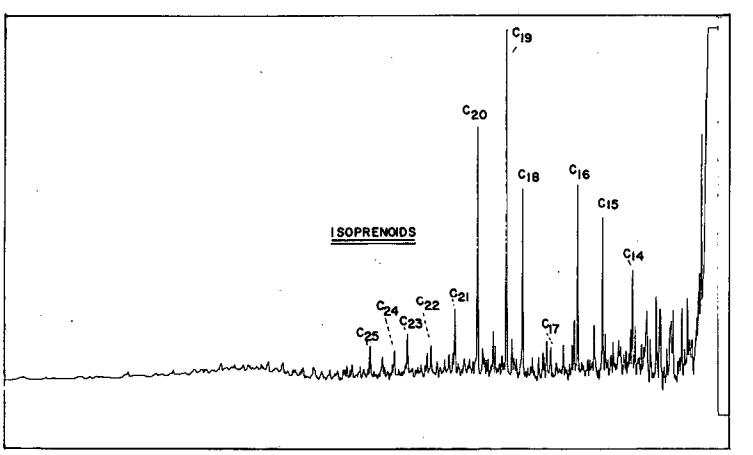

XBL6811-6690

Fig. 3. Gas chromatogram of the branched-cyclic alkane fraction of Bell Creek Crude Oil. All conditions are the same as for Fig. 1.

SF-96, were used for this analysis. Coinjections of isoprenoid standards, C_{15}, C_{17}, C_{19}, C_{20}, and C_{21} isoprenoid hydrocarbons, were made on all three columns. The locations of these standards coincide with the peaks labeled on Fig. 3.

The isoprenoids were isolated from the branched-cyclic fraction by preparative gas-liquid chromatography on an Aerograph Model A-90-P. The branched-cyclic fraction was chromatographed on a temperature-programmed 25 ft × 0.01 in. 3% SE-30 column. Fractions were collected and rechromatographed isothermally on a 25 ft × 1/8 in. HI-EFF-4B (butane-1, 4-diolsuccinate) column.

The final fractions collected from the polyester butandiol column were used for gas chromatograph–mass spectrometric analysis. A 100 ft. × 0.01 in. Apiezon L capillary column was used in the last step.

All mass spectra were taken by using a combination of an Aerograph 204 gas chromatograph and an A.E.I. MS-12 mass spectrometer. The gas chromatographic oven temperature was programmed from 90° to 300°C at 2°C/min with a helium flow rate of 2.5 ml/min. The effluent from the capillary column was split into two parts, 1.5 ml/min going to the flame ionization detector and 1 ml/min going through a 1 ft × 0.002 in. heated stainless steel tube at 220°C directly into the ion source of the mass spectrometer. The spectra were determined at an ionizing voltage of 70 eV and an ionizing current of 50 μA. The temperature of the ion source was 200°C. Each spectrum was scanned in 3 seconds. The spectra were recorded on an oscillograph recorder.

Results

The n-alkanes representing 2.75 ± 0.2% of the Bell Creek Crude Oil range from C_{10} to C_{33} (Fig. 2). Identifications were made by mass spectral analyses and by coinjections with standard samples on three different gas chromatographic capillary columns: Apiezon L, Polysev, and SF-96. There was no significant predominance of odd- over even-carbon-numbered n-paraffins. A similar observation was described by Bray.[9] The most prevalent n-alkane was n-C_{17}. This result coincided with our earlier reports[10, 11] that photosynthetic microorganisms, such as blue-green algae, green algae, and photosynthetic bacteria, contained more n-heptadecane than any other compound in the total hydrocarbon fraction.

Samples of C_{14} to C_{25} isoprenoid hydrocarbons were isolated from the branched-cyclic fraction (Fig. 3) and identified by their mass spectrometric fragmentation patterns. Figures 4 through 6 give the mass spectra of C_{14} to C_{25} isoprenoid alkanes isolated from this crude oil. For the C_{22}–C_{25} isoprenoids we suggest the structures I--2, 6, 10, 14-tetramethyloctadecane; II--2, 6, 10, 14-tetramethylnonadecane; III--2, 6, 10, 14, 18-pentamethylnonadecane; and IV--2, 6, 10, 14, 18-pentamethyleicosane, based on their mass spectra. All these compounds have regular head-to-tail condensations, having three methylene groups between two methyl branch sites. See Fig. 7.

The C_{22} isoprenoid, I, exhibits six major fragments: C_8, C_{11}, C_{13}, C_{16}, C_{18}, and C_{21}, corresponding to fragment ions at m/e 113, 155, 183, 225, 253, and 295. Structures II, III, and IV indicate the major fragment ions in Fig. 6. In Fig. 6, the spectrum for the C_{23} isoprenoid, a doublet at m/e 98 and 99 is observed; this phenomenon is described in our previous report.[12] When a fragment has a long straight chain the even peak, C_nH_{2n}, is intensified. This phenomenon is also seen in Fig. 5, the fragmentation pattern of the C_{18} isoprenoid. The C_{23} isoprenoid (Fig. 6) does show the doublet at m/e 98 and 99, indicating the presence of a long straight chain. Thus, Fig. 6, the C_{23} isoprenoid, could not

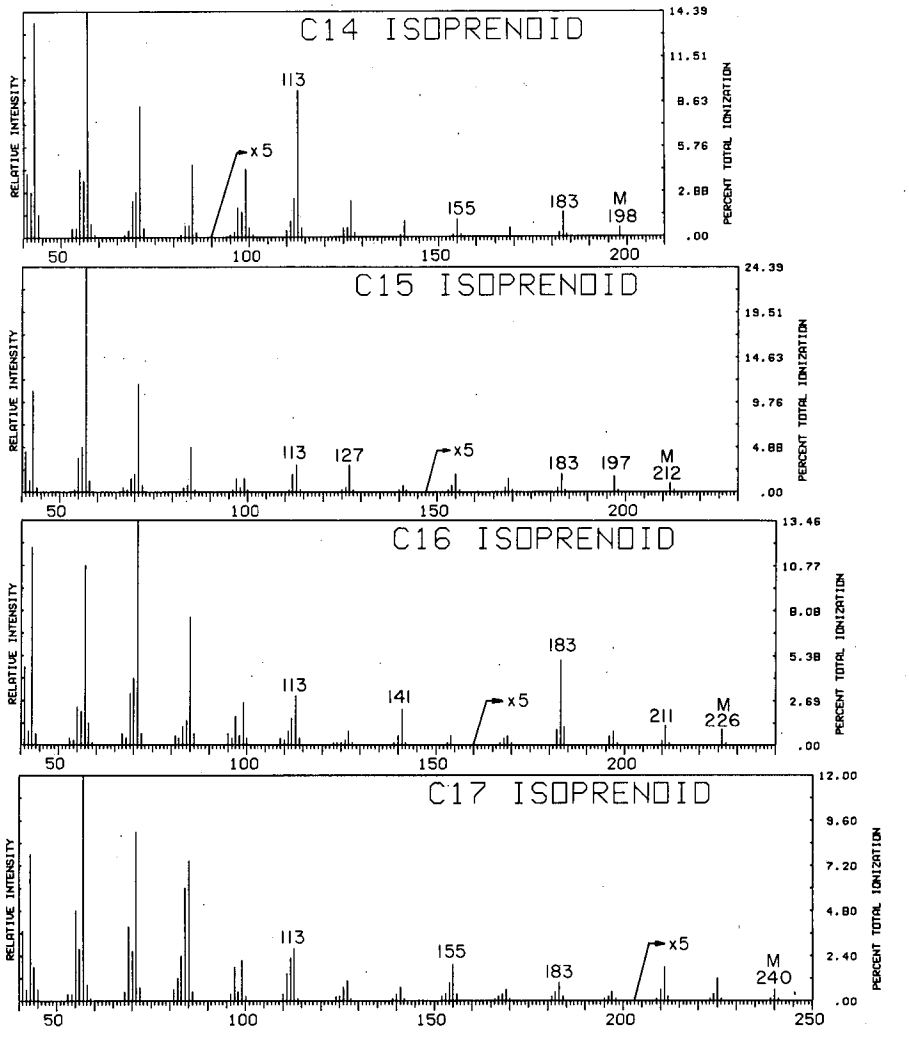

Fig. 4. Mass spectra of C_{14} to C_{17} isoprenoid hydrocarbons. They were taken as the components were eluted from a 100 ft × 0.01 in. i. d. Apiezon L capillary gas chromatographic column. The compounds were ionized by electron impact at 70 eV; ion source temperature 200°C; ionizing current 50 μA. Each peak was scanned within the range of 10-600 mass units in 3 sec on an A. E. I. MS-12 mass spectrometer.

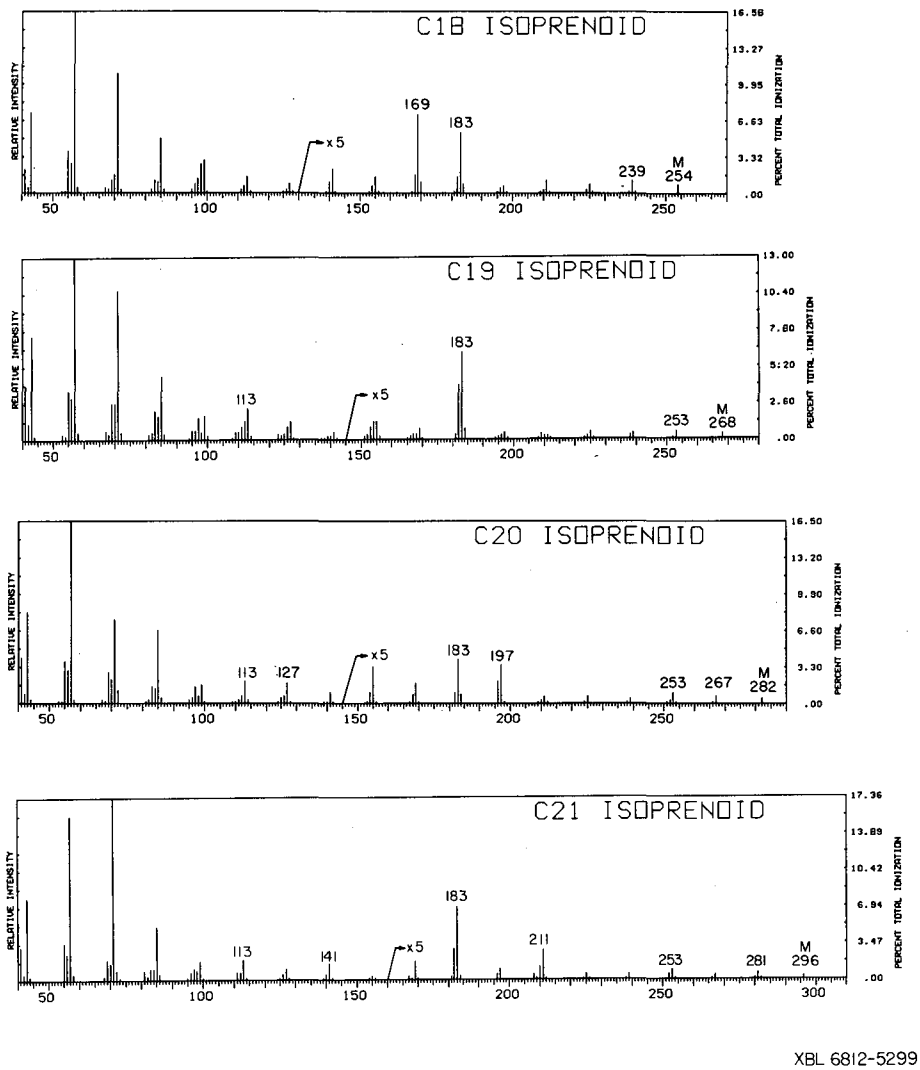

Fig. 5. Mass spectra of C_{18} to C_{21} isoprenoid hydrocarbons. All conditions are the same as for Fig. 4.

have the irregular structure, 2, 6, 10, 14, 17-pentamethyloctadecane, because it cannot produce a doublet at m/e 98 and 99. A double peak appears neither in the C_{24} nor the C_{25} isoprenoid of Fig. 6, which eliminates the irregular structures 2, 6, 10, 14-tetramethlyeicosane and 2, 6, 10, 14-tetramethylheneicosane. The C_{19} and C_{20} isoprenoids, pristane and phytane, do not show doublets at m/e 112 and 113 or m/e 126 and 127.

In Fig. 6, besides major fragments C_7, C_8, C_{12}, C_{13}, C_{17}, C_{18}, and C_{22} for the C_{23} isoprenoid, significant fragments are also observed at C_{15} and C_{20}, which requires the charge to remain on the primary carbon atom. The same effect is seen in the C_{24} isoprenoids,

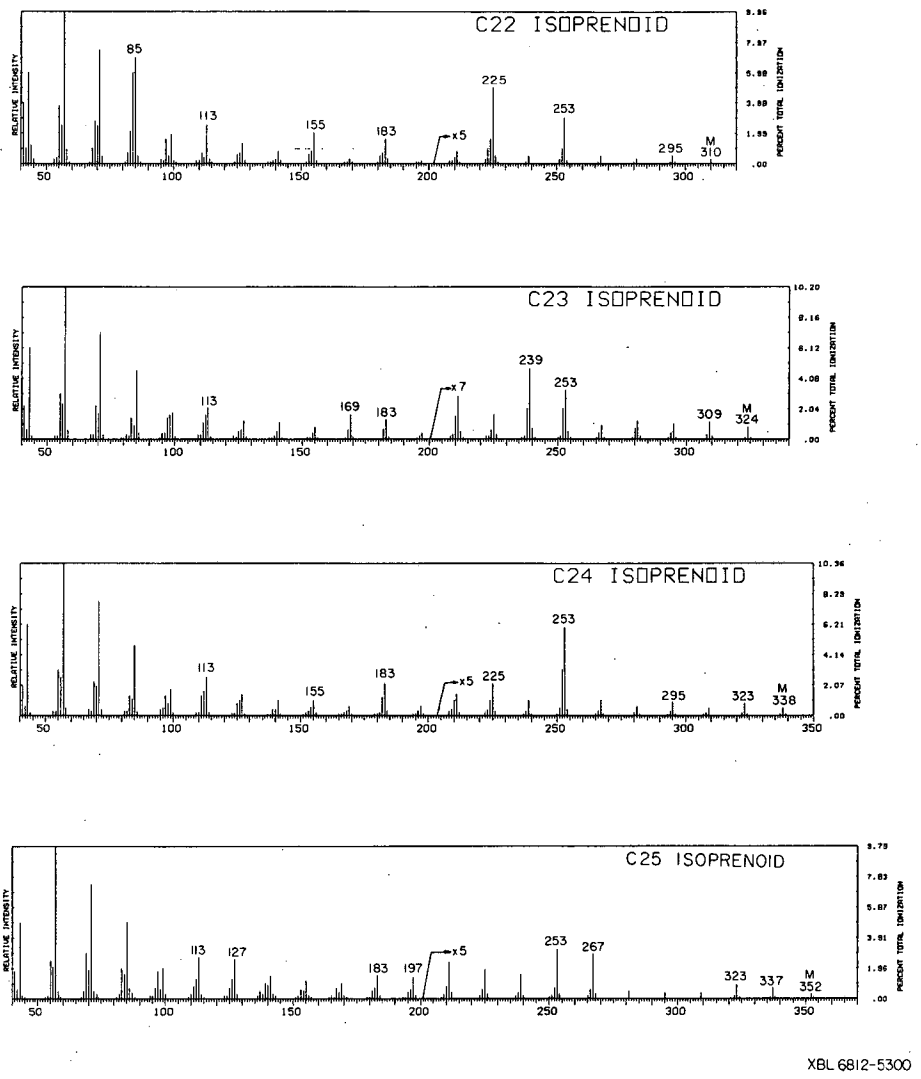

Fig. 6. Mass spectra of C_{22} to C_{25} isoprenoid hydrocarbons. All conditions are the same as for Fig. 4.

which have major C_{16} and C_{21} fragments. This phenomenon is observed in high-molecular-weight hydrocarbons. After bond cleavage adjacent to a methyl branch the charge normally stays on the secondary carbon. If the primary fragment is sufficiently large, the charge can sometimes remain on the primary carbon fragment.

An estimate has been made of the abundance of isoprenoid hydrocarbons, based on gas chromatographic data. This is shown in Table I by percentage by weight of the Bell Creek Crude Oil.

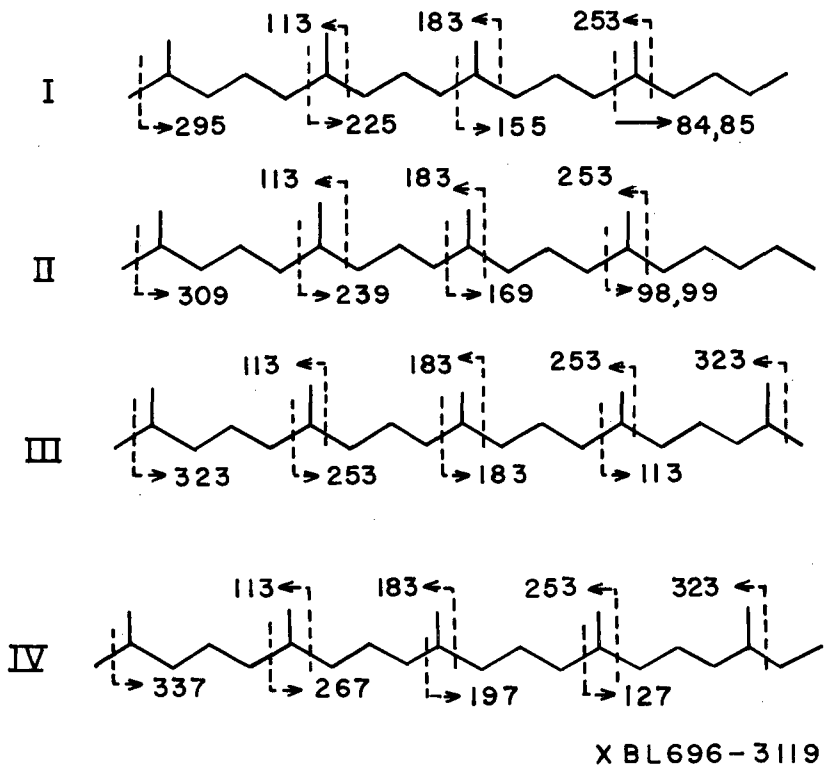

Fig. 7. C_{22} through C_{25} isoprenoids. Molecular weights: I (C_{22}), 310; II (C_{23}), 324; III (C_{24}), 338; IV (C_{25}), 352.

Table I. Isoprenoid content (in percent by weight) of the Bell Creek Crude Oil.

	Content		Content
C_{14}	0.11 ± 0.02	C_{20}	0.46 ± 0.04
C_{15}	0.20 ± 0.02	C_{21}	0.09 ± 0.01
C_{16}	0.30 ± 0.03	C_{22}	0.04 ± 0.01
C_{17}	0.05 ± 0.02	C_{23}	0.06 ± 0.01
C_{18}	0.32 ± 0.03	C_{24}	0.03 ± 0.01
C_{19}	0.68 ± 0.05	C_{25}	0.05 ± 0.01

Identified isoprenoid alkanes constitute approximately 2.4% of the crude oil.

Discussion

The biological precursors of the C_{19} and C_{20} isoprenoids, pristane and phytane, have been the subject of much interest. These two compounds are considered to be derived from the phytyl side chain of the chlorophyll molecule, a precursor orginally proposed by Bendoraitis et al.[1] In the Bell Creek Crude Oil, norpristane, pristane, and phytane together account for more than 60% of the total isoprenoids. Bendoraitis et al.[2] suggested that the sesquiterpenoid 2, 6, 10-trimethyldodecane (farnesane) and its degradation product, 2, 6, 10-trimethylundecane, also resulted from degradation of phytol in the source bed. However, another possibility should be considered. Since farnesol is the side chain of chlorophyll in some photosynthetic bacteria, for example Chlorobium,[13] it could be the precursor of farnesane. By a sequence of abiological diagenetic processes such as dehydration and reduction, it is possible to envisage the conversion of farnesol to farnesane. Again, oxidation, decarboxylation, and reduction could lead to the C_{14} isoprenoid.

The hypothetical reduction and oxidative cleavage products of polyenes, such as squalene and lycopene, have been considered by McCarthy et al.[14] and Bendoraitis et al.[2] Figure 8 illustrates how C_{19} to C_{25} hydrocarbons might be derived from squalene by one bond cleavage. The isoprenoids found in crude oil and sediments are all "regular" isoprenoids containing only head-to-tail linkages. For example, only the regular C_{25} isoprenoid, 2, 6, 10, 14, 18-pentamethyleicosane, has been found. The degradation products from squalene which contain four or five isoprenoids would be "irregular" isoprenoid alkanes. An "irregular isoprenoid" contains at least one head-to-tail or tail-to-tail linkage. In other words, a regular isoprenoid has three methylene groups between two methyl branch sites, but the irregular isoprenoid contains at least one unit which has either two methylene groups or four methylene groups between two methyl branch sites. The irregular C_{25} isoprenoid from squalene, 2, 6, 10, 15, 19-pentamethyleicosane, it is not present in any significant amount. Absence of the C_{19} isoprenoid, 2, 6, 10-trimethylhexadecane; the C_{20} isoprenoid, 2, 6, 10, 15-tetramethylhexadecane; the C_{21} isoprenoid, 2, 6, 10, 15-tetramethlyheptadecane; the C_{23} isoprenoid, 2, 6, 10, 15-tetramethylnonadecane; and the C_{24} isoprenoid, 2, 6, 10, 15-tetramethyleicosane; as well as the absence of the C_{25} isoprenoid, 2, 6, 10, 15, 19-pentamethyleicosane, indicates that squalene is not an important precursor of these isoprenoid hydrocarbons.

McCarthy et al.[14] suggested that lycopene (Fig. 9) could be the precursor of the C_{21} isoprenoid. If lycopene is an important precursor of lower-molecular-weight isoprenoid hydrocarbons, we would also expect it to be an

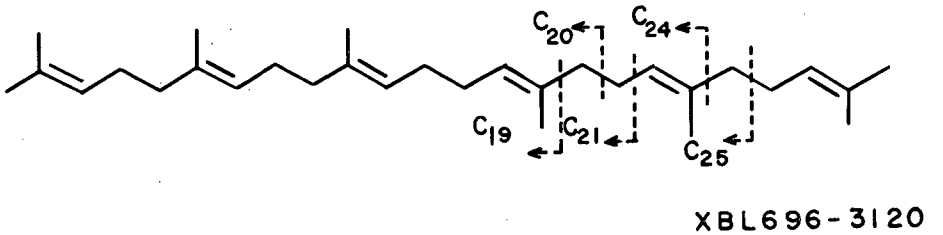

Fig. 8. Diagenetic pathway to "irregular" isoprenoid alkanes with squalene as precursor.

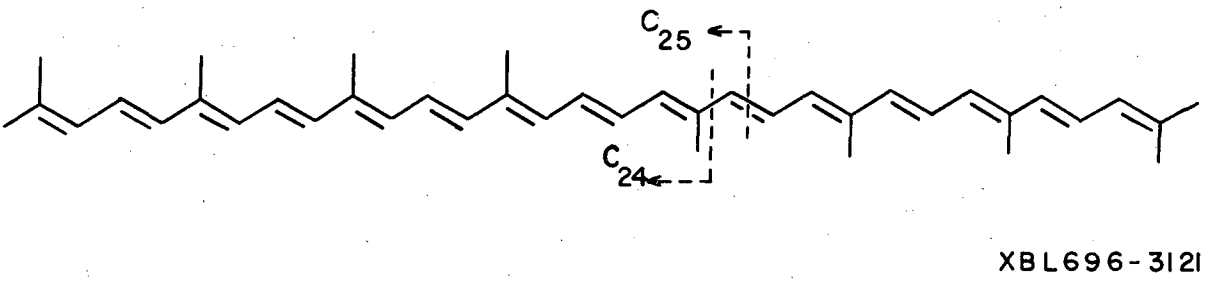

Fig. 9. Diagenetic pathway to "irregular" isoprenoid alkanes with lycopene as precursor.

important precursor of the C_{24} and C_{25} isoprenoid alkanes. Figure 9 shows how C_{24} and C_{25} isoprenoids can be derived from lycopene by one bond cleavage. Thus we would expect to obtain the irregular C_{24} isoprenoid, 2, 6, 10, 14-tetramethyleicosane, and the irregular C_{25} isoprenoid, 2, 6, 10, 14, 19-pentamethyleicosane, if lycopene were the precursor. However, the C_{24} and C_{25} isoprenoids identified in the Bell Creek Crude Oil have the regular isoprenoid structures, i.e., 2, 6, 10, 14, 18-pentamethylnonadecane and 2, 6, 10, 14, 18-pentamethyleicosane. No significant amounts of irregular C_{24} and C_{25} isoprenoid hydrocarbons were observed. Thus, it appears that the common, naturally occurring isoprenoid hydrocarbons, squalene and lycopene, did not play an important role in the diagenetic pathway to isoprenoid alkanes isolated from this crude oil. Many other precursors (such as regular isoprenyl alcohols) are, however, available in living organisms. Regular head-tail-head-tail oligoterpenyl alcohols are rather common in nature.

Solanesol was isolated by Rowland et al.[15, 16] from tobacco leaves, where it was found partly as fatty acid esters. The structure of solanesol,

$$H\text{—}(CH_2\text{-}\overset{CH_3}{\overset{|}{C}}\text{=}CH\text{-}CH_2)_n\text{-}OH,$$

where n = 9 is solanesol, n = 11 is bactoprenol n = 6 to 9 are betulaprenols, n = 20 is dolichol, was confirmed by Fukawa et al.[17] Burgos and his co-workers[18] have discovered dolichol in pig liver, and Lindgren[19] has isolated a series of C_{30}-C_{45} terpenols, betulaprenols, from birch wood. Thorne and his co-workers[20] gave the name bactoprenol to the most abundant lipid formed by three species of Lactobacillus from mevalonic acid. The structure of this compound was confirmed as a C_{55} regular isoprenyl alcohol. A C_{110} isoprenoid substance has been identified as a metabolic product of Aspergillum fumigatus by Burgos et al.[21], while Hemming and his co-workers[22] detected a C_{50} isoprenoid alcohol in the spadix of Arum maculatum.

All isoprenoid alcohols have regular head-tail structures from end to end. These alcohols may be converted into high-molecular-weight isoprenoid alkanes by geochemical processes, just as the low-molecular-weight compounds might be generated from a four-isoprenyl-unit alcohol, phytol. It is suggested that the initial degradation process has to take place by attack at the alcohol end of farnesol, phytol, betulaprenols, solanesol, etc. This could then be followed by reducing and thermal cracking mechanisms to give the C_{14} to C_{25} isoprenoid hydrocarbons found in the Bell Creek Crude Oil.

Summary

The aliphatic hydrocarbon content of the crude oil from the Bell Creek Oil Field of Powder River County, Montana, has been studied. Mass spectrometric fragmentation patterns indicate the presence of all twelve isoprenoid hydrocarbons ranging from C_{14} to C_{25} as well as head-to-tail conformations. Precursors of the compounds are discussed.

Acknowledgments

We thank Dr. C. J. Thompson for supplies of Bell Creek Crude Oil and Howard Ono for valuable discussion. The work described was supported in part by the National Aeronautics and Space Administration and in part by the U. S. Atomic Energy Commission.

References

1. J. G. Bendoraitis, G. L. Brown, and L. S. Hepner, Isoprenoid hydrocarbons in petroleum, Analyt. Chem. 34, 49-53 (1962).
2. J. G. Bendoraitis, B. L. Brown, and

L. S. Hepner, Isolation and identification of isoprenoids in petroleum, World Petroleum Congress, Frankfort-am-Main, Germany, June 19-26, 1963.

3. R. B. Johns, T. Belsky, E. D. McCarthy, A. L. Burlingame, P. Haug, H. K. Schnoes, W. Richter, and M. Calvin, The organic geochemistry of ancient sediments. Part II, Geochim. Cosmochim. Acta 30, 1191-1222 (1966).
4. E. D. McCarthy and M. Calvin, The isolation and identification of the C_{17} isoprenoid 2, 6, 10-trimethyltetradecane from a Devonian Shale: The role of squalene as a possible precursor, Tetrahedron 23, 2609-2619 (1967).
5. W. E. Robinson, J. J. Cummins, and G. U. Dineen, Changes in Green River oil-shale paraffins with depth, Geochim. Cosmochim. Acta 29, 249-258 (1965).
6. J. J. Cummins and W. E. Robinson, Normal and isoprenoid hydrocarbons isolated from oil-shale bitumen, J. Chem. Eng. Data 9, 304-307 (1964).
7. G. Eglinton and M. Calvin, Chemical fossils, Sci. Am. 216, 32-43 (1967).
8. J. G. O'Connor, S. H. Burrow, and N. S. Norris, Determination of Normal Paraffins in C_{20} to C_{32} Paraffin Waxes by Molecular Sieve Adsorption, Anal. Chem. 34, 82-85 (1962).
9. E. E. Bray and E. D. Evans, Distribution of n-paraffins as a clue to recognition of source beds, Geochim. et Cosmochim. Acta 22, 2-15 (1961).
10. J. Han, E. D. McCarthy, W. Van Hoeven, M. Calvin, and W. H. Bradley, Organic geochemical studies. II: A preliminary report on the distribution of aliphatic hydrocarbons in algae, in bacteria, and in a Recent lake sediment, Proc. Natl. Acad. Sci. U.S. 59, 29-33 (1968).
11. J. Han, E. D. McCarthy, M. Calvin, and M. H. Benn, The hydrocarbon constituents of the blue-gree algae, Nostoc muscorum, Anacystis nidulans, Phormidium loridum, and Chlorogloea fritschii, J. Chem. Soc. (C) 2785-2791 (1968).
12. E. D. McCarthy, J. Han, and M. Calvin, Hydrogen atom transfer in mass spectrometric fragmentation patterns of saturated aliphatic hydrocarbons, Anal. Chem. 40, 1475-1480 (1968).
13. H. Rapoport and H. P. Hamlow, Chlorobium chlorophyll-660. The esterifying alcohol, Biochem. Biophys. Res. Comm. 6, 134-137 (1961).
14. E. D. McCarthy, W. Van Hoeven, and M. Calvin, The synthesis of standards in the characterization of a C_{21} isoprenoid alkane isolated from Precambrian sediments, Tetrahedron Letters, 4437-4442 (1967).
15. R. L. Rowland, P. H. Latimer, and J. A. Giles, Flue-cured tobacco. I. Isolation of solanesol, an unsaturated alcohol, J. Am. Chem. Soc. 78, 4680-4683 (1956).
16. R. L. Rowland and J. A. Giles, Flue-cured tobacco. V. Polyisoprenoid compounds, Tobacco Sci. 4, 29-32 (1960).
17. H. Fukawa, M. Toyodo, T. Shimizu, and M. Murohashi, Isolation of new isoprenyl alcohols from silkworm feces, Tetrahedron Letters 49, 6209-6213 (1966).
18. J. Burgos, F. W. Hemming, J. F. Pennock, and R. A. Morton, Dolichol: A naturally occurring C_{100} isoprenoid alcohol, Biochem. J. 88, 470-482 (1963).
19. B. O. Lindgren, Homologous aliphatic C_{30}-C_{45} terpenols in birch wood, Acta Chem. Scand. 19, 1317-1326 (1965).
20. K. Thorne and E. Kodicek, The structure of Bactoprenol, a lipid formed by Lactobacilli from mevalonic acid, Biochem. J. 99, 123-127 (1966).
21. J. Burgos, P. H. W. Butterworth, F. W. Hemming, and R. A. Morton, The biosynthesis of long-chain polyisoprenoid alcohol by Aspergillus fumigatus, Fresenius,

Biochem. J. 91, 22 (1964).

22. F. W. Hemming, R. A. Morton, and J. F. Pennock, Constituents of the unsaponifiable lipid fraction from the spadix of Arum maculatum, Proc. Roy Soc. (London) B158, 219-310 (1963).

CONDENSATION REACTIONS OF AMINO ACIDS AND NUCLEOTIDES IN THE PRESENCE OF VARIOUS SYNTHETIC POLYPEPTIDES AND POLYNUCLEOTIDES

Loring Bjornson

One of the major problems in chemical evolution is how the amino acid and nucleotide polymer systems were brought together to give the present living systems in which the DNA, in conjunction with the RNA's, determines what proteins are synthesized. It has been shown that these types of polymers can be formed from the monomers under various abiogenic conditions.[1] The next question is what sort of interactions could take place between these polymers and their monomers that might lead eventually to a living system.

One of the most obvious interactions between the amino acid and nucleotide systems is the electrostatic attractions between the basic amino acids, e.g., lysine and arginine, and the acidic nucleotides. This type of interaction is well known, and examples such as the binding of histones to DNA,[2] or the binding of polylysine to various polynucleotides,[3] have been studied in detail. This type of complex is thought to be primarily due to ionic interactions. However, the fact that polylysine binds preferentially to polynucleotides and high adenine and thymine[3] content indicates that other interactions must exist also.

Thus, it was thought that perhaps polylysine would interact with adenosine-5'-monophosphate (AMP-5') in such a way that when a condensing agent was added adenylate oligomers would be formed. If such an interaction were strong enough, the polylysine could act as a catalyst for the condensation of nucleotides. Another possibility would be that polynucleotides, e.g., polyadenylic acid, could catalyze the formation of lysyl peptides by the same mechanism.

The experiments designed to test this hypothesis were simply the reactions of the monomers and condensing agent with and without the polymer present. The first reaction studied was that of AMP-5' and a water-soluble condensing agent, 1-ethyl-3-(3-dimethyl-aminopropyl) carbodiimide hydrochloride (EPCI·HCl), in the presence and absence of a basic polypeptide. The reaction of AMP-5' and EPCI·HCl has been studied previously in this and in another laboratory,[4] and the major product is $A^{5'}$ppA. The polypeptide used was a copolymer of L-lysine and L-phenylalanine in a 1 to 1 ratio. The ϵ-amino group of lysine was first quaternized to prevent reaction with AMP-5' by dissolving the copolymer in water, adding excess CH_3I and 1 N NaOH. A standard solution of ^{14}C-labeled AMP-5' (0.025 M), pH 7, was made up and 50-μl aliquots were added to a test tube containing various amounts of poly-L-Phe-L-Lys-ϵ-N$(CH_3)_3$I. The ratio of AMP-5' to Lys in these samples was 10, 2, and 1. A fivefold molar excess of EPCI·HCl

was added to these samples, including one with no polymer present, and the reaction mixtures were allowed to stand overnight at 0 to 5°. Five-μl aliquots were spotted on Whatman #1 paper and subjected to two-dimensional chromatography. The chromatography conditions and the final autoradiogram were the same as reported previously.[4] However, the results were just the opposite of what was expected. Instead of enhanced yields of product, the yields decreased with increasing amounts of polymer. Thus, although the yield of the AMP:EPCI·HCl adduct remained about constant at 4%, the yield of $A^{5'}$ppA decreased from 29.8% with no polymer present to 18.3% with the maximum amount of polymer present. Another effect of added polymer was to cause the $A^{5'}$ppA to "tail" on the chromatogram. It is possible that, whereas the polymer stayed at the origin with some movement in the acidic solvent, some $A^{5'}$ppA was bound to the polymer and held back. It is not clear at present why the yield of $A^{5'}$ppA decreases when the polypeptide is added, but one possibility would be that the polymer causes an increase in the hydrolysis of EPCI·HCl. Another possibility is that the ionic attraction between AMP-5' and the polymer could be completely disrupted by the addition of a large excess of the charged species, EPCI·HCl.

In another experiment in which L-Lys was reacted with EPCI·HCl in the presence and absence of polyadenylic acid, the preliminary results indicate that again there was no catalytic effect with the polymer.

Thus, the experiments performed so far have not substantiated the initial prediction that there could be binding between the oppositely charged polymer and monomer which would be sufficient for a catalytic effect. However, it is felt that the addition of an excess of charged condensing agent may be destroying any binding before a reaction can occur; therefore the experiments will be repeated, using an uncharged condensing agent. Work is now in progress on the synthesis of one such agent, 1,3-bis-(2-methoxy ethyl) carbodiimide.

References

1. S. W. Fox, ed., The Origins of Prebiological Systems (Academic Press, New York and London, 1965).
2. A. V. S. de Reuck and J. Knight, ed., Histones (Ciba Foundation Study Group No. 24, Little, Brown & Co., Boston, 1966).
3. M. Leng and G. Felsenfeld, Proc. Natl. Acad. Sci. U. S. 56, 1325 (1966).
4. J. Sulston, R. Lohrmann, L. E. Orgel, and H. Todd Miles, Proc. Natl. Acad. Sci. U. S. 59, 726 (1968).

SPECIFICITY IN REACTIONS OF AMINO ACIDS AND NUCLEOTIDES. I. DISCUSSION OF THE VARIOUS APPROACHES TO THE PROBLEM

Frederick A. Johnson

In 1958 Hecht and co-workers[1, 2] discovered that transfer ribonucleic acids (t-RNA's) required the 3'-terminal base triplet cytidylyl-cyticylyl-adenosine (or....pCpCpA) in order to be charged enzymically with amino acids. Lipmann,[3] Berg,[4, 5] and others simultaneously discovered that the amino acids were attached to t-RNA through an ester linkage to the 2'- or 3'-hydroxyl group on the ribose portion of the terminal adenosine residue. Ever since the discovery that the pCpCpA end group was necessary to t-RNA activity, chemical evolutionists have been wondering how this triplet evolved from primitive conditions to hold its present role in living systems.

The reasons for the evolution of pCpCpA probably lie somewhere between the two extremes of (a) pure chance and (b) strong chemical preference of amino acids to couple with this base triplet. Of course, the reason that pCpCpA is found at the terminus of all t-RNA's in living systems today is almost certainly due to enzymic "recognition" of this end group by the various aminoacyl-tRNA synthetase enzymes. However, it is still pertinent to ask how this particular base triplet was placed in the role it now has. Presumably there may have been a time when primitive cells had no enzymes capable of recognizing pCpCpA, and this enzyme was evolved after pCpCpA had proven itself to be chemically superior to other base triplets. Or else the first enzyme capable of coupling amino acids to nucleic acids fitted pCpCpA entirely by chance. There are a host of possibilities. It is reasonable to suspect that pCpCpA has some chemical property which, when the adenosine is charged with an amino acid, offers a substantial advantage for peptide synthesis.

One approach to this question has been to study the stability of the aminoacyl-nucleotide ester bond under cleavage conditions. Wieland was the first to offer data of this nature.[6] He reacted leucyl-2'(3')-adenosine-5'-phosphate (Leu-AMP), leucyl-uridine-5'-phosphate (Leu-UMP), and leucyl-guanosine-5'-phosphate (Leu-GMP) with hydroxylamine and recorded the half-lives of the cleavage of the ester bonds. His results (shown in Table I) indicated very little effect of the particular nucleotide base (A, G, or U) upon the reactivity of the active ester bond.

Table I. Wieland: Half-times of hydroxylamination of various leucyl-nucleotides.

Ester	$t_{1/2}$ (min)
Leucyl-2'(3')-AMP	4
Leucyl-2'(3')-UMP	5
Leucyl-2'(3')-GMP	7
Leucyl methyl ester	105

Although Wieland found no specificity for the chemical stabilities of aminoacyl-mono-nucleotides in hydroxylamine, Chladek and Zemlicka[7] in Czechoslovakia found that ethyl-

2', 3-cycloortho esters of glycyl derivatives of three dinucleoside monophosphates showed a wide range of resistance to hydrolysis in acetic acid with respect to the various nucleoside bases used. The reaction is shown below (CBZ = the carbobenzyloxy group, $C_6H_5CH_2OC(=O)$—):

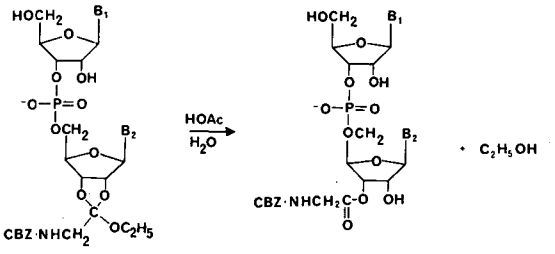

Formula #1

In Table II the results show that the ortho ester of CpA is the most resistant to acid hydrolysis, while UpU and UpA derivatives hydrolyze much faster.

Table II. Chladek and Zemlicka: Acid hydrolysis of ethyl N-carbobenzyloxyglycyl-2', 3'-cyclo ortho esters of dinucleotide monophosphates at room temperature.

B_1pB_2	Hydrolysis conditions	$t_{1/2}$ (min)
UpU	20% aqueous HOAC[a]	20
UpA	80% aqueous HOAC	120
CpA	80% aqueous HOAC	340

[a] The authors did not give the $t_{1/2}$ of hydrolysis of the UpU in 80% HOAC.

The major drawback to the significance of these results is that the rates of acid hydrolysis of 2', 3'-cyclic ortho esters is only tangentially related to the rates of coupling between amino acids and free 2', 3'-dihydroxy nucleotides. However, from the chemical evolutionist's point of view it is encouraging that the nucleoside bases have some role in the chemistry at the 2', 3'-terminal positions.

Studies pertaining to the facility of the coupling reaction itself have been carried out by Harpold in this Laboratory, and by Kraevsky[8] in Moscow. Harpold attached the nucleotides to an insoluble polystyrene support by a phosphate "benzyl" ester bond:

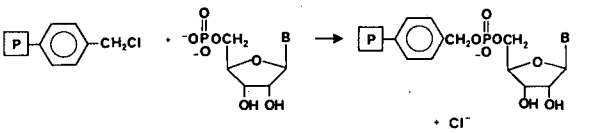

Formula #2

He then coupled N-carbobenzyloxyamino acids to the free 2', 3'-dihyoxyls by reacting the polymer-bound nucleotide with the N-protected amino acid anhydrides. By cleaving the aminoacyl-nucleotide from the solid support, he determined the percent yields of the coupling reactions:

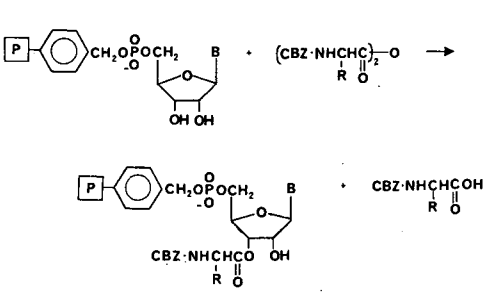

Formula #3

The results are shown in Table III.

Kraevsky performed the coupling of tert-butoxycarbonylalanine (t-BOC-Ala-OH) to four nucleoside phosphates in aqueous DMF, using N, N'-carbonyl diimidazole as the coupling agent:

Table III. Harpold: Yields of Aminoacyl Nucleotides recovered from the coupling of amino acid anhydrides to polymer-bound nucleotides.

Nucleotide	Amino acid	Amount of bound nucleotide reacted (%)
AMP	Glycine	10.0
AMP	Phenylalanine	7.0
CMP	Glycine	6.5
CMP	Phenylalanine	2.9

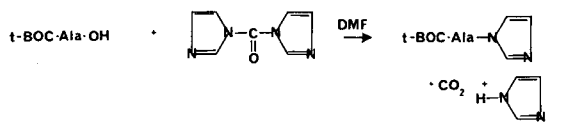

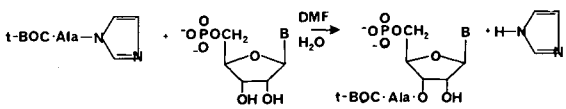

Formula #4

The data reported are percentages of coupled product formed after 3.5 hr of reaction, and these percent yields vary according to the molar ratio of amino acid to nucleotide used. See Table IV.

The two purine nucleotides couple in greater yield than does cytidine-5'-phosphate, a pyrimidine nucleotide, indicating a possible preference of the amino acid for purine nucleotides.

In the later two experiments it was never determined whether the differences in product yields corresponded to real differences in coupling reactivities (i.e., real rate differences), to differences in the stabilities of the products (e.g., to subsequent hydrolysis), or to differences in unknown factors of the

Table IV. Kraevsky: Yield of coupling of t-BOC-alanine to nucleotide-5'-phosphates.

Ratio of Amino acid to nucleotide	Nucleotide	Yield (%)
4:1	AMP	22.3
10:1	AMP	41.5
4:1	GMP	27.4
10:1	GMP	57.6
4:1	CMP	10.5
10:1	CMP	10.9
4:1	TMP[a]	45.6 [a]
10:1	TMP[a]	87.9 [a]

[a]Since the thymidine ribose has no 2'-hydroxyl group, the resulting ester has a much greater stability with respect to hydrolysis. This fact alone is enough to explain the high yields of the TMP ester as opposed to other 2', 3'-dihydroxy nucleotides.

experiment, such as diffusion and dispersion of the two nucleotides through their respective solid supports in Harpold's experiments.

Thus, there is a dearth of meaningful information concerning the reactivities of, and specificities between, the various nucleotides with respect to their coupling with amino acids.

It is the purpose of my work to determine this information by finding actual reaction rates, first between the various ribonucleotides and amino acids, and then between nucleotide dimers and trimers and the amino acids. Any such determination requires three essential conditions: (i) suitably modified substrates, (ii) a coupling agent sufficient to couple a carboxylic acid to a secondary alcohol, and (iii) a nearly quantitative method of following the course of the coupling reaction kinetically.

The problem of substrates applies to both the nucleotide and the amino acid under consideration. The α-amino group of the amino acid requires a covering group in order to prevent self-condensation in the presence of a

coupling agent, which would make peptide bonds instead of ester bonds. There are drawbacks to using the common N-protecting groups, such as carbobenzyloxy and t-butoxycarbonyl groups: (a) a large additional side chain might cover up any subtle variation in the interactions of the amino acid with nucleotides, and (b) hydrocarbon protecting groups render amino acids considerably less soluble in water. Since it is desirable that chemical evolution studies be done in dilute aqueous media, the advantages of using soluble reagents are obvious. Thus it was decided to use the smallest known polar N-protecting group--the formyl group--to protect the amino function. Phenylalanine was chosen as a representative amino acid of average bulk and reactivity. N-Formyl-DL-phenylalanine-3-^{14}C was synthesized in yields up to 69% (see Experimental Procedure).

The nucleotide must also be covered to prevent the formation of a 5'-phosphocarboxylic anhydride rather than a 2', 3'-carboxylic ester. (Wieland[9] found that amino acid thiophenyl esters couple at the 5'-phosphate rather than at the 2', 3'-hydroxyls. Kraevsky et al.[8] did not use 5'-protected phosphates, however, and reported no 5'-acylated products. For this reason the Kraevsky work is being repeated.) For this prevention the methyl ester of adenylic acid (AMP) was prepared as the principal nucleotide derivative for the initial studies (see Experimental Procedure). This phosphate diester should resist further reaction at phosphorus, since any condensation products would create a trialkylated phosphate, which would be highly unstable.

Two coupling agents have so far been considered: (i) carbodiimides, and (ii) carbonyl diimidazole. Carbodiimides can couple carboxylic acids to primary alcohols, but no report of coupling to secondary alcohols (such as the ribose hydroxyl groups) has yet been made. Carbonyl diimidazole was used by Kraevsky to couple t-BOC-alanine directly to the ribose hydroxyl groups. Although the diimidazole reagent hydrolyzes readily in water, Kraevsky's results indicated that the amino acyl imidazolide is stable enough to couple with secondary alcohols, even in aqueous solution. (This very strange result is also being checked at present in a repeat of the Kraevsky experiment.)

Attempts to prepare the methl 2'(3')-(N-formyl-DL-phenylalanyl) adenosine-5'-phosphate have so far been unsuccessful. Part of the problem determining the extent to which coupling takes place has been the lack of an analytical method of detecting this unstable ester. Earlier attempts to follow the disappearance of the vicinal 2', 3'-dihydroxyl groups by oxidizing them with periodate ion failed; repeated experiments gave irreproducible results. Presently under consideration is a thin-layer chromatographic method designed to separate the reagents from the aminoacyl-nucleotide ester.

Further problems were traced to the hydrolysis of the carbonyl diimidazole reagent upon storage, making it unsuitable for experimental use without further purification. It has been found that recrystallizing this reagent from benzene gives crystals whose melting point (115—117°) corresponds more closely to the reported melting point (116—117°) than does the reagent straight from the bottle (m.p. 100—111°).

Because of the rapid rate at which the active esters hydrolyze, it was decided to perform the coupling reaction first in a nonaqueous medium. Experiments are now under way using absolute dimethyl formamide (DMF) as solvent for the coupling reactions. As soon as the coupled product has been identified and characterized and a kinetic assay has been devised, aqueous systems may again be used. So far, however, no aminoacyl-nucleotide esters have been found in the coupling reactions.

Experimental Procedure

N-Formyl-DL-phenylalanine-3-^{14}C (procedure taken from Ref. 10): A 100-ml round-bottom flask was fitted with a 5-in. reflux condenser, two rubber septa through which a thermometer and a 25-ml addition funnel were placed, and a magnetic stirring bar. DL-Phenylalanine-3-^{14}C (1 g, 6 mmoles, 100 μCi was dissolved in 15 ml of 88% formic acid (18.3 g, 350 mmoles). Five ml of acetic anhydride (5.4 g, 53 mmoles) was added dropwise with stirring over 5 min. The temperature rose to 45°, and within 1 hr had dropped back to 25°. Five ml of ice-cold water was stirred in to quench the acetic anhydride. The solvents were removed under vacuum, leaving a white solid residue.

N-Formyl-DL-phenylalanine-3-^{14}C was recrystallized from hot water and was dried *in vacuo* over P_2O_5 for 4 hr at 100°, giving 800 mg (69%) of product, m.p. 169.5 – 170.5° (reported m.p. 169 – 170°). Elemental analysis showed %C calcd: 62.16; found: 61.88. %H calcd: 5.74; found: 5.63. %N calcd: 7.25; found: 7.24.

Ammonium methyl adenosine-5'-phosphate (procedure taken from Ref. 11): The dihydrate of adenosine-5'-phosphate (1.15 g, 3 mmoles) was suspended in 750 ml of absolute methanol in a 1-l round-bottom flask that was previously dried by flaming and protecting with a $CaSO_4$ drying tube. Tri-n-butylamine (2.23 g, 6 mmoles) was added with magnetic stirring; the suspension became transparent. N, N'-Dicyclohexylcarbodiimide (6.16 g, 30 mmoles) was dissolved into the solution and was stirred for 22 days. A 75-microliter aliquot of the reaction solution was spotted on a Whatman #1 paper alongside a 100-μg spot of authentic AMP, and the paper was developed in EtOH-NH_4OH-H_2O (7:1:2). The uv handlamp showed the authentic AMP at R_f = 0.20. The reaction mixture spot gave no spot at R_f = 0.20, but showed a new one at R_f = 0.60.

The methanol was removed under vacuum, leaving a residue which was then slurried with 40 ml of water containing 370 mg (9 mmoles) of NaOH. The slurry was vacuum filtered, and the filtrate was washed with 3 x 10 ml of diethyl ether to remove dicyclohexylcarbodiimide and its urea. The aqueous bottom layer was freeze-dried, leaving a white solid residue.

The residue was dissolved in 9 ml of water and the solution was eluted through a Dowex-50W cation-exchange resin (NH_4^+ form; 1.7 × 37-cm cylindrical column). After 100 ml had eluted, the eluate was freeze-dried, giving a white solid residue. Two crops of product were recrystallized from MeOH-acetone (1:20), washed with acetone and diethyl ether, and dried *in vacuo* over P_2O_5 at 58° for 1 day, giving about 500 mg (45%) of pure product, m.p. 200° with decomposition. Elemental analysis showed %P 8.01. This corresponded to the hemihydrate of ammonium methyl adenosine-5'-phosphate, where %P calc is 8.09. A uv spectrum of the product showed a λ_{max} at 259 mμ. The product was chromatographically pure.

References

1. L. I. Hecht, P. C. Zamecnik, M. L. Stephenson, and J. F. Scott, J. Biol. Chem. 233, 954 (1958).
2. L. I. Hecht, M. L. Stephenson, and P. C. Zamecnik, Proc. Natl. Acad. Sci. U.S. 45, 505 (1959).
3. H. G. Zachau, G. Acs, and F. Lipmann, ibid. 44, 885 (1958).
4. P. Berg and J. Ofengand, ibid. 78 (1958).
5. J. Preiss, P. Berg, E. J. Ofengand, F. H. Bergmann, and M. Dieckmann, ibid. 45, 319 (1959).
6. T. Wieland, H. Merz, and G. Pfleiderer, Chem. Ber. 93, 1816 (1960).

7. S. Chladek and J. Zemlicka, Collection Czech. Chem. Commun. 32, 1776 (1967).
8. A. A. Kraevsky, P. P. Purygin, L. N. Rudzite, Z. S. Belova, and B. P. Gottikh, Izvest. Akad. Nauk SSSR, Ser. Khim. 1968, 378.
9. T. Wieland, F. Jaenicke, H. Merz, and M. Ossorio, Ann. Chem. 613, 95 (1958).
10. J. C. Sheehan and D.-D. H. Yang J. Am. Chem. Soc. 80, 1154 (1958).
11. M. Smith, J. G. Moffatt, and H. G. Khorana, ibid. 6204 (1958).

Biophysical Chemistry and Biophysics

FOURIER TRANSFORM NMR SPECTROSCOPY

J. A. Despotakis, M. P. Klein, T. Mahan, and D. E. Phelps

It is widely recognized that high-resolution NMR offers one of the few methods of learning details of the solution structure of macromolecules and of studying the interactions between molecules and the conformational changes of these molecules. Basically, three types of information are contained in an NMR spectrum: (a) the intensities of the peaks; (b) the positions of the peaks--i.e., the chemical shifts and spin coupling constants; and (c) the time dependencies of these peaks. The first type of information is the most basic, since without adequate signal-to-noise ratio nothing can be learned about the other two. The Fourier transform method affords a very significant improvement in the attainable signal-to-noise ratio because it increases by two to three orders of magnitude the rate at which data are accumulated. Since the data rates are increased, we are enabled to acquire time-dependent spectral information not otherwise accessible. The chemical shift information can be improved only by resort to higher magnetic fields, and for this purpose we have recently acquired a 220-MHz spectrometer.

To exploit fully the inherent advantages of the Fourier transform method we have developed an extremely versatile small computer system with a unique hardware and software complement. Employing this system in its incompleted form, we have been able to demonstrate the feasibility of measuring simultaneously all the spin relaxation times in a high-resolution spectrum, thus rendering accessible information about the correlation times of the various chemically distinct groups in a molecule. We have also demonstrated that the theoretical sensitivity improvement may be realized in practice and applied to the study of proteins. One immediate gain is that very broad lines may be detected simultaneously with the usual narrow lines, thus rendering visible protons coupled to nitrogen, as well as protons shifted by paramagnetic ions within the proteins.

All of the foregoing work has been carried out with our 60-MHz spectrometer. The extension of this method to the 220-MHz spectrometer is an immediate goal, but must be approached cautiously because of the structure of the probe and the solid-state receiver circuitry. When this development is completed it will permit us to obtain spectra from many more compounds than is currently feasible while operating in the conventional mode.

This is of great interest to us because of the large number of proteins and co-factors that are to be studied.

CHEMICAL EFFECTS ON CORE-ELECTRON BINDING ENERGIES IN IODINE AND EUROPIUM*

C. S. Fadley, S. B. M. Hagstrom, M. P. Klein, and D. A. Shirley

A theoretical and experimental study was made of the shift in atomic core-electron binding energies caused by the chemical environment. Two models are presented to account for these "chemical shifts." The first uses an energy cycle to break the core-electron binding energies into a free-ion contribution and a classical Madelung energy contribution. The Madelung energy contributes a significant part of the binding-energy shift. It can, in principle, be evaluated rigorously, although there is some ambiguity as to a surface correction. The reference level for binding energies must also be considered in comparing theory with experiment (or in comparing experimental shifts with one another). Electronic relaxation could also introduce errors of ≈ 1 eV in shift measurements. The second, more approximate, model consists of a "charged-shell" approximation for bonding electrons in atomic complexes. It gives semiquantitative estimates of shifts and demonstrates the relationship between bond polarity and core-electron binding-energy shifts. These models indicate that several features of the free-ion state will be reflected also in chemical shifts. Free-ion Hartree-Fock calculation were made on F, Cl, Br, I, and Eu in several oxidation states. These indicate that the removal of a valence electron shifts the binding energies of all core levels by nearly equal amounts (10–20 eV). This shift decreases with increasing atomic number in a given chemical family. The removal of an inner "valence" electron (e.g., 4f in europium) gives rise to relatively large shifts (≈ 20 eV). These features were also found in the experiment chemical shifts. Chemical shifts were measured for iodine in KI, KIO_3, and KIO_4 and for europium in $EuAl_2$ and Eu_2O_3, by the technique of photoelectron spectroscopy. Binding energies in iodine were found to increase by ≈ 0.8 eV per unit increase in oxidation number. A Madelung energy calculation indicates that this corresponds to a loss of ≈ 0.5 electronic charge from the valence shell per unit increase in oxidation state, and this value agrees approximately with previous results obtained from Mössbauer measurements. A shift of 10 eV was found between Eu^{2+} and Eu^{3+}. This very large shift is due largely to the loss of a full 4f electron in this change of oxidation state. With some refinements, the above technique could produce very useful information about bonding in ionic solids, in particular, allowing the determination of the charge on each atom. Their application to such problems as a determination of the oxidation states of metals in biological molecules seems even more promising.

---

* Abstract from J. Chem. Phys. 48, 3779 (1968).

EMISSION MÖSSBAUER SPECTROSCOPY FOR BIOLOGICALLY IMPORTANT MOLECULES. VITAMIN B_{12}, ITS ANALOGS, AND COBALT PHTHALOCYANINE*

A. Nath, M. Harpold, M. P. Klein,
and W. Kündig

It has been shown that complex molecules with conjugated ring systems, such as vitamin B_{12}, its analogs, and cobalt phthalocyanine, escape fragmentation during the Auger event following electron-capture decay of cobalt-57. Consequently, Mössbauer spectra are characteristic of the entire molecules. This opens up very interesting possibilities for the use of emission Mössbauer spectroscopy for biologically important molecules.

*Abstract from Chem. Phys. Letters 2, 471 (1968).

MÖSSBAUER STUDIES OF AFTEREFFECTS OF AUGER IONIZATION FOLLOWING ELECTRON CAPTURE IN COBALT COMPLEXES

Amar Nath, M. P. Klein, W. Kündig, and D. Lichtenstein

A cobalt-57 nucleus undergoes radioactive decay by capturing an orbital electron--most frequently from the K shell. An electron from the less tightly bound L shell hops in to fill the vacancy, while the excess energy is utilized in ejecting another electron from the L shell of the atom. These two vacancies in the L shell are in turn filled by electrons from the next outer shell or subshell. Thus, the vacancy cascades traverse to the valence shell, resulting in a multiply charged ionic species. Pollak[1] has worked out this Auger cascade scheme for $^{57}Co^{3+}$, and estimates the maximum charge buildup for the daughter ^{57}Fe as +8 (viz., Fe^{8+}). This Auger vacancy cascade is believed[2] to take place in 10^{-15} to 10^{-16} sec. If the cobalt atom is incorporated into a molecule, the multiply charged daughter iron ion is rapidly neutralized by transfer of electrons from neighboring atoms in the molecule. The positive charges are driven to the extremities of the molecule due to electrostatic repulsion. This redistribution of charges in the molecule probably occurs within 10^{-15} sec and hence without any change in the relative positions of the individual constituent nuclei. In the gaseous phase, where the molecules are isolated, there is considerable experimental evidence to suggest that the multicenter Coulombic repulsion virtually explodes the molecule, leading to the formation of several fragments.[2,3] A similar picture of disruption of molecules in liquids, with the additional formation of radicals in the immediate vicinity by the Auger electrons, has been used by Libby,[4] Willard,[5] their co-workers, and others. Little is known about the phenomenon in solids, however.

For molecules incorporating ^{57}Co, the 14.4-keV Mössbauer emission can convey information regarding the chemical forms in which the daughter ^{57}Fe is "stabilized" within 10^{-7} sec following the electron capture. Wertheim et al.[6] studied the chemical consequences of electron capture in Co(III) acetyl-

acetonate, and their interpretation is summarized here. The highly ionized iron ion undergoes electronic relaxation until it acquires the charge of +3, at which stage it is stabilized as $Fe(III)(acac)_3$ in the $Co(III)(acac)_3$ lattice and the sequence is terminated. A charge state of 2+ results if the electronic relaxation permits the transfer of an additional electron to the valence orbitals of the iron atom before the ligands rearrange to accommodate a 3+ charge state. An atom of this charge state may then be stabilized, within a time short compared with 10^{-7} sec, as an impurity atom in the $Co(III)(acac)_3$ matrix, or it may be reoxidized by the near-neighbor environment and then stabilized as an Fe(III) atom in a regular lattice site, which differs only slightly from its Co(III) neighbors.

The aforementioned authors had not considered the possibility of fragmentation of the molecule as a consequence of the Auger event.

In the work reported here, we have carried out a systematic study of the chemical consequences of Auger ionization in several cobalt chelates labeled with ^{57}Co. Fragmentation of the molecule was identified by the presence of degraded high-spin Fe^{2+} and Fe^{3+} species. Parallel experiments using chelates doped with $^{57}Co^{++}$ (or preferably with the citrate complex) were conducted to help identify Fe^{2+} and Fe^{3+} species, as their respective isomer shifts and quadrupole splittings are determined by the environment. Although the presence of ionic high-spin iron species can be regarded as unequivocal evidence of fragmentation, the reverse may not be true; that is, the presence of coordinated Fe(III) or Fe(II) may reflect failure to fragment or may be a consequence of reentry of the degraded iron ion (resulting from fragmentation) into a neighboring cobalt chelate molecule through exchange to form the coordinated species. The possibility of exchange can also be examined with the help of doping experiments.

Experimental Procedure

The labeled cobalt complexes, with the exception of vitamin B_{12}, were either synthesized by conventional methods--for instance, the phthalocyanine and indenyl chelates--or obtained by solid-state isotopic exchange.[7] The exchanges were carried out with complexes doped with ^{57}Co and heated at appropriate temperatures, followed by purification.

The inactive cobalt complexes were generally doped with carrier-free cobalt-57(III) citrate. The latter was prepared by treating carrier-free cobalt-57 chloride with an aqueous solution containing hydrogen peroxide and traces of sodium citrate. A few milligrams of the powdered cobalt complex was moistened with a couple of drops of the cobalt-57(III) citrate solution. The moisture was permitted to evaporate. The powder was then repeatedly moistened with water so that the citrate completely percolated inside the crystallites. In a few cases, doped complexes were prepared through freeze-drying. Either procedure yielded the same Mössbauer spectrum. For water-insoluble complexes, such as $Co(III)(acac)_3$, acetone was used to moisten the powder. For Co(II) phthalocyanine an acetone solution of carrier-free $^{57}CoCl_2$ was used, followed by repeated moistening with chloronaphthalene. Some doped samples, especially the tris-dipyridyl Co(III) perchlorate, were analyzed to check for isotopic exchange during doping.

For producing dispersion of water-soluble complexes, a milligram or so of the labeled complex was dissolved in a viscous solution of polyethylene oxide or agar-agar. The solution was then freeze-dried. The $Co(III)(acac)_3$ dispersion in cellulose acetate was obtained by rapid evaporation of a warm viscous solution by flowing a current of air onto the swirling mass.

The active samples were maintained at liquid nitrogen temperature unless specified otherwise. Sodium ferrocyanide (containing 1 mg of ^{57}Fe per cm^2) was used as the Mössbauer absorber, and all the chemical shifts are referred thereto.

Data and Observations

In the earlier phase of this work, we were doping cobalt complexes with carrier-free $^{57}Co^{++}$. Subsequently it was realized that this procedure does not simulate faithfully the environment of the degraded iron species resulting from Auger fragmentation of the parent molecule, for the following reasons. In a labeled cobalt complex, molecular fragmentation results as a consequence of Coulombic repulsion as discussed earlier, and therefore the iron ion may possess some kinetic energy and may come to rest in a new intermolecular site, which is relatively free of fragments resulting from the original Auger event. On the other hand, in $^{57}Co^{++}$-doped complexes, since $^{57}Co^{++}$ is not attached to any coordinating ligands, the daughter ion is unlikely to acquire any kinetic energy (as a consequence of the Auger event and buildup of charge) to move it away from its original site. Hence, it is likely to reside in a "dirtier" environment, possibly having some fragments in the neighborhood, formed during the Auger event. To overcome this difficulty, we have used carrier-free cobalt-57(III) citrate as a dopant. From an independent experiment, we know that the citrate complex fragments in almost 100% of the Auger events, forming ionic Fe^{2+} and Fe^{3+} (Fig. 1). This fragmentation is likely to give some kinetic energy to the degraded iron species, which will then find itself in a new site in the host matrix. This rationale for using carrier-free cobalt-57(III) citrate instead of $^{57}Co^{++}$ is amply justified by our data on doped acetylacetonate and dipyridyl complex, which is discussed later.

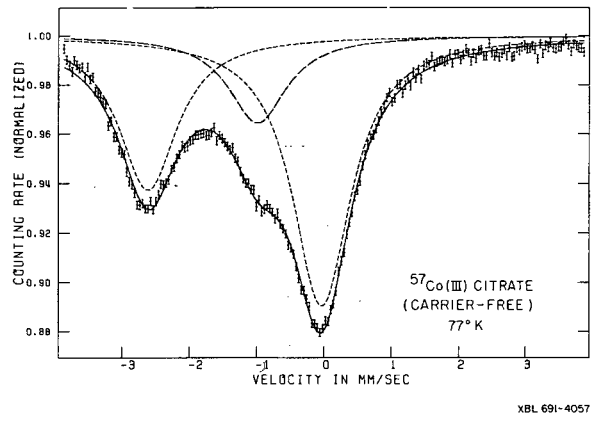

Fig. 1. Emission Mössbauer spectrum of labeled ^{57}Co(III) citrate at 77°K. The two outer peaks are the quadrupolar split doublet of uncoordinated Fe^{2+}. The asymmetry is discussed in the text. The central line corresponds to uncoordinated Fe^{3+}.

Before discussing the spectra of individual complexes, we would like to comment on the manner in which we analyzed our spectra. It is known that the degraded high-spin Fe^{2+} is characterized by a large isomer shift and quadrupolar splitting. In some cases the asymmetry of the peaks is very marked. One of the reasons for this asymmetry appears to be the anisotropy in the amplitude of thermal vibration of an Fe^{++} ion as an interstitial in the bulk. We find that the asymmetry decreases considerably at liquid helium temperature. However, in several cases the spectra of Fe^{3+} ions have a quadrupole component (presumably due to neighboring polar groups or fragments) superimposed on the Fe^{2+} peak near zero velocity, thereby exaggerating the apparent asymmetry. We have not included this Fe^{3+} component in our curve analysis, as it is not likely to affect the main trend of the interpretation of data. Thus we have consistently analyzed the degraded Fe^{3+} as a single peak centered around 1 mm/sec and have ignored its quadrupolar component, if any, in the vicinity of zero velocity.

The spectra of individual complexes are now discussed.

Sodium ethylenediamine tetraacetate-Co(III) [Co(III) EDTA]

Figures 2 and 3 are the spectra of labeled sodium ^{57}Co(III) EDTA and the doped chelate, respectively. One can see the quadrupolar splittings of Fe^{2+} and the single peak of Fe^{3+}. Peaks corresponding to sodium Fe(III) EDTA (Refs. 8, 9) are expected to occur at about -1 and 0 mm/sec, the former being more prominent. It is apparent from the figures that if there is any sodium Fe(III) EDTA, it must be present in relatively small amounts. Thus we can conclude that the EDTA chelate molecule ruptures in a great majority of Auger events, forming the degraded ionic Fe^{2+} and Fe^{3+} species.

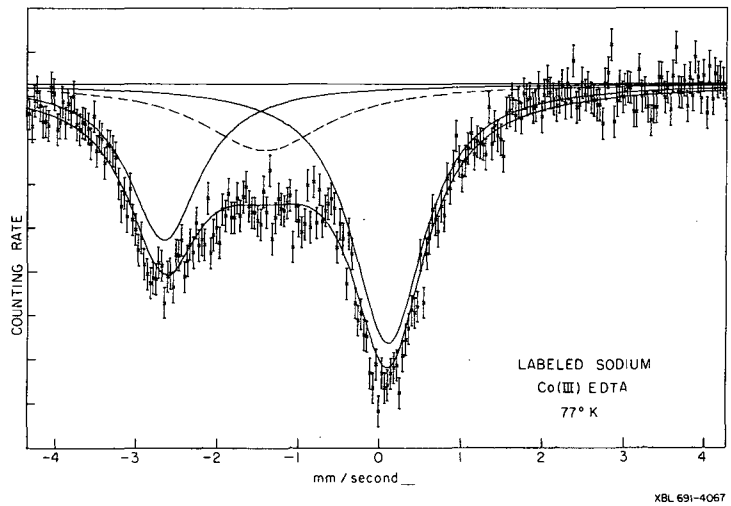

Fig. 2. Emission Mössbauer spectrum of labeled sodium ethylenediamine tetra-acetato ^{57}Co(III) at 77°K. The two outer peaks are the quadrupolar split doublet of uncoordinated Fe^{2+}. The central peak corresponds to uncoordinated Fe^{3+}.

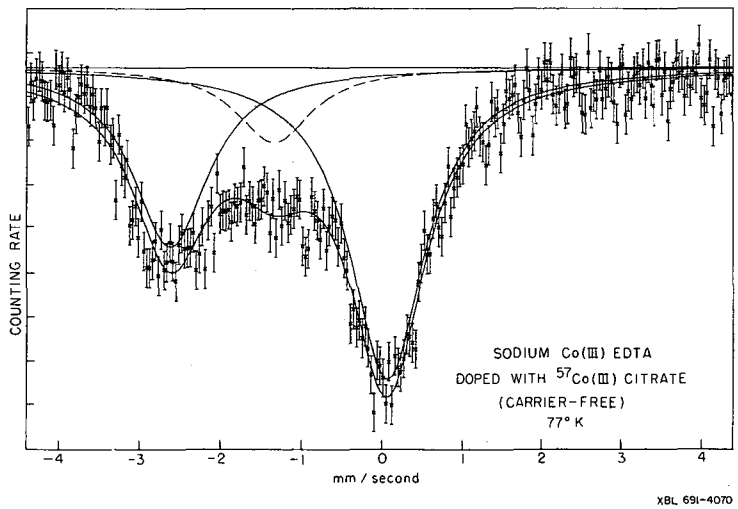

Fig. 3. Emission Mössbauer spectrum of sodium ethylenediamine tetra-acetato Co(III) doped with "carrier-free" ^{57}Co(III) citrate at 77°K. The two outer peaks are the quadrupolar split doublet of uncoordinated Fe^{2+}. The central peak corresponds to uncoordinated Fe^{3+}.

Bis-salicylaldehyde triethylenetetramine cobalt(III) chloride $[Co(III)TS_2]Cl$

The behavior of this chelate is similar to that of the EDTA complex. There is evidence for fragmentation of molecules in a large majority of the events (Figs. 4 and 5) The $Fe(III)TS_2 \cdot Cl$ is expected to have peaks at -1.44 and 1.16 mm/sec (determined in an independent absorption experiment), and it can be present, if at all, in relatively small amounts (Fig. 4).

Bis-indenyl Co(III) nitrate

Figures 6 and 7 show the spectra of the labeled and the doped complex. The spectrum of the labeled bis-indenyl complex (Fig. 6) bears no resemblance to that of the doped complex (Fig. 7), unlike the EDTA and TS_2 complexes discussed earlier. Hence, there is no

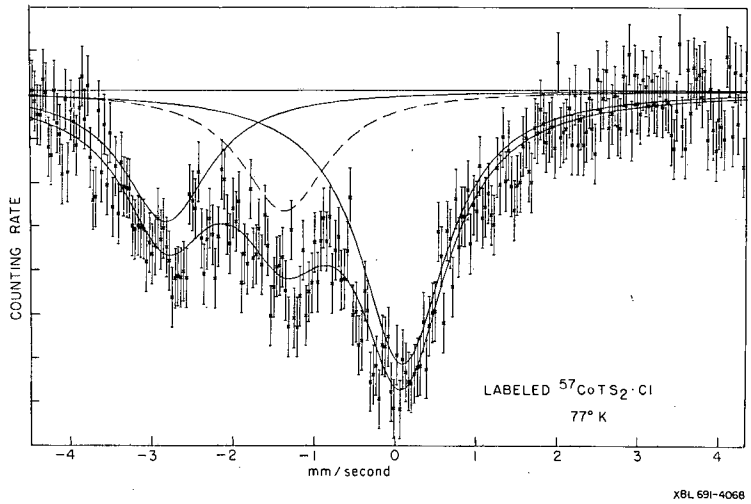

Fig. 4. Emission Mössbauer spectrum of labeled bis-salicylaldehyde triethylene-tetramine $^{57}Co(III)$ chloride at 77 °K. The two outer peaks are the quadrupolar split doublet of uncoordinated Fe^{2+}. The central peak corresponds to uncoordinated Fe^{3+}.

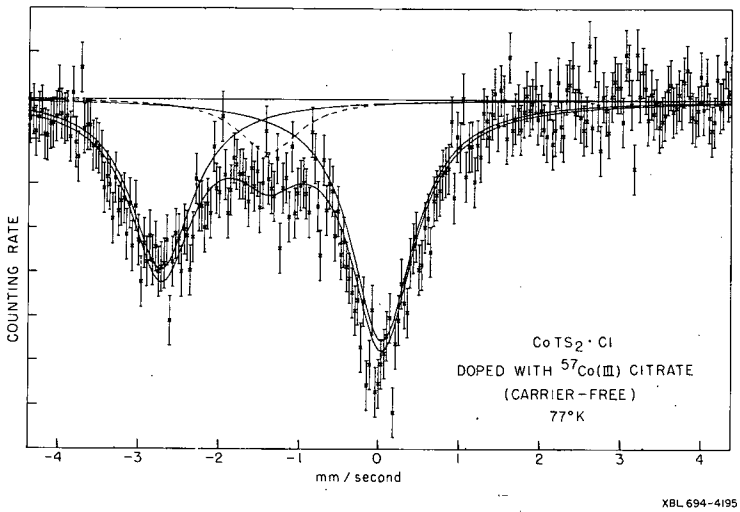

Fig. 5. Emission Mössbauer spectrum of bis-salicylaldehyde triethylene-tetramine Co(III) chloride doped with "carrier-free" $^{57}Co(III)$ citrate at 77 °K. The two outer peaks are the quadrupolar split doublet of uncoordinated Fe^{2+}. The central peak corresponds to uncoordinated Fe^{3+}.

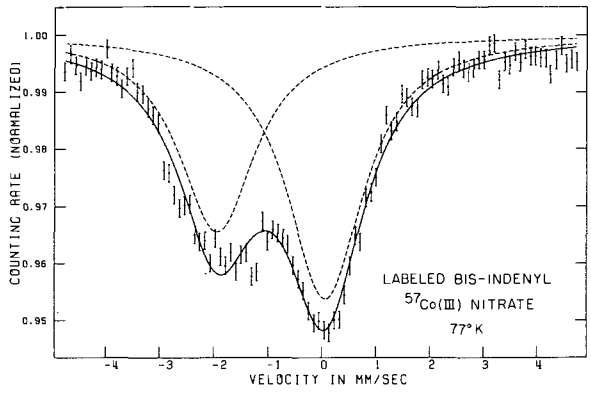

Fig. 6. Emission Mössbauer spectrum of labeled bis-indenyl $^{57}Co(III)$ nitrate at 77°K. The doublet arises from the coordinated form, C_9H_7Fe.

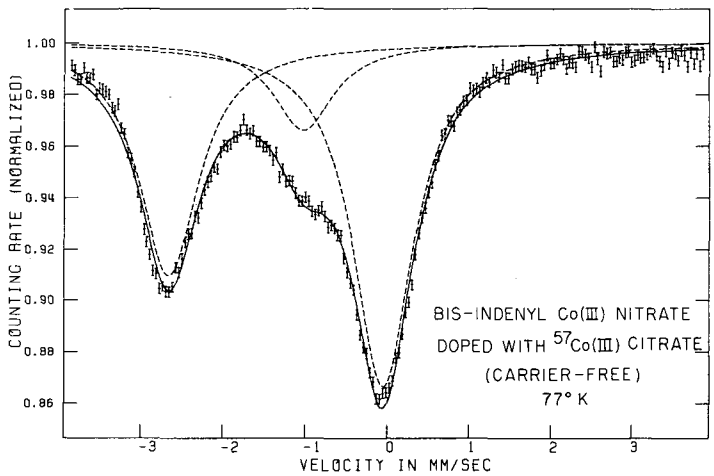

Fig. 7. Emission Mössbauer spectrum of bis-indenyl Co(III) nitrate doped with "carrier-free" $^{57}Co(III)$ citrate at 77°K. The two outer peaks are the quadrupolar split doublet of uncoordinated Fe^{2+}. The central peak corresponds to uncoordinated Fe^{3+}.

evidence for the presence of Fe^{2+} or Fe^{3+} in the spectrum of the labeled indenyl complex. Neither does it correspond to the spectrum of the bis-indenyl Fe(II), where the expected peak positions[10] are -1.82 and 0.72 mm/sec, nor to that of the chemically unstable [bis-indenyl Fe(III)] $^{+}$, which, on the basis of analogy with [bis-cyclopentadienyl Fe(III)] $^{+}$, would have a single peak at approximately -0.35 mm/sec.[11] Also, the lines are unusually wide, i.e., 1.73 mm/sec--as a matter of fact, the widest observed for all emission experiments. We attribute the spectrum to the radical C_9H_7Fe formed as a result of detachment of one of the rings from the sandwich compound. Hence, in this case also, fragmentation occurs as a consequence of Auger ionization.

Cobalt(III) acetylacetonate

Figures 8 and 9 show the spectra of the labeled and doped acetylacetonate complex. With such a close resemblance between the two spectra, one is at first sight led to believe that there is complete fragmentation of labeled molecules resulting in the formation of high-spin Fe^{3+} and Fe^{2+} ions. However, on closer scrutiny, one realizes that the peak for Fe(III)-$(acac)_3$ is expected[12] to occur at approx. -0.5 mm/sec, but it would be broadened and distorted due to partial paramagnetic hyperfine splitting as a result of dilution in a diamag-

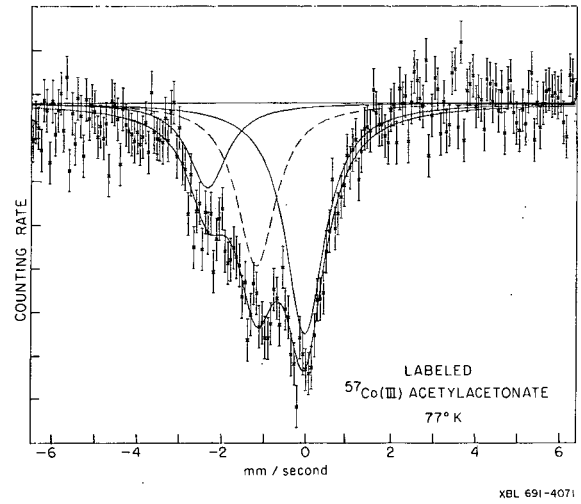

Fig. 8. Emission Mössbauer spectrum of labeled ^{57}Co(III) acetylacetonate at 77°K. The two outer peaks are the quadrupolar split doublet of uncoordinated Fe^{2+}. The central peak corresponds to uncoordinated Fe^{3+}.

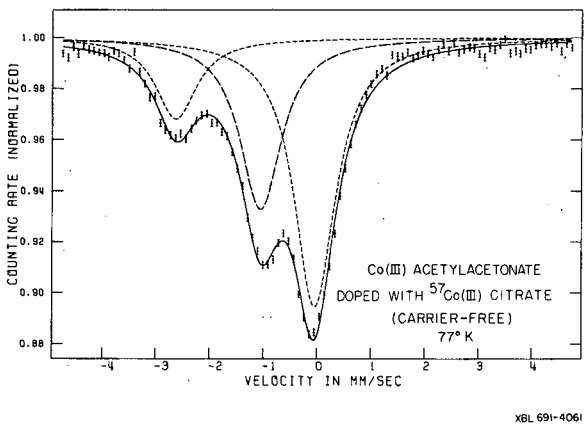

Fig. 9. Emission Mössbauer spectrum of Co(III) acetylacetonate doped with "carrier-free" ^{57}Co(III) citrate at 77°K. The two outer peaks are the quadrupolar split doublet of uncoordinated Fe^{2+}. The central peak corresponds to uncoordinated Fe^{3+}.

netic matrix of $Co(III)(acac)_3$. This region also overlaps with the peaks of Fe^{2+} and Fe^{3+}, and hence it is not worthwhile analyzing for $Fe(III)(acac)_3$. We decided rather to detect the presence of $Fe(acac)_3$ by looking at the positions of the four outer lines at liquid helium temperature. In Fig. 10, the positions of these lines and their centroid (≈ 0.63 mm/sec) indeed do correspond with those of $Fe(acac)_3$ determined earlier[13] in a diamagnetic matrix. This spectrum shows that a certain fraction of iron is present in the coordinated form, viz., $Fe(acac)_3$.

Now the question arises whether the $Fe(acac)_3$ originates as a consequence of failure of molecular fragmentation or reentry following fragmentation in the following manner. A higher charged iron ion, for instance, $\tilde{>}4+$, resulting from molecular fragmentation, comes to rest at a new site between some molecules of $Co(III)(acac)_3$. It captures an electron to form an electronically excited Fe^{3+} ion, which in turn can undergo exchange with a molecule of $Co(acac)_3$ forming $Fe(acac)_3$. Exchange of this type in solids, excited by electron capture, has received considerable attention[7,14] in a different context. To ascertain whether some fraction of the $Fe(acac)_3$ detected is formed through this reentry process, we ran a sample of $Co(acec)_3$ doped with carrier-free ^{57}Co(III)

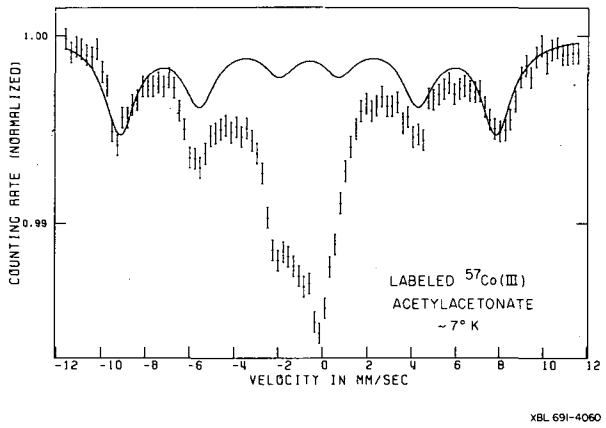

Fig. 10. Emission Mössbauer spectrum of labeled ^{57}Co(III) acetylacetonate at about 7° K. The four outer peaks of the hyperfine sextet arise from the coordinated species Fe(III)$(acac)_3$.

citrate at liquid helium temperature (Fig. 11). It shows the outer four peaks of the hyperfine sextet at the expected positions. It may be mentioned that when $^{57}Co^{++}$ is used as the dopant instead of the citrate, these four peaks are barely detectable. From this, we can conclude that the citrate simulates the conditions of the labeled complex better than Co^{++} for the reasons discussed earlier.

Therefore, one may conclude that in labeled $Co(acac)_3$ a large percentage of molecules fragments in consequence of Auger ionization, and subsequently a certain fraction of the degraded iron species reenters into the coordinated form through electronically excited exchange. A small percentage of molecules remains unfragmented.

Tris-dipyridyl Co(III) perchlorate

The spectra for the labeled and the doped dipyridyl complex are shown in Figs. 12 and 13, respectively. In Fig. 12, the two prominent peaks belong to $Fe(III)(dipy)_3 \cdot (ClO_4)_3$; the remaining two weak lines belong to the quadrupolar split lines of Fe^{2+}. Thus the major contribution is from $Fe(III)(dipy)_3(ClO_4)_3$. From the doped run (Fig. 13) we learn that a certain fraction of the iron becomes incorporated into the dipyridyl complex by means of reentry. Consequently, we infer that the majority of the spectrum (Fig. 12) arises from complexed iron atoms that have escaped fragmentation, while a much smaller portion may represent fragmentation followed by reentry.

It is noteworthy that if the dipyridyl chelate is doped with carrier-free ^{57}Co(III) EDTA,

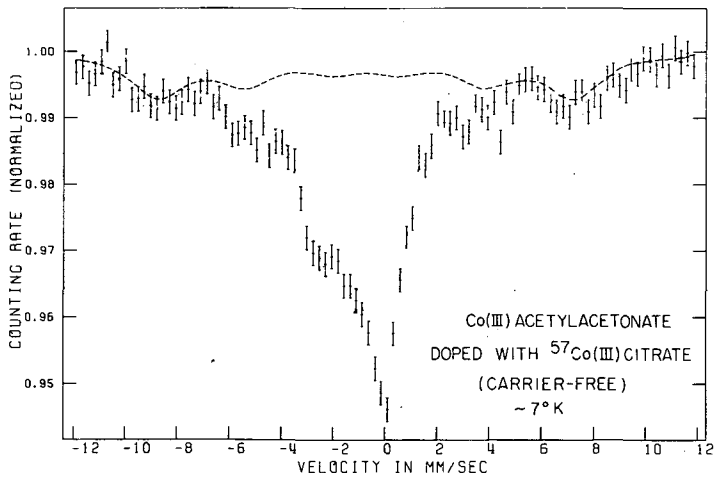

Fig. 11. Emission Mössbauer spectrum of Co(III) acetylacetonate doped with "carrier-free" ^{57}Co(III) citrate at about 7 °K. The four outer peaks of the hyperfine sextet arise from the coordinated species Fe(III) $(acac)_3$.

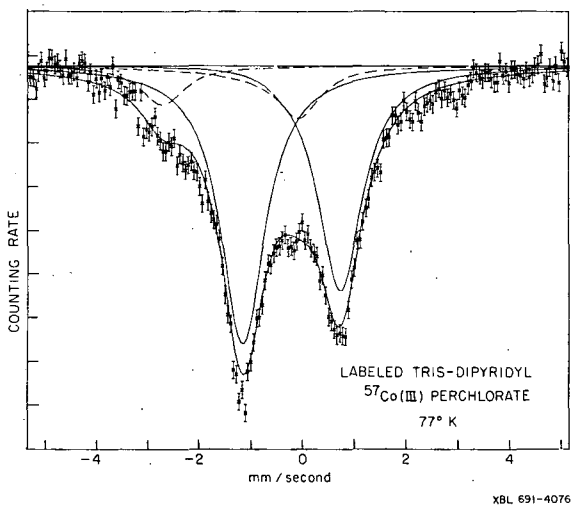

Fig. 12. Emission Mössbauer spectrum of labeled tris-dipyridyl ^{57}Co(III) perchlorate at 77° K. The prominent doublet arises from the coordinated dipyridyl complex. The weaker doublet corresponds to the uncoordinated Fe^{2+}.

the results are similar. However, if $^{57}Co^{++}$ is used as the dopant, there is no evidence for the presence of $Fe(III)(dipy)_3 \cdot (ClO_4)_3$ in the spectra. This, again, shows that presence of $^{57}Co^{++}$ as such does not simulate the conditions encountered during fragmentation of a labeled molecule. On the other hand, if the ion is coordinated to citrate or EDTA, its presence does seem to simulate the environment, for reasons discussed earlier.

Dilution Experiments

We dispersed $^{57}Co(III)(acac)_3$ in cellulose acetate and $^{57}Co(III)(dipy)_3(ClO_4)_3$ in polyethylene oxide and agar-agar. These are presumably molecular dispersions in inert matrices. Figures 14 and 15 show the spectra. Dilution results in a considerable diminution of the intensities of the four hyperfine lines attributable to $Fe(acac)_3$, as is evident from a comparison of Fig. 14 with Fig. 10. Dispersal of the dipyridyl complex in polyethylene oxide results in an even more pronounced diminution of intensity of the parent species, as is apparent from a comparison of Figs. 15 and 12. Thus, dispersal of the complexes in foreign matrices leads to a larger fraction of fragmented molecules.

It seems that in dilute dispersals, not only is the reentry process inhibited (for obvious reason), but the probability of survival of the molecule after the Auger event is considerably diminished.

Cobalt(II) phthalocyanine

Figures 16 and 17 show the spectra of labeled and doped Co(II) phthalocyanine, respec-

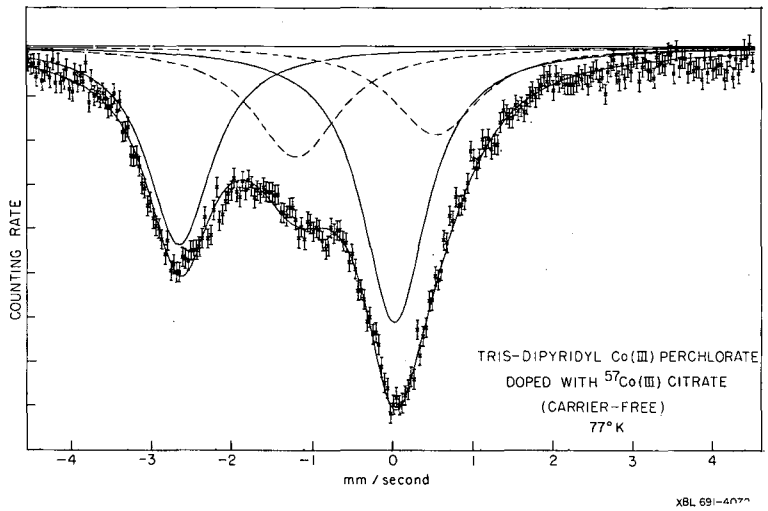

Fig. 13 Emission Mössbauer spectrum of tris-dipyridyl Co(III) perchlorate doped with "carrier-free" ^{57}Co(III) citrate at 77 °K. The prominent doublet arises from the uncoordinated Fe^{2+}. The weaker pair corresponds to the coordinated dipyridyl complex.

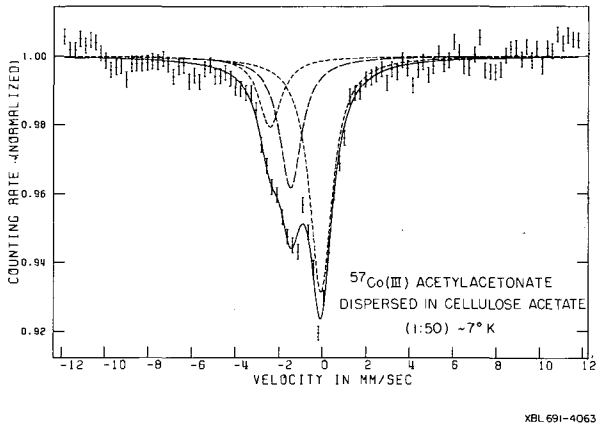

Fig. 14. Emission Mössbauer spectrum of ^{57}Co(III) acetylacetonate dispersed in cellulose acetate (1:50 by weight) at about 7° K. The four outer peaks arising from the coordinated species Fe(III) $(acac)_3$ are hardly perceptible.

tively. In Fig. 16 we see no evidence for the presence of the degraded Fe^{2+} or Fe^{3+} species, and the spectrum corresponds to that of Fe(II) phthalocyanine only, and so the question regarding reentry does not arise. One may conclude that the labeled molecules escape fragmentation in 100% of the Auger events.

Vitamin B_{12}

Earlier[15] we have observed systematic variations in chemical shifts and quadrupolar splittings upon substituting the cyanide and the benzimidazole ring of the vitamin B_{12} molecule, showing the complete absence of fragmentation.

It is appropriate here to comment on some aspects of the doping experiments. In general, doping the complexes with carrier-

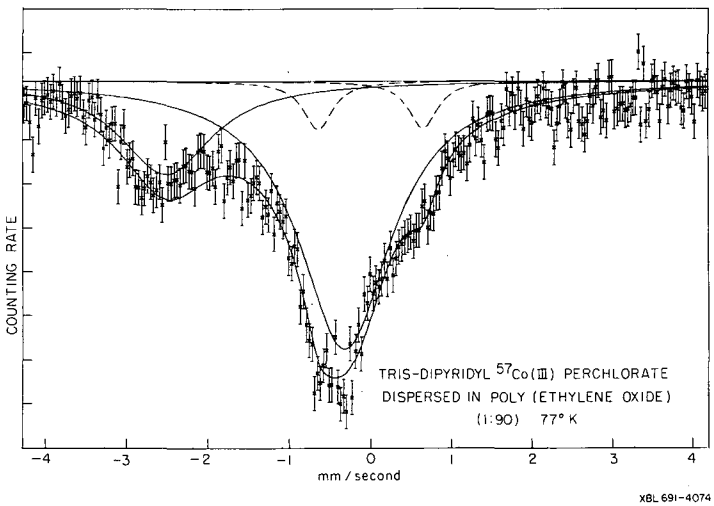

Fig. 15. Emission Mössbauer spectrum of tris-dipyridyl ^{57}Co(III) perchlorate dispersed in polyethylene oxide (1:90 by weight) at 77° K. The weak dotted doublet corresponds to the coordinated dipyridyl complex. The peak at about -2.5 mm/sec is one of the two components of uncoordinated Fe^{2+}, while the other component along with Fe^{3+} lies near zero velocity.

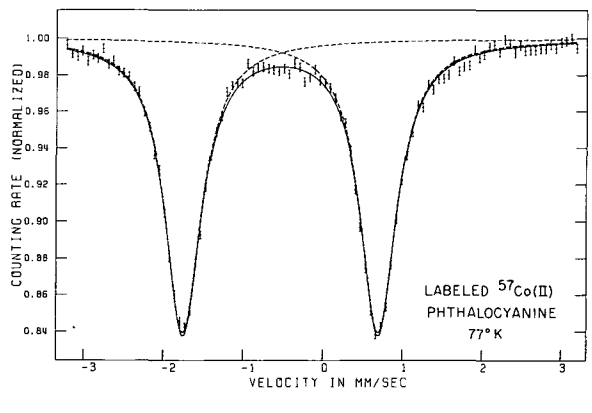

Fig. 16. Emission Mössbauer spectrum of labeled ^{57}Co(II) phthalocyanine at 77° K. The doublet arises from Fe(II) phthalocyanine.

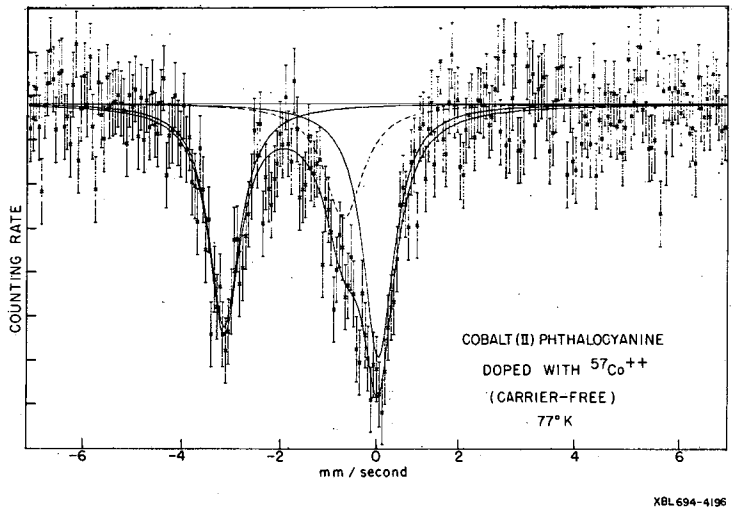

Fig. 17. Emission Mössbauer spectrum of Co(II) phthalocyanine doped with "carrier-free" $^{57}Co^{++}$ at 77°K. The two outer peaks are the quadrupolar split doublet of uncoordinated Fe^{2+}. The central dotted line corresponds to uncoordinated Fe^{3+}.

free ^{57}Co(III) citrate seems to simulate the environment encountered by the degraded iron in labeled complexes. For instance, the isomer shifts and quadrupolar splittings observed for Fe^{++} in labeled and citrate-doped Co(III) EDTA (Figs. 2 and 3) are about the same. The same behavior obtains for Co(III)TS_2 (Figs. 4 and 5). Again, the same values are observed for Fe^{++} in doped $Co(dipy)_3(ClO_4)_3$ irrespective of whether it is doped with carrier-free ^{57}Co(III) citrate or with ^{57}Co(III) EDTA. On the other hand, Fe^{++} exhibits different values for doped and labeled $Co(acac)_3$ (Figs. 8 and 9). When $^{57}Co(acac)_3$ is dispersed in polyethylene oxide, the values for Fe^{++} still correspond with the labeled case. The above observations can perhaps be rationalized if we assume that during fragmentation of $^{57}Co(acac)_3$, the recoiling iron species carries an acetylacetone fragment loosely bound to it, and so the Fe^{++} will have a different environment as compared to the doped case. (It will not be out of place to mention recent observations on Auger fragmentation of $Pb(CH_3)_4$ in the gaseous phase (Ref. 16). The authors find that the lead ion possesses little kinetic energy (<0.1 eV), while H^+, C^+, and C^{2+} have a few tens of eV energy. The authors suggest that since the methyl groups are placed in a tetrahedral configuration, the Coulombic repulsion between the central Pb and its methyl groups tends to cancel each other, as the highly charged molecular ion explodes from a common center. It does not appear likely that an identical situation would arise in the cobalt complexes under study, as the configurations are not as symmetrical as the $Pb(CH_3)_4$. However, it may be stressed that even if the iron species does not possess appreciable kinetic energy in any of the cobalt complexes, it will make no essential change in the model which we propose later.)

Discussion

We recapitulate briefly our experimental observations.

Cobalt chelates with hexadentate ligands, such as EDTA and TS_2, which are chemically very stable, fragment in a large majority of events as a consequence of the Auger ionization. The same is true of the indenyl sandwich compound.

In Co(III)$(acac)_3$, the spectra reveal a small fraction of coordinated iron, viz., $Fe(acac)_3$. This coordinated iron arises by way of two paths, viz., the parent molecule escaping fragmentation and the reentry of the degraded iron ion undergoing excited exchange

with a host cobalt chelate molecule. Dispersal of the chelate in cellulose acetate inhibits reentry and may also enhance the probability of fragmentation.

For the system $Co(III)(dipy)_3(ClO_4)_3$, a majority of molecules escape fragmentation;[17] a small contribution to the coordinated form comes about from reentry. Dispersal of the dipyridyl complex in an inert matrix considerably enhances the probability of fragmentation. Inhibition of reentry will have a minor contribution, too.

There is no evidence of fragmentation in $^{57}Co(II)$ phthalocyanine or in vitamin B_{12}.

In phthalocyanine and vitamin B_{12}, the cobalt atom is coupled to large and highly conjugated systems (unlike the EDTA and TS_2 complexes). One can visualize that after the Auger event, the multiply charged ^{57}Fe ion extracts electrons from the ring, and the resulting positive charges on the ring are dispersed to its periphery. Due to the rapid dispersal of charge through the conjugated system and because of the large size of the ring, the multicenter Coulombic repulsion is inadequate to fragment the molecule. Thus, the molecule escapes fragmentation at this stage. Now let us consider the second stage. The charges built up on the ring are expected to disperse through neighboring molecules before the bonds get a chance to miss the electrons, viz., within 10^{-13} sec. The rapid charge dispersal through neighboring molecules is perhaps also facilitated as the relative positions of atoms remain fixed during this interval and Franck-Condon restrictions would not arise. As a consequence of charge neutralization, one would expect several tens of electron volts of energy to be deposited in the parent molecule and its immediate vicinity. This is the crucial stage. The fact that the molecules do not fragment at this stage either shows that the large amount of energy is very efficiently dispersed from the epicenter. To the best of our knowledge, this is the first time that experimental evidence is available for suggesting rapid intermolecular transport of such amazingly large amounts of energy.

To a lesser extent, this picture appears to be true for neat $Co(III)(dipy)_3(ClO_4)_3$. When the dipyridyl molecules are dispersed in a foreign inert matrix, the original lattice is broken down and the dissipation of charge and energy is no longer rapid and efficient, and thus the probability of fragmentation is considerably enhanced.

It is pertinent to mention that in light of the interpretation given above, that molecules with conjugated structure can escape fragmentation during the Auger event, one can now interpret the earlier observations on tetraphenyl tin.[18] It was reported that when $^{119m}Sn(phenyl)_4$ is used as a Mössbauer source, the major component is that associated with the single resonance line observed with an unlabeled $Sn(phenyl)_4$ absorber. The de-excitation of ^{119m}Sn occurs by the emission of 65.3-keV and 23.8-keV gamma rays in cascade. The 65.3-keV gamma radiation preceding the 23.8-keV Mössbauer emission undergoes internal conversion almost completely. Hence, the Mössbauer emission is preceded by Auger ionization as in the case of cobalt-57. Therefore, one can conclude that tin tetraphenyl, which is a conjugated system like the cobalt dipyridyl complex, escapes fragmentation in a majority of events.

The work reported here may have an important bearing on the role of Auger ionization in radiation biology and chemistry.[19]

In the case of acetylacetone and dipyridyl complexes, we have experimental evidence which suggests that a certain fraction of parent chelate can arise from reentry of the multiply charged degraded iron ion through the process of electronically excited exchange, discussed earlier. Naturally, the question arises as to why exchange does not occur, at least in noticeable amounts, in the case of EDTA and TS_2

complexes. The highly ionized iron species relaxes by capturing electrons from neighboring molecules. Some of the molecules in the immediate vicinity of a $^{57}Fe^{n+}$ ion, with which it could have exchanged, collapse by virtue of the energy deposited during charge neutralization.

For bis-indenyl Co(II) nitrate, Co(II) phthalocyanine, and vitamin B_{12} one should not expect noticeable exchange, as shown by earlier studies.[7,20,21] It appears that in these compounds, the stereochemistry of the molecules does not permit the configuration needed for exchange.

We have observed differences in Mössbauer parameters (isomer shift and quadrupolar splittings) obtained by emission spectroscopy versus the conventional absorption experiments. For instance, the average values observed for $Fe(III)(dipy)_3(ClO_4)_3$ which originates in a $Co(III)(dipy)_3(ClO_4)_3$ lattice (both in the case of labeled dipyridyl as well as when dipyridyl is doped with $^{57}Co(III)$ citrate or $^{57}Co(III)$ EDTA), are I.S., 0.28 mm/sec and Q.S., 1.84 mm/sec as compared to the values of 0.0 and 1.76 mm/sec respectively, determined through absorption spectroscopy of the iron compound.[22] Again, the Mössbauer parameters are different for dispersals in inert matrices. The values obtained for $^{57}Co(III)$-$(dipy)_3(ClO_4)_3$ dispersed in polyethylene oxide and agar-agar are 0.0 and 1.36 mm/sec. One can perhaps explain these differences by virtue of the different matrices in which the Mössbauer emitter or absorber is situated. For the labeled and doped experiments, the Mössbauer emitter, $^{57}Fe(dipy)_3(ClO_4)_3$, is situated in the lattice of $Co(dipy)_3(ClO_4)_3$, unlike the absorption experiment. Again, in dilute dispersals the emitters are situated in polyethylene oxide and agar-agar matrices, where the configuration is obviously not the same as it is in the cobalt or iron dipyridyl lattice.

Summary

The electron-capture decay of a cobalt-57 atom triggers an Auger event resulting in the loss of several electrons from the molecule in which it is incorporated. The 14.4-keV Mössbauer emission conveys information regarding the chemical forms in which the daughter ^{57}Fe is "stabilized" within 10^{-7} sec following electron capture. During this time the electronic relaxation occurs completely and several tens of electron volts energy is deposited in the molecule as a result of neutralization. We find that the ethylenediamine tetra-acetate, bis-salicylaldehyde triethylenetetramine, and indenyl chelates fragment in a large majority of events, resulting in the formation of degraded ionic Fe^{2+} and Fe^{3+} in the former two cases and C_9H_7Fe in the latter. To a somewhat lesser extent, the acetylacetonate behaves similarly. On the other hand, highly conjugated compounds such as cobalt phthalocyanine and vitamin B_{12} escape fragmentation in 100% of the Auger events. Tris-dipyridyl Co(III) perchlorate also escapes fragmentation in a majority of events. Apparently, the large amount of excitation energy deposited in the molecule as a consequence of charge neutralization is very rapidly (in less than 10^{-13} sec) and efficiently dispersed through neighboring molecules. It is a novel phenomenon.

When the dipyridyl chelate molecules are dispersed in a foreign matrix, the dissipation of charge and energy is no longer rapid and efficient and the probability of fragmentation is considerably enhanced.

We also find that part of the coordinated parent species for the labeled chelates of acetylacetone and dipyridyl arises through fragmentation followed by interaction of the electronically excited degraded iron species with a neighboring chelate molecule, resulting in replacement of cobalt with an iron atom. This finding was made possible by using chelates

doped with "carrier-free" ^{57}Co citrate.

Emission spectroscopy yields values for the isomer shifts and quadrupole splittings which differ from those obtained by absorption spectroscopy. The apparent disparities are attributed to the dissimilarities of the matrices in which the Mössbauer emitter or absorber is situated.

Acknowledgments

Two of the authors (A. N. and D. L.) are particularly grateful to Dr. W. F. Libby for several valuable discussions.

The authors also express their gratitude to Mr. W. Erin and Miss L. Marton for their help during the course of this work.

References and Footnotes

1. H. Pollak, Phys. Stat. Sol. 2, 720 (1962).
2. S. Wexler, in Actions Chimiques et Biologiques des Radiations, M. Haissinsky, Ed., Vol. 8 (Masson, Paris, 1965), pp. 103-241.
3. A. H. Snell, Alpha-, Beta-, and Gamma-Spectroscopy, K. Siegbahn, Ed. (Interscience Publishing Co., New York, 1964), p. 1545.
4. A. R. Kazanjian and W. F. Libby, J. Chem. Phys. 42, 2778 (1965).
5. P. R. Geissler and J. E. Willard, J. Phys. Chem. 67, 1675 (1963).
6. G. K. Wertheim, W. R. Kingston, and R. H. Herber, J. Chem. Phys. 37, 687 (1962).
7. Amar Nath, S. Khorana, P. K. Mathur, and S. Sarup, Indian J. Chem. 4, 51 (1966).
8. L. M. Epstein, J. Chem. Phys. 36, 2731 (1962).
9. J. J. Spijkerman, L. H. Hall, and J. L. Lambert, J. Am. Chem. Soc. 90, 2039 (1968).
10. R. H. Herber, R. B. King, and G. K. Wertheim, Inorg. Chem. 3, 101 (1964).
11. G. K. Wertheim and R. H. Herber, J. Chem. Phys. 38, 2106 (1963).
12. G. M. Bancroft, A. G. Maddock, W. K. Ong, R. H. Prince, and A. J. Stone, J. Chem. Soc. A, 1966 (1967).
13. J. W. G. Wignall, J. Chem. Phys. 44, 2462 (1966).
14. Amar Nath and S. P. Vaish, J. Chem. Phys. 46, 4660 (1967).
15. Amar Nath, Michael Harpold, and Melvin P. Klein, Chem. Phys. Letters 2, 471 (1968).
16. T. A. Carlson and R. M. White, J. Chem. Phys. 48, 5191 (1968).
17. Recently, Hazony and Herber [J. Inorg. Nucl. Chem. 31, 321 (1969)] have suggested that in the spectrum of labeled $^{57}Co(acac)_3$, the quadrupolar split doublet belonging to Fe^{2+} arises by virtue of the fact that the unit cell of $Co(acac)_3$ is more compact (density 1.43 g/cm^3) than that of $Fe(acac)_3$ (density 1.33 g/cm^3) and therefore the Fe substitutional impurity which is formed by the ^{57}Co decay in $Co(acac)_3$ is accommodated in a strongly compressed lattice site in which it experiences a marked compression ($\approx 7\%$). They imply that fragmentation of the molecule does not occur, which is contrary to our experimental observations. We do not agree with their speculation for the following reasons: First, $Co(acac)_3$ and $Fe(acac)_3$ are not isomorphous, the former being monoclinic while the latter is orthorhombic, so that the differences in density may arise mainly because of the mode of packing of molecules and not because of differences in molecular size; therefore, a newly born molecule of $Fe(acac)_3$ may not experience any appreciable compression in the $Co(acac)_3$ lattice. Second, when $^{57}Co(acac)_3$ is molecularly dispersed in cellulose ac-

etate, the relative intensity of Fe^{2+} lines increases (cf. Figs 10 and 14). Again, when ^{57}Co(III) EDTA is dispersed in polyethylene oxide, the spectrum differs little from that of the neat compound. These observations, as well as several others on a variety of complexes already mentioned in the text, can be easily understood on the basis of fragmentation of the molecule rather than on the basis of the fact that the unfragmented molecule undergoes compression in a foreign matrix.

18. R. H. Herber and H. A. Stöckler, Proceedings of the Symposium on Chemical Effects of Nuclear Transformations, I. A. E. A., Vienna, Vol. II, 403 (1965).
19. Aadne Ore, The Role of Multiple Ionization in Radiation Action, Proceedings of the Third International Congress of Radiation Research, June-July 1966, G. Silani, Ed. (Wiley and Sons), p. 54.
20. Amar Nath and J. Shankar, Proc. Symp. Chemical Effects of Nuclear Transformations, Prague (1960), I. A. E. A. 1, 409 (1961).
21. J. Shankar, Amar Nath, and M. H. Rao, Radiochim. Acta 3, 26 (1964).
22. R. L. Collins, R. Pettit, and W. A. Baker, Jr., J. Inorg. Nucl. Chem. 28, 1001 (1966).

COMPLETE DETERMINATION OF THE ALIGNMENT OF CH_2Cl_2-CD_2Cl_2 MOLECULES IN POLY-γ-BENZYL-L-GLUTAMATE SOLUTION BY THE NUCLEAR MAGNETIC RESONANCE OF ^{35}Cl, ^{2}D, AND ^{1}H. COMPARISON OF ELECTRIC AND MAGNETIC ORDERING

D. Gill, M. P. Klein, and G. Kotowycz

Concentrated solutions of poly-γ-benzyl-L-glutamate dissolved in CH_2Cl_2 (and CD_2Cl_2) are liquid crystalline[1] and acquire order when placed in magnetic[2, 3] and electric[4, 5] fields. Solute ordering constrains the motion of the solvent molecules so that their intramolecular traceless tensor interactions are not averaged to zero.

We have determined additional NMR characteristics of the solvent in the liquid crystalline state of this system.[2, 3] Comparison of the integrated signal intensity of the high-resolution (HR) proton magnetic resonance (PMR) with that of a measured quantity of added TMS indicates that to within experimental error all the solvent molecules contribute to the HR PMR spectra.

We have extended the NMR measurements to the ^{35}Cl and ^{2}D nuclei to extract, insofar as possible, information about the ordering of the solvent. The anisotropic motion is reflected by the residual dipolar splitting of the PMR,[6, 7] by the quadrupolar splitting of the deuterium magnetic resonance (DMR),[7] and by the occurrence of quadrupolar-induced satellites in the ^{35}Cl NMR spectrum, reported here for the first time.

For calculating the "distortion theory" orientation parameters, S_{ii},[6] we defined a molecule-fixed frame in which the 1 = x axis is parallel to the Cl-Cl direction, the 2 = y axis is parallel to the H-H direction, and 3 = z is the C_{2v} axis, and assumed that the axis of constraint[6] of the solvent was directed along the

magnetic field $H_0(\Omega = 0)$. If asymmetry parameters are neglected, the frequency (separation, in hertz, between the two lines in the DMR in CD_2Cl_2 is[6,7]

$$\Delta_D Q = \pm \frac{e^2Qq(D)}{2h}[-S_{11} + S_{22}(3\sin^2\alpha - 1) + S_{33}(3\cos^2\alpha - 1)], \quad (1)$$

where eq(D) is the gradient along the CD bond, assumed to be the largest component of the electric field gradient, and $2\alpha = 112.0$ deg is the DCD bond angle.

The frequency separation between the outer two lines of the triplet ^{35}Cl NMR is

$$\Delta_{Cl} Q = \pm \frac{e^2Qq(^{35}Cl)}{3h}[S_{11}(3\sin^2\beta - 1) - S_{22} + S_{33}(3\cos^2\beta - 1)], \quad (2)$$

where $2\beta = 111.8$ deg is the Cl-C-Cl bond angle.

The separation, in hertz, between the two dipolar components of the solvent PMR is

$$\Delta_{HH} = \pm 3h(\gamma/2\pi)^2 R_{HH}^{-3} S_{22}, \quad (3)$$

where $\gamma/2\pi = 4.257 \times 10^3$, and $R_{HH} = 1.771$ Å.

For ^{35}Cl, $e^2Qq/2h$ is 36.2 MHz.[8] We deduced $e^2Qq(D)/h = 150$ kHz for deuterium from a DMR T_1 measurement.[9] The values of $\Delta_{Cl}Q$, $\Delta_D Q$, and Δ_{HH} measured at 24° in solutions which contained ten solvent molecules for each monomer residue are given in Table I.

Eight sets of solutions to Eqs. 1-3 are possible when all combinations of signs are considered. From the magnitudes of the splittings alone it is not possible to select the correct set of S parameters, and additional information is necessary. In our case it was obtained from the PMR "powder pattern"[10] and the orientation by an electric field. Either of these observations yields the sign of S_{22}.

Table I. Measured residual quadrupole splittings of the NMR spectra of deuterium ($\Delta_D Q$) and of ^{35}Cl ($\Delta_{Cl}Q$) and the residual dipolar splitting of the proton NMR (Δ_{HH}) in the $CH_2Cl_2 + CD_2Cl_2$ solvent molecules of a magnetically aligned concentrated solution of PBLG.

$\Delta_D Q$	$\pm(368 \pm 3)$ Hz
$\Delta_{Cl}Q$	$\pm(112 \pm 20) \times 10^3$ Hz
Δ_{HH}	$\pm(107 \pm 2)$ Hz

Immediately after the cholesterically ordered sample[1a] is placed in the magnetic field, the PMR and DMR spectra replicate those of proton pairs in polycrystalline solids[10] except that the interaction in the liquid crystal is attenuated by 10^3.

We draw the analogy and attribute the intensity at the shoulders of the PMR spectrum to proton pairs aligned parallel to H_0. In the course of alignment the intensity of the PMR and DMR shoulders increases at the expense of that in the center of the pattern, and we interpret this change as a proliferation of proton pairs aligned parallel to H_0. This conclusion provides us with the additional information necessary to establish the signs of Eqs. 1-3. These conditions are, then, (a) $\Sigma S_{ii} = 0$, (b) $S_{22} > 0$, and (c) $S_{22} > S_{11}$.

From Eq. 3 and restriction b, we obtain $S_{22} = +1.7 \times 10^{-3}$, and from the molecular bond angles the remaining S parameters are calculated by Eqs. 2 and 3 (Table II).

S parameters corresponding to $\Delta_D Q(+)$ and $\Delta_{Cl}Q(-)$ are self-consistent, as are those corresponding to $\Delta_D Q(-)$ and $\Delta_{Cl}Q(+)$. The former set is chosen to conform with condition c and to be consistent with the molecular geometry.

Using the S parameters derived from the PMR and ^{35}Cl NMR and substituting into Eq. 1,

Table II. The S_{ii} parameters as calculated from the data of Table I, Eqs. 1-3, and restrictions a-c.

Signs of Δ_D^Q, Δ_{Cl}^Q	Nucleus: Deuterium $\Delta_D^Q(+)$	Deuterium $\Delta_D^Q(-)$	^{35}Cl $\Delta_{Cl}^Q(+)$	^{35}Cl Δ_{Cl}^Q
$S_{22} \times 10^3$	+ 1.7	+ 1.7	+ 1.7	+ 1.7
$S_{11} \times 10^3$	- 3.2	+ 6.6	+ 6.0	- 2.8
$S_{33} \times 10^3$	+ 1.5	- 8.3	- 7.7	+ 1.1

we calculate $e^2Qq(D)/h$ = 160 kHz, in agreement with the T_1- derived value of 150 kHz.

We emphasize that the unique assignment of the S parameters was possible because the PMR and DMR "powder patterns" reveal the parallel and perpendicular splittings; the time development of the spectra establishes $S_{22}>0$. Similar use of such observations has been made by others.[11] For mesophases which have short reorientation times the "powder pattern" would not be observable. The sign ambiguity in such cases may be resolved by the application of electric fields which orient the mesophases; the dependence of the spectrum upon the angle between the electric and magnetic fields should suffice to establish the sign of the orientation parameters.

The PMR spectra observed when the samples were subjected to electric fields revealed that electric-field ordering is prompt and always dominates the magnetic ordering for fields of 5 kV cm^{-1}. For periods shorter than 30 min between successive applications of E fields, the ordering influence of H_0 may be neglected. When $\vec{E}$ is parallel to $\vec{H}_0$, the PMR spectra are unperturbed; the dipolar splitting exhibits the angular dependence ($3\cos^2\Omega - 1$) when Ω is the angle between $\vec{E}$ and $\vec{H}_0$. We deduce that the pattern of ordering is identical in $\vec{E}$ and in $\vec{H}$ fields.

References

1. (a) C. Robinson, Tetrahedron 13, 219 (1961); (b) A. Saupe and G. Englert, Phys. Rev. Letters 11, 462 (1963).
2. S. Sobajima, J. Phys. Soc. Japan 23, 1070 (1967).
3. M. Panar and W. D. Phillips, J. Am. Chem. Soc. 90, 3880 (1968).
4. A. Wada, Poly-α-Amino Acids, G. D. Fasman, Ed. (Marcel Dekker, Inc., New York, N. Y., 1967), p. 369.
5. J. C. Powers and W. L. Peticolas, Advances in Chemistry Series, No. 63, American Chemical Society, Washington, D. C., 1967, p. 217.
6. A. D. Buckingham and K. A. McLauchlan, in Progress in High Resolution NMR Spectroscopy, Vol. 2, J. W. Emsley, J. Feeney, and L. H. Sutcliff, Ed. (Pergamon Press, Oxford, 1967).
7. J. C. Rowell, W. D. Phillips, L. R. Melby, and M. Panar, J. Chem. Phys. 43, 3442 (1965).
8. R. L. Livingston, ibid. 19, 1434 (1951).
9. A. Carrington and A. D. McLachlan, Introduction to Magnetic Resonance (Harper and Row, New York, N. Y., 1967), p. 196.
10. G. E. Pake, J. Chem. Phys. 16, 327 (1948).
11. K. D. Lawson and T. J. Flautt, J. Am. Chem. Soc. 89, 5489 (1967).

MOLECULAR BASIS OF NERVE CONDUCTION

Gerald Entine and Howard H. Wang

Since the basis of learning and memory is dependent upon nerve conduction, an understanding of the molecular mechanisms underlying nerve conduction is of fundamental importance. It is generally believed that some molecular foundation for the electrical behavior of neuronal conduction must exist, but as yet no direct observation of these molecular changes, other than electrical phenomena, have been described.

We have undertaken to detect, by direct observational methods, changes in the molecular arrangement, or shape, during the passage of a nerve impulse. We have so far employed three different kinds of observation. The first of these is the possible change in the direct optical properties of the neuronal membrane during the passage of the action potential. By the use of polarized light oriented at a specific angle to the direction of the nerve membrane we have been able to observe changes in what appears to be birefringence correlated with the passage of the action potential. This has been done in the region of visible light and has not allowed us as yet to conclude what kinds of molecules are changing and in what way. We have therefore developed ultraviolet light sources which will permit us to make some identification of those molecules which are moving and observe how they move.

Attempts to observe fluorescence changes in this same manner intrinsic to the nerve have not succeeded. Attempts to stain the nerve with fluorescent dyes as probes have only just begun.

Finally, we have used a biradical probe of unique design. This biradical probe depends upon the fact that the two radical ends of the molecule may interact and that this interaction produces a very profound change in the electron spin resonance spectrum of the biradical. Modifications of that interaction produced by changes in the molecular environment have been explored in model systems. For example, the biradical in a flexible environment, so that the two radicaloid ends can exchange, produces a spectrum of five equal lines, brought about by the equivalence of two nitrogen atoms, each with a spin of one. If, however, the ends are prevented from encountering each other, the spectrum is that of an independent monoradical in the form of three equal lines from a single nitrogen with a spin of one. The sensitivity of the system to changes in the molecular environment is so great that it led us to the conviction that if we could attach such a sensitive geometrical probe to the proper place in the nerve membrane, we would have no difficulty in observing and interpreting the molecular changes that are presumably responsible for nerve conduction.

Our first step was, therefore, to determine the behavior of the biradical in the resting nerve. This we have done and found that the biradical does indeed change very markedly upon contact with the nerve. The interaction between the two ends of the biradical seems to be sharply inhibited. The interpretation of this observation in molecular terms is complicated by an additional chemical reaction in which the probe itself is chemically changed, and the separation of the two effects has not yet been achieved. The possible use of a similar double fluorescing system, sensitive to the geometric relation of the two fluorescing centers to each other and their control by the microenvironment, is under construction.

CIRCULAR DICHROISM SPECTRA AND THE MOLECULAR ARRANGEMENT OF BACTERIOCHLOROPHYLLS IN THE REACTION CENTERS OF PHOTOSYNTHETIC BACTERIA*

Kenneth Sauer, Edward A. Dratz, and Lelia Coyne

Studies of the circular dichroism and absorption spectra of the bacteriochlorophyll molecules in chromatophore fragments of R. spheroides (R-26 mutant), with antenna pigments removed, suggest that there are large exciton interactions among the reaction center molecules. The evidence from the CD spectra supports an interpretation in which the reaction center contains a trimer of bacteriochlorophylls. Upon activation by visible light or upon chemical oxidation, one of the molecules is converted to its oxidized form, and the remaining two molecules no longer exhibit evidence of any strong electronic interaction. A model is proposed in which the reaction center consists of two bacteriochlorophyll molecules separated by a third, which in turn is in close proximity to an electron acceptor and an electron donor (cytochrome).

*Abstract from Proc. Natl. Acad. Sci. U. S. 61, 17 (1968).

OPTICAL PROPERTIES OF THE PROTOCHLOROPHYLL PIGMENTS. I. ISOLATION, CHARACTERIZATION, AND INFRARED SPECTRA*

Claude Houssier and Kenneth Sauer

A method for the large-scale preparation of the protochlorophyll pigments from pumpkin seed coats is described. Use is made of polyethylene and sugar chromatographies, currently employed for the preparation of the chlorophyll pigments. The procedure permits the isolation of pure solid samples, in relatively large amounts (20–50 mg from 2 kg of seeds) and with good yields (higher than 40%).

In confirmation of other reports, two protochlorophyll pigments are obtained. One is the true protochlorophyll α and the other one is 4-vinyl protochlorophyll α, also called the "bacterial" protochlorophyll or Mg-2,4-divinylpheoporphyrin α_5, esterified with phytol. The pigments were characterized as regards their chromatographic sequence compared with the chlorophylls, their purity, the presence of the phytol, and by their visible and infrared absorption spectra.

Protochlorophyll α and 4-vinyl protochlorophyll α show clear differences in their visible absorption spectra. The small differences observed in their infrared spectra can be ascribed to the presence of the additional vinyl substituent in 4-vinyl protochlorophyll α. The infrared spectra present several distinguishing features. The absence of the skeletal (C = C) vibrations indicates a much higher symmetry of the macrocycle in these molecules than in the chlorophylls. In carbon tetrachloride, the "aggregated" ketone carbonyl band was observed for protochlorophyll α and 4-vinyl protochlorophyll α at 1668 cm^{-1}, indicating that this molecule aggregates in a way similar to the chlorophyll pigments.

*Abstract from Biochim. Biophys. Acta 172, 476 (1969).

OPTICAL PROPERTIES OF THE PROTOCHLOROPHYLL PIGMENTS. II. ELECTRONIC ABSORPTION, FLUORESCENCE, AND CIRCULAR-DICHROISM SPECTRA*

Claude Houssier and Kenneth Sauer

The electronic absorption spectroscopic properties of the protochlorophyll pigments are analyzed by means of the fluorescence excitation and emission spectra, fluorescence polarization, and circular dichroism. From the fluorescence emission and polarization spectra, assignments of the visible absorption bands to four electronic transitions and their vibrational components are made, and their relative orientations are deduced. The main red and blue bands of the protochlorophyll pigments show parallel polarization to each other, in contrast with the case of the chlorophylls, where they are perpendicular. On the other hand, the first vibrational overtone of the red band presents a mixed x-y polarization. The circular-dichroism spectra correlate with the fluorescence polarization data, the red and blue regions each showing two circular-dichroism bands of opposite signs.

The results are discussed in connection with the theoretical data available for the porphyrin pigments.

*Abstract from Biochim. Biophys. Acta 172, 492 (1969).

PIGMENT ANTENNAS AND REACTION CENTERS IN PHOTOSYNTHESIS

Kenneth Sauer and Edward A. Dratz

An antenna of light-harvesting chlorophyll molecules surrounding and feeding electronic excitation energy to a small group of molecules in a reaction center has been proposed as a model for energy focusing in the photosynthetic apparatus.[1] The studies by Emerson and Arnold, using brief flashes of illumination, showed that photons absorbed by any one of an array of hundreds of chlorophyll molecules lead to the activation of a single dark-reaction site.[2,3] There is an obvious advantage for organisms with large pigment antennas in that even at relatively low light levels they are able to carry out the necessary metabolic reactions to maintain their cellular vitality. For other purposes--for example, the commercial production of algal carbohydrates and proteins in ponds at high light intensity, or the maintenance of a thermal balance under desert conditions--it may be advantageous to have relatively small antennas associated with each reaction center.

Chlorophyll Antennas

The composition and size of the pigment antennas can be determined from activation spectra of photosynthesis, from measurements of maximum yields of photosynthetic electron transport in saturating flashes, from stoichiometric ratios of pigments to active components such as P700, P870, cytochromes, fluorescence quenchers, etc., and from the threshold levels for the action of certain inhibitors.

Until recently it has been generally assumed that the simplest situation exists in the photosynthetic bacteria, in which the pigments consist of bacteriochlorophyll and carotenoids. It appeared that only one light reaction was involved in initiating bacterial photosynthetic electron transport, and that very probably all the pigment molecules belonged to a single light-harvesting antenna. Clayton has estimated the ratio of total bacteriochlorophyll to the reaction center pigment P870 to be 10–20 to 1 in R. spheroides, on the basis of absorption band areas.[4,5] This is, as we shall see, a rather small antenna size in comparison with those observed in higher plants and algae. At the same time there is kinetic evidence that the antenna molecules with their reaction centers are not separated into individual packages. It appears that a given antenna molecule is able to transfer its excitation to any one of at least seven reaction centers in its vicinity.[6] The close proximity and strong interactions that exist among the antenna chlorophyll molecules account for the highly efficient transfer and utilization of electronic excitation energy originating in molecules throughout the antenna. Evidence is also seen in the long-wavelength shifts in the absorption spectra and, more specifically, in the enhanced optical rotatory dispersion (ORD) and circular dichroism (CD) of the light-harvesting pigments from a variety of photosynthetic bacteria.[7]

New evidence based on the activation spectra of complex cytochrome absorption changes suggests that there are at least two light reactions and two distinguishable antenna arrays in several photosynthetic bacteria.[8,9] The precise disposition and function of the pigments in these two photosystems can only be guessed at present. Significant differences have been reported for the quantum yields for P870 photoxidation and for associated cytochrome oxidation. In the former case estimates indicate that one P870 is oxidized in a one-electron reaction for each two photons absorbed,[10,11] although a higher value of approximately one electron per photon has been reported recently.[12] The oxidation of the cytochrome C423.5 in Chromatium, in which it appears to be closely coupled to $P870^+$ reduction, occurs with a quantum yield at least twice as large.[13-15] This may come about as a consequence of the transfer of two equivalents of electrons from cytochrome to an acceptor for each quantum absorbed leading to photoconversion of P870, as suggested by Loach.[15] At the same time, under some experimental circumstances the P870 photooxidation occurs with a quantum yield of only 0.5, which may be because only half the antenna bacteriochlorophyll (BChl) molecules transfer their electronic excitation energy to this reaction-center molecule. The final decision on the antenna size and composition in photosynthetic bacteria clearly must await more detailed experimental findings.

In higher plants and algae, the antenna systems have been somewhat better studied. Starting with the pioneering experiments of Emerson and Arnold in the early 1930's, long series of studies using saturating, brief flashes of light have been reported.[16] We will follow the suggestion of Kok[17] in reporting antenna sizes on the basis of electrons transferred and assuming a value of eight photons absorbed in two light reactions per O_2 evolved. Most of the early values should be reduced eightfold to compare with numbers quoted more recently. On this basis antenna sizes of about 300 chlorophylls per functional photosynthetic unit were observed under a variety of experimental conditions and for several species of plants and

algae. A larger unit is observed for submillisecond flashes than for those of 2 to 100 msec duration,[17-19] and some increase occurs with increasing age of algal cultures.

Recently we have studied the antenna sizes for electron transport reactions associated with only photosystem 1 on the one hand and only photosystem 2 on the other.[20] Not only are these two pigment systems distinguishable on an absorption- or activation-spectrum basis,[21,22] but they also exhibit different functional unit sizes in flashing light experiments. Photosystem 1 appears to consist of 440 chlorophylls per rate-limiting step, whereas photosystem 2 has only 55 to 70. The 440-to-1 stoichiometric ratio of chlorophyll to P700,[23,24] or to cytochrome f,[25] in photosystem 1 suggests that this represents the actual size of a single unit. There is no evidence that either the P700 or the cytochrome f is involved in a kinetic pool, which would make the actual unit some integral multiple of 440 molecules.

For photosystem 2 there is good evidence that such a pool does exist. One candidate for a pool of electron acceptors for photosystem 2 is plastoquinone, which exists as several molecular species in chloroplasts[26] and is present at a total concentration some 90 times as large as P700 or cytochrome f.[27] Kinetic experiments give evidence of pools 8 to 18 times that of P700 for the acceptor of photosystem 2.[28-32] This could easily account for the fact that the number of chlorophylls in the functional photosynthetic unit for the ferricyanide or DCPIP Hill reaction is only one eighth that for a photosystem 1 reaction.[20] Whether there are eight reaction centers in system 2 for each one in system 1, or whether the reaction centers in system 2 are equal in concentration to those in system 1 but feed a pool containing an eightfold larger concentration of electron acceptors, is currently a subject of controversy.[17,33] The latter hypothesis is favored by the observations that for submillisecond flashes the functional unit for photosystem 2 increases in size[17] and that very small absorption changes appear to be associated with the reaction-center chlorophyll in system 2.[34]

At present there are no convincing experiments which indicate whether the reaction centers in higher plant chloroplasts are immersed in large continuous pools of chlorophylls. The question of the possibility of energy transfer between photosystems 1 and 2 has led to the formulation of "spillover" and "separate package" hypotheses. This problem has been much studied, but no clear decision between the two alternatives is possible at present.[35-37] The twofold decrease in quantum yields for photosystem 1 reactions in going from long to short wavelengths indicates that energy absorbed by system 2 at short wavelengths cannot be used to drive a system 1 reaction.[22,38,39] This would appear to support the separate-package hypothesis. On the other hand, kinetic analysis by Malkin of a wide variety of data on enhancement of photosynthesis using two wavelengths of light generally supports the spillover hypothesis.[36] Similar analysis by Williams of different experimental data comes to the opposite conclusion and supports the separate-package hypothesis.[37]

The results reported by Avron in these proceedings show that in two cases reactions which are thought to involve only photoreaction 1 are able to make full use of the entire pigment complement of chloroplasts.[40] These important observations, together with his determination of a quantum yield of unity for the ferricyanide Hill reaction at wavelengths below 670 nm, require a profound reevaluation of existing models for the pig-

ment system–reaction center relationships in higher plant photosynthesis.

From studies of the minimum amount of the oxygen evolution inhibitor DCMU sufficient to block electron flow from water, Izawa and Good reached the conclusion that one molecule of DCMU per 2500 chlorophylls in chloroplasts is enough to stop the reaction.[41] Apart from complications associated with the presence of bound but apparently inactive DCMU, this evidence suggests that a much larger unit is present if oxygen evolution sites are used as the point of reference. It may be that several of the smaller quantasome-size units cooperate for this purpose, and that oxygen evolution occurs at more thinly distributed locations in the chloroplast lamellae. The direct interference of DCMU with electron transport, as witnessed by its effect on fluorescence and absorption transients, appears to be in conflict with such a picture, however.

Reaction Centers

The reaction centers of the purple bacteria contain the pigment absorption components designated P800 and P870, which arise from molecules involved along with an electron acceptor and a cytochrome in the trapping of photons absorbed by the antenna BChl and in the initiation of electron transport.[1] The preparation by Clayton and others of bacterial chromatophores from which the antenna pigments have been removed permits the detailed study of the optical properties of the reaction-center pigments.[4,5,42,43]

For R. spheroides, Clayton has shown that P800 and P870 exist in a ratio of 2 to 1, and that upon illumination by visible light a complete bleaching of the P870 occurs, accompanied by a blue shift of the P800 band.[43] Furthermore, there is present an amount of oxidizable cytochrome very nearly equivalent stoichiometrically to the P870 and closely coupled to it. These observations suggest that the reaction center (RC) contains three (or some integral multiple of three) bacteriochlorophyll molecules, one of which becomes oxidized upon illumination.

We have studied the circular dichroism spectra of RC preparations made from chromatophores of a carotenoidless mutant of R. spheroides (R-26) either by oxidation with excess chloroiridate[44] or by extraction with the nonionic detergent Triton X-100[5] to remove the antenna pigments. CD measurements were made by using a special instrument, already described.[7,45] The absorption and CD spectra of these preparations have been presented in detail[46] and some of the results are summarized in Fig. 1. The solid curves show the RC sample in its normal, reduced condition; the dashed curves show the spectra of the same material when it is being illuminated simultaneously from the side by use of visible light from a tungsten lamp. Complementary color filters are used to prevent the activating light from interfering with the CD measurements.

In its unactivated or reduced state, the RC preparation exhibits a positive CD component at 860 nm and a negative double CD with a crossing at 802 nm. The latter feature presumably arises from an exciton splitting of the P800 absorption that is too small to resolve in the absorption spectrum. Thus, we have evidence from the CD spectrum of the presence of three BChl exciton components in the reaction center. It can be shown by straightforward theoretical arguments that the three CD components can arise from no fewer than three different BChl molecules. The negative CD component at 748 nm almost certainly is associated with the absorption band at 758, which probably arises from

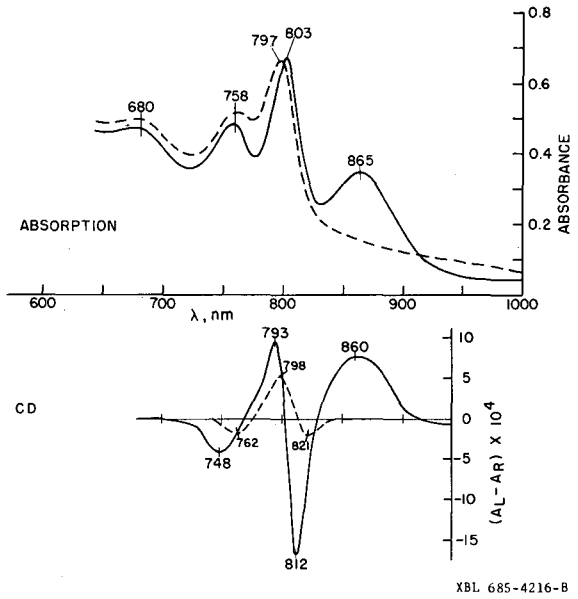

Fig. 1. Absorption and CD spectra of the reaction centers of R. spheroides, R-26 mutant, isolated by the Triton X-100 method of Reed and Clayton (Ref. 5). Solid curves: normal or reduced preparation. Dashed curves: sample under simultaneous side illumination with strong visible light. Path lengths 0.5 cm.

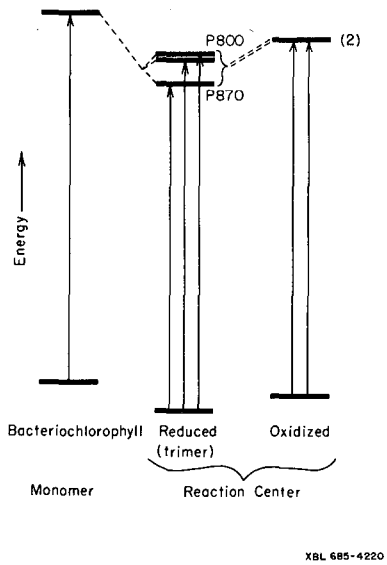

Fig. 2. Electronic energy level diagram for bacteriochlorophyll monomers and reaction-center trimers.

bacteriopheophytin. The close correspondence in behavior of the P870 and the P800 features[44] strongly suggests that the three molecules are all interacting with one another in a trimer. An energy level diagram which illustrates this interaction is shown in Fig. 2.

Upon illumination or upon chemical oxidation with ferricyanide or chloroiridate, the P870 bleaches and the P800 absorption band at 803 shifts to 797 nm, with no change in band area. The overall effect is that one-third of the total absorption is lost in this conversion. At the same time the CD band at 860 disappears and a new positive CD component forms, centered at 798 nm.[46] This can be accounted for most easily if we assume that in the oxidized state the two remaining BChl molecules no longer interact electronically with one another, either because they are too far apart or because they are unfavorably oriented with respect to each other. A detailed description of this argument is given by Sauer, Dratz, and Coyne.[46]

On the basis of this interpretation of the CD spectra we propose an elaboration of Clayton's model[1] for illustrating the nature and function of the reaction center in photosynthetic bacteria. In this expanded model three BChl molecules are arranged, pre-

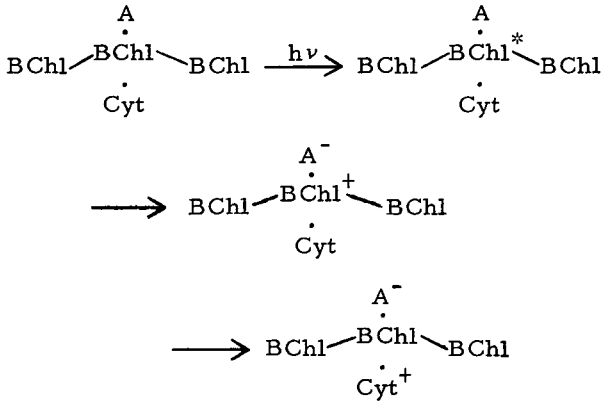

sumably, in a strongly interacting trimer and are closely associated with an electron acceptor (probably ubiquinone) and an electron donor, cytochrome. Upon illumination one of these BChl molecules is converted to the oxidized form ($BChl^+$), which has a different set of electronic energy levels and, hence, a different absorption spectrum. The two remaining BChl molecules do not interact strongly with one another, perhaps because they are located more or less on opposite sides of the bleached molecule. In an ensuing dark step the $BChl^+$ picks up an electron from a cytochrome and returns to its reduced state. All of this occurs within 2 μsec if a brief flash of activating light is used.[47]

In higher plants and algae less is known about the nature of the molecular structure of the reaction centers. For photosystem 1 there exists a well-documented chlorophyll species,[22,45] designated P700, which has many characteristics similar to that of P870 in bacteria. Nothing analogous to the P800 blue shift has been observed, so we have no indication as yet that chlorophyll a trimers are involved in chloroplasts. It has not yet been possible to purify reaction centers from higher plants. Döring et al.[32] have recently reported evidence based on photo-induced absorption changes that there is an analogous reaction-center pigment for photosystem 2; however, it has not been characterized in any detail. When we come to know better the similarities and differences among the reaction-center molecular structures for the different kinds of photosynthetic organisms, we may be in a position to guess the pathway along which they evolved and the nature of the responses which arose in response to pressures from the environment.

References

1. R. K. Clayton, Science 149, 3690 (1965).
2. R. Emerson and W. Arnold, J. Gen. Physiol. 15, 391 (1932).
3. R. Emerson and W. Arnold, ibid. 16, 191 (1932).
4. R. K. Clayton, Biochim. Biophys. Acta 75, 312 (1963).
5. D. W. Reed and R. K. Clayton, Biochem. Biophys. Res. Commun. 30, 471 (1968).
6. R. K. Clayton, J. Theoret. Biol. 14, 173 (1967).
7. E. A. Dratz, A. J. Schultz, and K. Sauer, Brookhaven Symposia in Biology 19, 303 (1966).
8. S. Morita, Biochim. Biophys. Acta 153, 241 (1968).
9. C. Sybesma and C. F. Fowler, Proc. Natl. Acad. Sci. U. S. 61, 1343 (1968).
10. R. K. Clayton, Photochem. Photobiol. 1, 305 (1962).
11. W. J. Vredenberg and L. N. M. Duysens, Nature 197, 355 (1963).
12. T. Beugeling, Biochim. Biophys. Acta 153, 143 (1968).
13. J. M. Olson, Science 135, 101 (1962).
14. W. J. Vredenberg and L. N. M. Duysens, Biochim. Biophys. Acta 79, 456 (1964).
15. P. A. Loach, Biochemistry 5, 592 (1966).
16. E. Rabinowitch, Photosynthesis, Vol. II, Part 2 (Interscience Publishers, New York, 1956), p. 1274.
17. B. Kok, Biochim. Biophys. Acta 21, 245 (1956).
18. H. Gilmour, R. Lumry, J. Spikes, and H. Eyring, Nature 173, 31 (1954).
19. F. Allen and J. Franck, Arch. Biochem. Biophys. 58, 124 (1955).
20. J. Kelly and K. Sauer, Biochemistry 7, 882 (1968).

21. K. Sauer and R. B. Park, ibid. 4, 2791 (1965).
22. J. Kelly and K. Sauer, ibid. 4, 2798 (1965).
23. B. Kok and G. Hoch, in Light and Life, W. D. McElroy and B. Glass, Eds. (Johns Hopkins University Press, Baltimore, Md., 1961), p. 397.
24. J. M. Anderson, D. C. Fork, and J. Amesz, Biochem. Biophys. Res. Commun. 23, 874 (1966).
25. N. K. Boardman and J. M. Anderson, Biochim. Biophys. Acta 143, 187 (1967).
26. M. D. Henninger and F. L. Crane, J. Biol. Chem. 241, 5190 (1966); 242, 1155 (1967).
27. H. K. Lichtenthaler and R. B. Park, Nature 198, 1070 (1963).
28. P. Joliot, J. Chim. Phys. 58, 570, 584 (1961).
29. P. Joliot, Biochim. Biophys. Acta 102, 116 (1965).
30. H. T. Witt, G. Döring, B. Rumberg, P. Schmidt-Mende, V. Siggel, and H. H. Stiehl, Brookhaven Symposia in Biology 19, 161 (1966).
31. S. Malkin and B. Kok, Biochim. Biophys. Acta 126, 413 (1966).
32. B. Kok, in Proceedings of the International Congress on Photosynthesis, Freudenstadt, Germany, June 1968 (in press).
33. S. Malkin, Biochim. Biophys. Acta 126, 433 (1966).
34. G. Döring, H. H. Stiehl, and H. T. Witt, Z. Naturforsch. 22b, 639 (1967).
35. T. T. Bannister and M. J. Vrooman, Plant Physiol. 39, 622 (1964).
36. S. Malkin, Biophys. J. 7, 629 (1967).
37. W. P. Williams, Biochim. Biophys. Acta 153, 484 (1968).
38. G. Hoch and I. Martin, Arch. Biochem. Biophys. 102, 430 (1963).
39. K. Sauer and J. Biggins, Biochim. Biophys. Acta 102, 55 (1965).
40. M. Avron, in Proceedings of the International Congress on Photosynthesis, Freudenstadt, Germany, June 1968 (in press).
41. S. Izawa and N. E. Good, Biochim, Biophys. Acta 102, 20 (1965).
42. I. D. Kuntz, Jr., P. A. Loach, and M. Calvin, Biophys. J. 4, 227 (1964).
43. R. K. Clayton, Photochem. Photobiol. 5, 669 (1966).
44. R. K. Clayton and W. R. Sistrom, ibid. 5, 661 (1966).
45. E. A. Dratz, Ph. D. Thesis, University of California, Berkeley, 1966.
46. K. Sauer, E. A. Dratz, and L. Coyne, Proc. Natl. Acad. Sci. U. S. 61, 17 (1968).
47. W. Parson, Biochim. Biophys. Acta 153, 248 (1968).
48. B. Kok, ibid. 48, 527 (1961).

BASE SEQUENCE STUDIES OF NUCLEIC ACIDS

I. Tinoco, Jr.

The research has been mainly in two areas: the sequence determination of bases in nucleic acids and the conformation of nucleic acids. The sequence studies reported here were done by Dr. David Lloyd in collaboration with Dr. Stanley Mandeles of the Space Sciences Laboratory. The optical properties for different conformations of nucleic acids discussed in this report were calculated by Dr. W. C. Johnson, Jr.

Tobacco mosaic virus ribonucleic acid (TMV-RNA) contains about 6400 bases. When a T-1 ribonuclease hydrolysate of TMV-RNA is chromatographed in a system designed to separate oligonucleotides on the basis of chain length, the elution profile shown in Fig. 1 is obtained. Mandeles[1] has designated the longest-chain-length component of the elution profile as the Ω fraction and the second to the last peak as the ψ fraction. No uv-absorbing material is eluted beyond these two peaks, even in 1 M NaCl. The yields of oligonucleotide in the ψ and Ω fractions resulting from the chromatography of 200 mg of hydrolyzed TMV-RNA were found to be approximately 1.5 and 2.0 mg, respectively, as determined from the 260-mμ absorbance.

When the ψ and Ω fractions were rechromatographed in a chain-length separation system it was found that no further resolution was obtained. However, since the rechromatography did appear to remove small amounts of impurities contained in the original ψ and Ω fractions, this step was retained in the routine isolation of these oligonucleotide fractions.

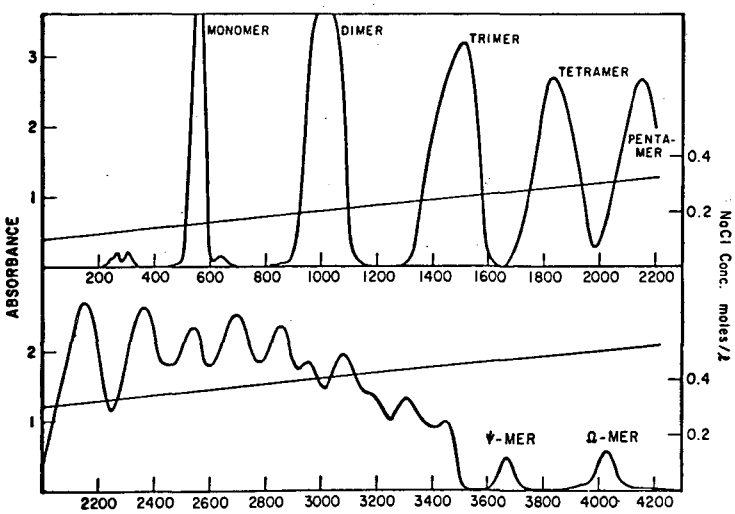

XBL 696-810

Fig. 1. The chromatographic separation of oligonucleotides according to chain length. A column (1.5×60 cm) containing 100 ml of DEAE Sephadex, A-25, was loaded with 200 mg of a T-1 RNase hydrolysate of TMV-RNA. The elution was performed with a linear concentration gradient from 0.1 to 0.6 M NaCl in 5 liters of 7 M urea, pH 7.5, at a flow rate of 40 ml/hr.

When the rechromatographed fractions were subjected to further chromatography at pH 2.8 to effect a separation on the basis of uridine content, the ψ fraction was resolved into two components containing equal amounts of oligonucleotide, as judged from the 260-mμ absorbancies. These fractions were designated ψ-1 and ψ-2 in the order in which they were eluted. In contrast to the behavior of the ψ fraction, Ω fraction was eluted as a single peak upon chromatography at pH 2.8. The results of the low-pH chromatography also indicated that the rechromatographed Ω fraction was free of minor contaminants.

On the basis of the results obtained from the isolation procedure described above, it appeared that each of the three oligonucleotide fractions was homogeneous and probably contained a nucleotide sequence unique to some location in the TMV-RNA molecule. We shall refer to these unique oligomers as the ψ-1-mer, ψ-2-mer, and Ω-mer.

The ψ-mers and Ω-mer were each subjected to treatment with pancreatic ribonuclease. The products of the pancreatic ribonuclease digestion were then separated and identified to provide pancreatic fingerprints of the three oligonucleotides. The pancreatic ribonuclease hydrolysates were separated chromatographically on a DEAE sephadex column by use of a combination of linear KCl and HCl gradients. The identities of oligomers eluted from the column were assigned from their elution positions and a knowledge of the specificities of T-1 and pancreatic ribonuclease. These assignments were checked by comparing the uv absorption spectra of the oligomers eluted from the column with known oligomers and, where necessary, by rechromatography with known oligomers. In all cases the results lead to an unambiguous identification. The profiles shown in Fig. 2a, b, c show the elution positions of the fragments obtained by pancreatic ribonuclease digestion of the ψ-1-mer, ψ-2-mer, and Ω-mer.

The portions of the eluent containing the pancreatic ribonuclease digestion products were quantitatively collected, and their volumes were accurately measured. The uv absorption spectrum of each fraction was measured and the number of 260-mμ absorbance units present in the fraction was computed. These values were converted to micromolar values. The three oligomers being investigated are the products of complete digestion with T-1 ribonuclease, which causes cleavage after guanine, and should therefore each contain a single terminal guanine residue. Thus, the mole ratios of each oligomer isolated from the pancreatic ribonuclease digest, relative to guanadylic acid, should have integral values equal to the number of moles of each oligomer per mole of ψ-1-mer, ψ-2-mer, or Ω-mer. Table I shows the mole ratios obtained for two different digests of each of the three T-1 ribonuclease fragments.

A study of the fragments produced by pancreatic ribonuclease hydrolysis of the ψ-mers and Ω-mer reveals a number of intriguing facts. Knowledge of the genetic code[2] allows one to work backwards from the amino acid sequence of TMV coat protein[3] to determine the nucleotide sequence of the coat protein gene. Because of the degeneracy in the code, one arrives at not one but a number of possible nucleotide sequences. An examination of these sequences reveals that none of them could give rise to the ψ-mers or Ω-mer upon T-1 ribonuclease digestion. This observation is in agreement with the findings of Knight and his co-workers,[4] who have determined that both the local lesion gene and the coat protein gene are located in the 3' linked half of the RNA strand. The ψ-mers and Ω-mer are all located nearer to

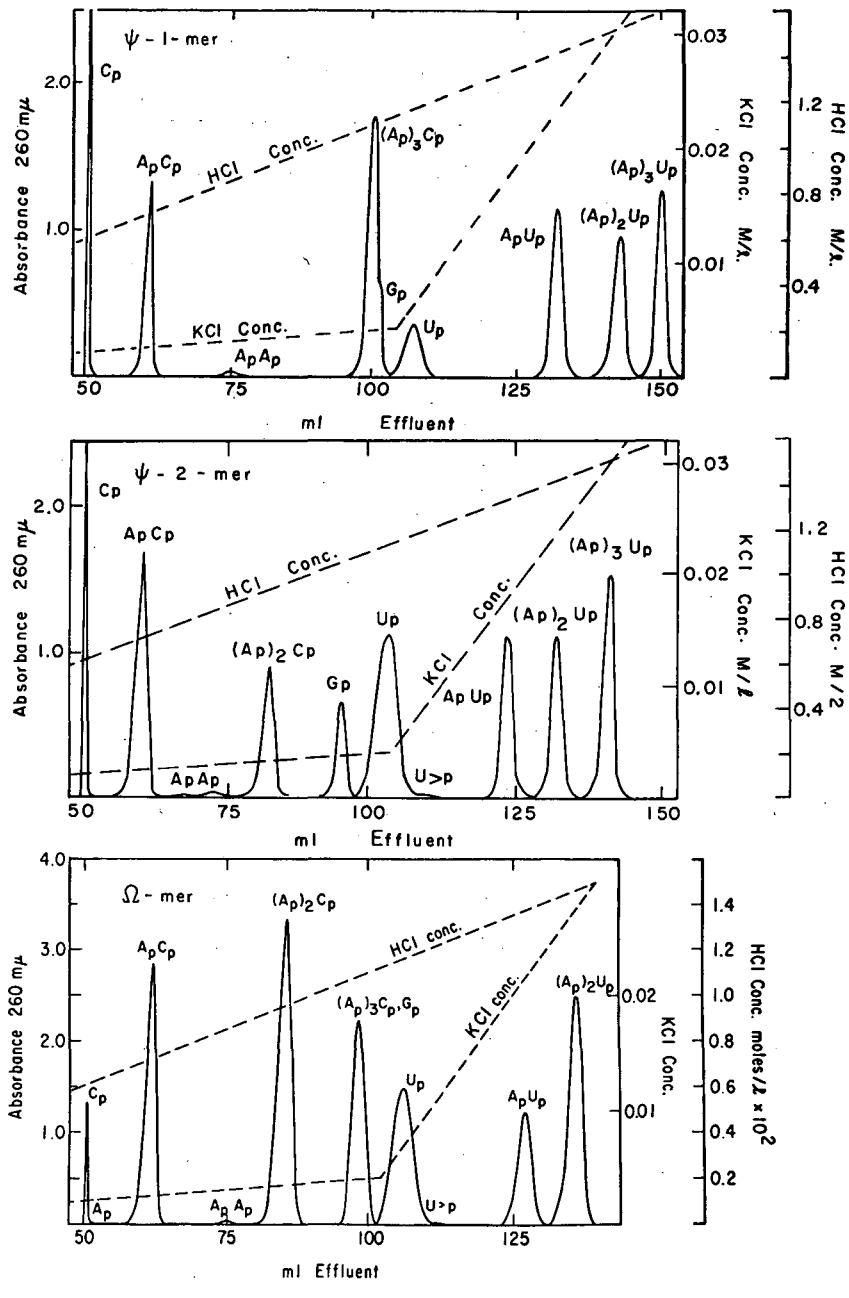

Fig. 2. The separation of the pancreatic RNase digestion fragments of (a) the ψ-1-mer, (b) the ψ-2-mer, (c) the Ω-mer. A column (0.4 × 35 cm) containing 4 ml of DEAE Sephadex, A-25, was loaded with 0.5 to 2.0 mg of a pancreatic RNase hydrolysate of the ψ-1-mer, ψ-2-mer, or Ω-mer. The elution was performed with a combination of gradients linear in KCl and HCl concentration.

Table I. Pancreatic fingerprints of the Ω-mer and ψ-mers.

	Ω-mer		ψ-1-mer		ψ-2-mer	
Digestion fragment	Fragment concentration[a] (μmoles per μmole Gp)	Closest integral value	Fragment concentration[a] (μmoles per μmole Gp)	Closest integral value	Fragment concentration[a] (μmoles per μmole Gp)	Closest integral value
Gp	1.00	1	1.00	1	1.00	1
Cp	1.05	1	3.86	4	2.08	2
ApCp	6.08	6	1.94	2	2.02	2
$(Ap)_2Cp$	6.04	6	not present	0	1.06	1
$(Ap)_3Cp$	1.96	2	0.92	1	not present	0
Up	12.00	12	2.04	2	5.30	5
ApUp	2.96	3	1.90	2	2.00	2
$(Ap)_2Up$	3.96	4	0.98	1	1.05	1
$(Ap)_3Up$	not present	0	0.93	1	1.04	1
Ap	0.10	0	0.04	0	0.05	0
ApAp	0.03	0	0.02	0	0.02	0
	$A_{35}U_{19}C_{15}G$		$A_{12}U_6C_7G$		$A_{11}U_9C_5G$	

a. Average of the values obtained from two experiments.

the 5' linked end of the TMV-RNA molecule.

The Ω-mer stands out among the three fragments that have been investigated, both because of its base composition and because of its nearest-neighbor frequencies. It possesses a sequence of 69 nucleotides from which Gp is totally absent. Furthermore, roughly half of the 69 nucleotides are Ap. Out of the total of 19 uracil residues, 7 are preceded by adenine and 12 are preceded by a pyrimidine; but of the 15 cytosine residues, only a single residue follows a pyrimidine. The remaining cytosine residues all follow adenine. The nucleotide composition and nearest-neighbor frequencies severely restrict the amino acids for which the Ω-mer could code. The absence of guanine in the sequence excludes all amino acids whose code words must contain G. The nearest-neighbor frequencies restrict the occurrence of lysine and those amino acids whose code words contain a C following a pyrimidine. Finally, the large A content demands that between 12 and 19 of the 23 amino acids being coded must come from the group asparagine, glutamine, methionine, and threonine.

References

1. S. Mandeles, J. Biol. Chem. 243, 3671 (1968).
2. M. Nirenberg, T. Caskey, R. Marshall, R. Brimacombe, D. Kellogg, B. Doctor, D. Hatfield, J. Levin, F. Rottman, S. Peska, M. Wilcox, and F. Anderson, Cold Spring Harbor Symp. Quant. Biol. 21, 11 (1966).
3. G. Fantatsu, A. Tsugita, and H. Fraenkel-Conrat, Arch. Biochem. Biophys. 103, 25 (1964).
4. C. I. Kado and C. A. Knight, Biochemistry 55, 1276 (1966); J. Mol. Biol. 36, 15 (1968).

CONFORMATION OF NUCLEIC ACIDS

I. Tinoco, Jr.

One important problem in science today is the understanding of how the chemical structure of nucleic acids controls their biological properties. To study this problem, many workers have measured the circular dichroism (CD) or the optical rotatory dispersion (ORD) of both natural and synthetic polynucleotides in aqueous solution. Interpretation of these spectra can give information about the conformation of each polymer in solution and perhaps help determine its sequence. To aid in the interpretation of measured CD spectra, we have applied a particularly simple theory of circular dichroism to the polynucleotides.

The quantum mechanical theory of optical activity was derived in 1928.[1] Since then many specific (but approximate) equations based on the general theory have been developed.[2,3] We have applied a particularly simple method[4] to the circular dichroism of polynucleotides. The resulting equation is

$$\epsilon_L - \epsilon_R(\nu) = \frac{\pi\nu}{c} f(\nu - \bar{\nu}) \times \sum_{i,j}{}' \sum_{a} \nu_{i0a} \left[\sum_{s,t} \frac{\rho_s^{i0a}}{r_{st}^3} \underset{\sim}{r}_{st} \right] \times a_t^j \times \underset{\sim}{\mu}_{i0a} \cdot \underset{\sim}{R}_{it} + \frac{\pi}{2c} \frac{\partial f(\nu - \bar{\nu})}{\partial \nu} \times \sum_{i,j}{}' \sum_{a,b} \nu_{i0a} \left[\sum_{s,t} \frac{\rho_s^{i0a} \rho_t^{i0b}}{r_{st}} \right] \times \underset{\sim}{R}_{ij} \cdot \underset{\sim}{\mu}_{i0a} \times \underset{\sim}{\mu}_{j0b} \cdot \qquad (1)$$

The notation is the same as in Ref. 4.

Equation (1) is particularly easy to apply. Only the properties of the monomers need be known, and the sums can be carried out on a computer. The first sum in each term shows that we must consider each monomer and its interaction with every other monomer. Consider a typical monomer buried in the middle of the polymer. If we consider DNA and RNA, the monomer may be any one of four bases--adenine, cytosine, guanine, or uracil. It may interact with any one of the four bases, so that, in general, there are sixteen possible types of base-base interactions. In practice, since the rotational strength varies with distance roughly as $1/R^2$, only one turn above and below the typical base need be calculated to insure convergence. We neglect end effects, which is a reasonable approximation for a larger polymer when the interactions fall off rapidly with distance.

The second sum in each term involves the transitions in the region of interest, here the near-ultraviolet region, above 220 mμ. We consider each base to have two $\pi \rightarrow \pi$ transitions in this region (this is predicted by H. Berthold et al.[5] for all bases, including adenine and uracil), with maxima between 240 and 280 mμ. We take $\bar{\nu} = 38\,400$ cm^{-1} (260 mμ). The third sum is over monomer "groups." We divide each base into "groups," where a group is any major atom (not a hydrogen atom) together with its hydrogen atoms.

The CD curves for various polynucleotides, calculated by using Eq. (1), are given in Figs.

1 through 3. They are compared with measured CD curves whenever possible. In some cases, measured ORD curves were transformed to CD, by use of the Kronig-Kramers relation, for comparison with the calculated curves. Note that the scale of the ordinate varies with each section of the figures. In all cases the measured or transformed curves are given by the solid line, and the calculated curves by the broken lines.

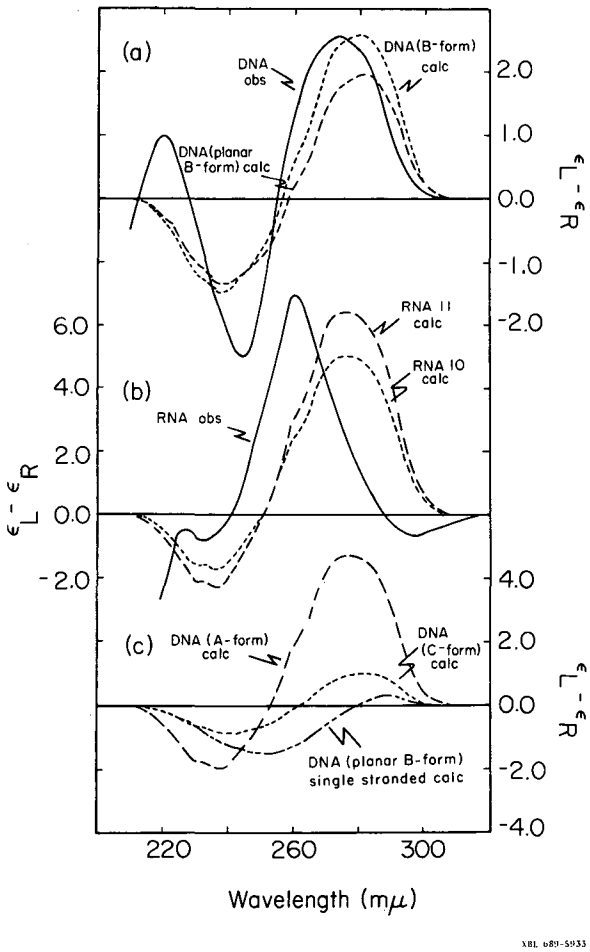

Fig. 1. (a) Measured CD of DNA together with the calculated curves for two possible configurations. (b) Measured CD of RNA compared with the calculated spectra for two conformations. (c) Calculated CD curves for A-form, C-form, and single-stranded DNA.

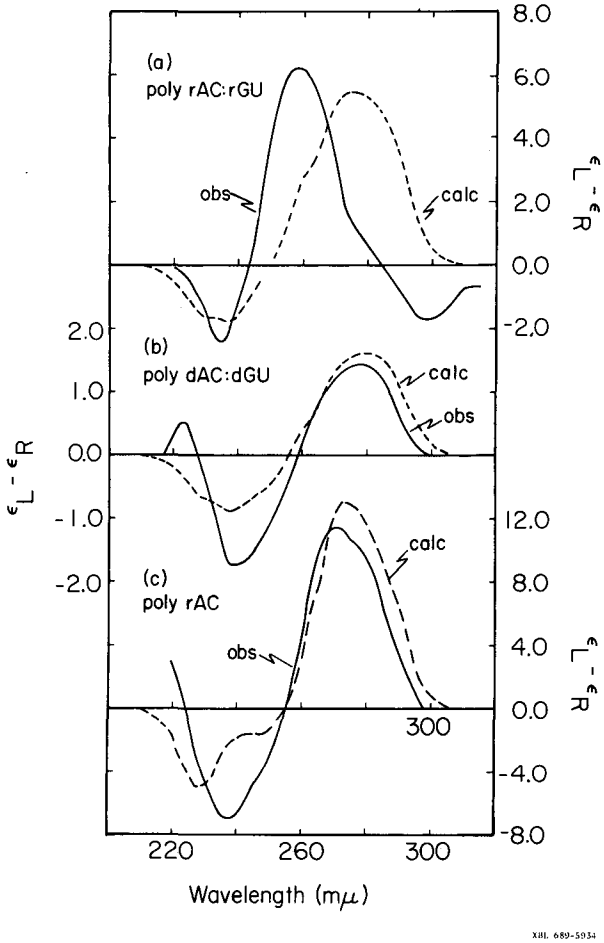

Fig. 2. (a) Calculated and observed CD spectra for poly rAC:rGU. (b) Calculated and observed curves for poly dAC:dGU. (c) CD spectrum of poly rAC, calculated and observed.

The simple theory does a surprisingly good job of predicting the optical properties of polynucleotides. Its primary weakness is its inability to predict the position of extrema accurately. At present we are not able to say whether the other weaknesses in our calculations are due to inaccuracies in the theory, the conformations assumed for the polymers, or the data used.

The theory has many strengths. It shows that the circular dichroism of polynucleotides can be calculated from base-base interactions,

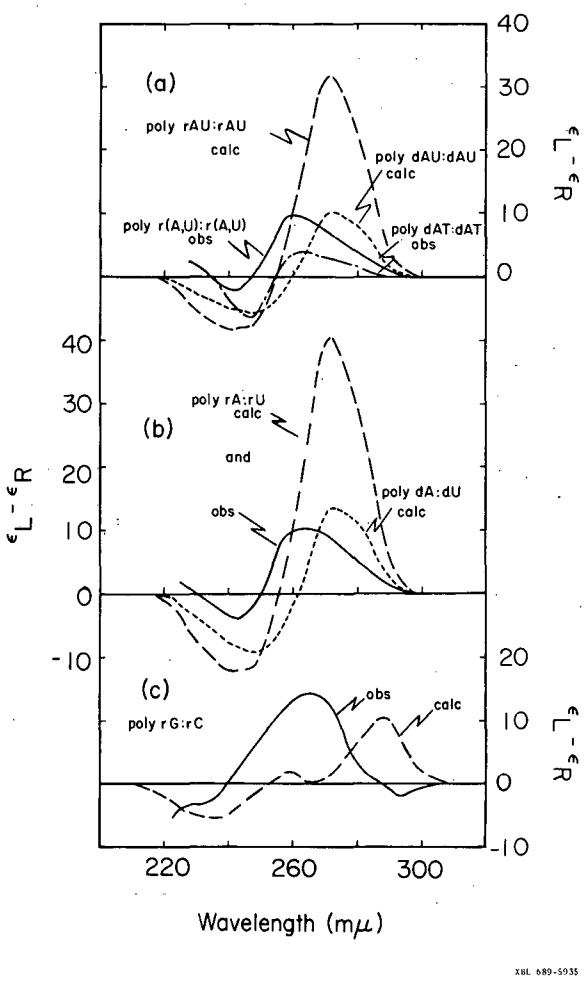

Fig. 3. (a) Calculated and measured CD spectra of the ribo- and deoxy- forms of poly AU:AU. (b) Measured and calculated spectrum of poly rA:rU and calculated curve for poly dA:dU. (c) CD spectrum of poly rG:rC observed and calculated.

rather than base-sugar interactions, and that it arises for the most part from the $\pi \rightarrow \pi^*$ transitions, rather than $n \rightarrow \pi^*$ transitions. For the nucleic acids, the simple theory predicts (as observed) that DNA will have a conservative spectrum while RNA will have a more intense nonconservative spectrum because its tilted bases allow the polarizabilities to contribute. The anomalously low magnitude of nucleic acid CD is shown to come naturally from the cancellation of the rotation strengths of the many bands. However, the theory may predict the wrong dependence of DNA rotational strength[6] on GC content. If the conformation of DNA changed with G-C content, or if the DNA were more rigid for a higher G-C content, the experimental change in CD could be understood. Although all we can say with certainty is that DNA in 80% alcohol solution[7] has its bases tilted, calculation of the CD of the A-form of DNA leads us to tentatively suggest that DNA in 80% alcohol is in this form. We predict a CD spectrum for single-stranded DNA which is quite different from its spectrum in its other forms, so that it should be possible to test the hypotheses of Luzzati et al.[8] about their intermediate form of DNA in formaldehyde-saline solution. In contrast, we predict essentially the same CD spectrum for both single- and double-stranded RNA. Comparison with measurement[9] indicates that single-stranded RNA is in the same conformation as a single strand of a double-stranded RNA.

Comparison of measured[10] and calculated CD spectra of poly rAC:rGU and poly dAC:dGU show good agreement, confirming the observation[11] that the polydeoxynucleotide is in DNA configuration and allowing us to predict that the polyribonucleotide is in RNA form. These results indicate that the difference in optical properties between DNA and RNA is primarily due to difference in geometry caused by the different sugar backbone, and that the anomalously low intensity of the CD of the nucleic acids is not a consequence of their antiparallel sugar backbone. Calculations for poly rAU:rAU and poly dAU:dAU indicate that they are in RNA and DNA configuration respectively, in solution. However, the predicted magnitudes are too high. Results are not clear-cut for poly rA:rU. There is no agreement between cal-

culated and observed spectra for any of the four GC polymers.

Single-stranded polymers were also calculated, although it is hard to evaluate the results. Here are the highlights. Poly rA is predicted to be in single-stranded DNA conformation and nearly completely stacked at -2°C. Poly rAC appears to be completely stacked and in RNA conformation in solution at room temperature, while poly rGU is not stacked.

This work brings to light other points. The circular dichroism of DNA and RNA in aqueous solution appears to be consistent with the conformation found for the nucleic acids in the fibers used for x-ray work.[12-14] The magnitude of a CD spectrum is not an index of the degree of asymmetry (compare poly rA and DNA), as has been suggested.[15] In fact, it does not appear that the shape or magnitude of a CD spectrum can be used a priori to determine whether a polynucleotide is single- or double-stranded. Finally, it appears that nearest-neighbor calculations are often not valid. In RNA, for instance, the second and third neighbors together contribute more intensity to the circular dichroism curve than do the nearest neighbors.

References

1. L. Rosenfeld, Z. Physik 52, 161 (1928).
2. A. Moskowitz, Adv. Chem. Phys. 4, 67 (1962).
3. I. Tinoco, Jr., Adv. Chem. Phys. 4, 113 (1962).
4. I. Tinoco, Jr., J. Chim. Phys. 65, 91 (1968).
5. H. Berthold, C. Giessner-Prettre, and A. Pullman, Intern. J. Quantum Chemistry 1, 123 (1967).
6. T. Samejima and J. T. Yang, J. Biol. Chem. 240, 2094 (1965).
7. J. Brahms and W. F. H. M. Mommaerts, J. Mol. Biol. 10, 73 (1964).
8. V. Luzzati, A. Mathis, F. Mason, and J. Witz, J. Mol. Biol. 10, 28 (1964).
9. C. R. Cantor, S. R. Jaskunas, and I. Tinoco, Jr., J. Mol. Biol. 20, 39 (1966).
10. Donald Gray (Chemistry Department, University of California), personal communication.
11. R. Langridge, Abstract WB14 of the 10th National Meeting of the Biophysical Society, Boston, Massachusetts, 1966.
12. R. Langridge, D. A. Marvin, W. E. Seeds, and H. R. Wilson, J. Mol. Biol. 2, 38 (1960).
13. W. Fuller, F. Hutchinson, M. Spencer, and M. H. F. Wilkins, J. Mol. Biol. 27, 507 (1967).
14. S. Arnott, M. H. F. Wilkins, W. Fuller, and R. Langridge, J. Mol. Biol. 27, 535 (1967).
15. G. D. Fasman, C. Lindblow, and L. Grossman, Biochemistry 3, 1015 (1964).

PUBLICATIONS AND PAPERS PRESENTED, 1968

1. David F. Ilten, Maurits E. Kronenberg, and M. Calvin, Reversible EPR Photosignals in Charge-Transfer Complexes, Photochem. Photobiol. 7, 331 (1968).

2. A. Alkaitis and Melvin Calvin, The Photochemistry of Pyridine-N-Oxide, Chem. Commun. 1968, 292.

3. A. Yamamoto, L. K. Phillips, and M. Calvin, Coordination of Pyridine to Phthalocyaninomanganese and Etioporphyrin I Manganese Complexes, Inorg. Chem. 7, 847 (1968).

4. Jerry Han, E. D. McCarthy, Willian Van Hoeven, Melvin Calvin, and W. H. Bradley, Organic Geochemical Studies. II. The Distribution of Aliphatic Hydrocarbons in Algae, Bacteria, and in a Recent Lake Sediment: A Preliminary Report, Proc. Natl. Acad. Sci. U. S. 59, 29 (1968).

5. Melvin Calvin, New Keys to Life Processes, Perspectives Biol. Med. 11, 555 (1968).

6. Janet S. Splitter and Melvin Calvin, Irradiation of 3-Substituted 2-Phenyloxaziridines, Tetrahedron Letters, 1445 (1968).

7. Jerry Han, E. D. McCarthy, Melvin Calvin, and M. H. Benn, The Hydrocarbon Constituents of the Blue-Green Algae Nostoc muscorum, Anacystis nidulans, Phormidium loridium, and Chlorogloea fritschii, J. Chem. Soc. 1968, 2785.

8. Michael A. Harpold and Melvin Calvin, AMP on an Insoluble Solid Support, Nature 219, 486 (1968).

9. E. D. McCarthy, J. Han, and Melvin Calvin, Hydrogen Atom Transfer in Mass Spectrometric Fragmentation Patterns of Saturated Aliphatic Hydrocarbons, Anal. Chem. 40, 1475 (1968).

10. Melvin Calvin, Life's Origin and Its Implications, Sci. J. (London) 4, No. 7, 76 (1968).

11. J. A. Bassham, Martha Kirk, and R. G. Jensen, Photosynthesis by Isolated Chloroplasts. I. Diffusion of Labeled Photosynthetic Intermediates between Isolated Chloroplasts and Suspending Medium, Biochim. Biophys. Acta 153, 211 (1968).

12. R. G. Jensen and J. A. Bassham, Photosynthesis by Isolated Chloroplasts. II. Effects of Addition of Cofactors and Intermediate Compounds, Biochim. Biophys. Acta 153, 219 (1968).

13. R. G. Jensen and J. A. Bassham, Photosynthesis by Isolated Chloroplasts. III. Light Activation of the Carboxylation Reaction, Biochim. Biophys. Acta 153, 227 (1968).

14. J. A. Bassham and M. R. Kirk, Dynamic Metabolic Regulation of the Photosynthetic Carbon Reduction Cycle, in Comparative Biochemistry and Biophysics of Photosynthesis, ed. by K. Shibata, A. Takamiya, A. T. Jagendorf, and R. C. Fuller (University of Tokyo Press, Tokyo, Japan, 1968), 365-378.

15. Kam-sik Ng and J. A. Bassham, The Quantum Requirement of Photosynthesis in Chlorella, Biochim. Biophys. Acta 162, 254 (1968).

16. J. A. Bassham, P. Sharp, and I. Morris, Effect of Mg^{2+} Concentration on the pH Optimum and Michaelis Constant of the Spinach Chloroplast (Ribulose Diphosphate Carboxylase), Biochim. Biophys. Acta 153, 898 (1968).

17. Edward L. Bennett and Mark R. Rosenzweig, Brain Chemistry and Anatomy: Implications for Theories of Learning and Memory, in Mind as A Tissue, Charles Rupp, ed. (Hoeber Medical Division, Harper and Row, New York, 1968), 63-86.

18. Richard M. Lemmon, Abiogenic Synthesis of Biologically Relevant Organic Compounds ("Chemical Evolution") (UCRL-18108, March 1968), to appear in Foundations of Space Biology and Medicine.

19. Melvin P. Klein and Edward A. Dratz, Derivative Spectroscopy with Recording Spectrometers, Rev. Sci. Instr. 39, 397 (1968).

20. David E. Downie and Melvin P. Klein, Electroluminescence in Potassium Dihydrogen Phosphate, Appl. Optics 7, 1245 (1968).

21 D. Gill, M. P. Klein, and G. Kotowycz, Complete Determination of the Alignment of CH_2Cl_2-CD_2Cl_2 Molecules in Poly-γ-benzyl-L-glutamate Solution by the Nuclear Magnetic Resonance of ^{35}Cl, ^{2}D, and ^{1}H. Comparison of Electric and Magnetic Ordering, J. Am. Chem. Soc. 90, 6870 (1968).

22. A. Nath, M. Harpold, M. P. Klein, and W. Kündig, Emission Mössbauer Spectroscopy for Biologically Important Molecules: Vitamin B-12, Its Analogs, and Cobalt Phthalocyanine, Chem. Phys. Letters 2, 171 (1968).

23. C. S. Fadley, S. B. M. Hägstrom, M. P. Klein, and D. A. Shirley, Chemical Effects on Core-Electron Binding Energies in Iodine and Europium, J. Chem. Phys. 48, 3779 (1968).

24. R. L. Vold, J. S. Waugh, M. P. Klein, and D. E. Phelps, Measurement of Spin Relaxation in Complex Spin Systems, J. Chem. Phys. 48, 3831 (1968).

25. D. Gill, M. P. Klein, and M. Harpold, Spin Interactions in a Flexible Biradical in Nematic Liquid Crystals, Bull. Am. Phys. Soc. 13, 1671 (1968).

26. J. Palmer and V. Moses, The Role of the Regulator-Gene Product (Repressor) in Catabolite Repression of β-Galactosidase Synthesis in Escherichia coli., Biochem. J. 106, 339 (1968).

27. D. C. H. McBrien and V. Moses, Compartmentalization of the Metabolism of Lactose, Galactose, and Glucose in Escherichia coli, J. Gen. Microbiol. 51, 159 (1968).

28. V. Moses and M. D. Yudkin, Catabolite Repression in Escherichia coli: A Study of Two Hypotheses, Biochem. J. 110, 135 (1968).

29. D. A. Webster, D. P. Hackett, and R. B. Park, The Respiratory Chain of Colorless Algae. III. Electron Microscopy, J. Ultrastructure Res. 21, 514 (1968).

30. R. B. Park and L. K. Shumway, The Ultrastructure of Fracture and Deep Etch Faces of Spinach Thylakoids, in Comparative Biochemistry and Biophysics of Photosynthesis, ed. by K. Shibata, A. Takamiya, A. T. Jagendorf, and R. C. Fuller (University of Tokyo Press, Tokyo, Japan, 1968), 57-68.

31. Roderic B. Park and A. O. A. Pheifhofer, The Continued Presence of Quantasomes in Ethylenediaminetetra-acetate-Washed Chloroplast Lamellae, Proc. Natl. Acad. Sci. U. S. 60, 337 (1968).

32. T. Trosper, R. B. Park, and K. Sauer, Excitation Transfer by Chlorophyll a in Monolayers and the Interaction with Chloroplast Glycolipids, Photochem. Photobiol. 7, 451 (1968).

33. H. Rapoport, U. Eppenberger, and M. B. Warren, Jr., Stereochemie der Umwandling von Dihydrothebain in Thebain. Synthese von markierten Thebainen, Helv. Chim. Acta 51, 381 (1968).

34. Jeffrey Kelley and Kenneth Sauer, Functional Photosynthetic Unit Sizes for Each of the Two Light Reactions in Spinach Chloroplasts, Biochemistry 7, 882 (1968).

35. Kenneth Sauer, Edward A. Dratz, and Lelia Coyne, Circular Dichroism Spectra and the Molecular Arrangement of Bacteriochlorophylls in the Reaction Centers of Photosynthetic Bacteria, Proc. Natl. Acad. Sci. 61, 17 (1968).

36. Terry Trosper and Kenneth Sauer, Chlorophyll a Interactions with Chloroplast Lipids in vitro, Biochim. Biophys. Acta 162, 92 (1968).

37. R. C. Davis and I. Tinoco, Jr., Temperature-Dependent Properties of Dinucleoside Phosphates, Biopolymers 6, 223 (1968).

38. D. Glaubiger, D. A. Lloyd, and I. Tinoco, Jr., Temperature-Dependent Optical Properties of a Torsional Oscillator Model for Dinucleoside Phosphates, Biopolymers 6, 409 (1968).

39. S. R. Jaskunas, C. R. Cantor, and I. Tinoco, Jr., Association of Complementary Oligonucleotides in Aqueous Solution, Biochemistry 7, 3164 (1968).

40. Gordon Tollin, Magnetic Circular Dichroism and Circular Dichroism of Riboflavin and Its Analogs, Biochemistry 7, 1720 (1968).

41. A. Bobst, Charakterisierung des 5, 6, 7, 8-Tetrahydropterin-(THP)-Radikals in saurer Lösung, Helv. Chim. Acta 51, 607 (1968).

42. E. A. Oakberg and Ann M. Hughes, Deuterium Oxide Effect on Spermatogenesis in the Mouse, Experimental Cell Res. 50, 306 (1968).

43. Lance L. Simpson, Effects of Intraperitoneally Injected Botulinum Toxin on Rat Cerebral Cortex Levels of Acetylcholine, J. Neurochem. 15, 359 (1968).

44. Lance L. Simpson, The Interaction between 5-Hydroxytryptamine and Botulinum Toxin Type A, Toxicol. Appl. Pharmacol. 12, 249 (1968).

45. Lance L. Simpson, Evidence for the Nonspecificity of the Interaction between 5-Hydroxytryptamine and Botulinum Toxin, Toxicol. 5, 239 (1968).

46. Lance L. Simpson, Daniel A. Boroff, and U. Fleck, Examination of the Possible Pathophysiology of the Central Nervous System during Botulinas Poisoning, Exptl. Neurol. 22, 85 (1968).

47. M. R. Rosenzweig, D. Krech, E. L. Bennett, and M. C. Diamond, Modifying Brain Chemistry and Anatomy by Enrichment or Impoverishment of Experience, in Early Experience and Behavior, G. Newton and S. Levine, Eds. (C. C. Thomas, Springfield, Ill., 1968), 258-298.

48. M. R. Rosenzweig and E. L. Bennett, Drugs and Modulate Effects of Environment on Brain Growth, Proc. 76th Ann. Conv. Am. Psychol. Assoc. 3, 269 (1968).

49. E. L. Bennett and M. R. Rosenzweig, Brain Chemistry and Anatomy: Implications for Theories of Learning and Memory, in Mind as a Tissue, C. Rupp, Ed. (Hoeber Medical Div., Harper and Rowe, New York, 1968), 63-86.

50. M. R. Rosenzweig, W. Love, and E. L. Bennett, Effects of a Few Hours a Day of Enriched Experience on Brain Chemistry and Brain Weights, Physiol. Behavior 3, 819 (1968).

51. M. R. Rosenzweig, W. Love, and E. L. Bennett, Enriched Experience for Two Hours a Day Alters Brain Chemistry, Fed. Proc. 27, 278 (1968) (Abstract).

52. E. L. Bennett, M. R. Rosenzweig, A. Orme, and S. Rosenbaum, Cholineacetyl Transferase Activity Difference in Brain Regions of Ten Rat Strains, Related to Acetylcholinesterase Activity, Acetylcholine Concentration, and Environmental Enrichment, Fed. Proc. 27, 836 (1968)(Abstract).

THESES

Work for the following Ph. D. theses was completed during 1968:

1. Jon Carl Palmer.
   The Control of Catabolite Repression of β-Galactosidase in Escherichia coli (Molecular Biology), UCRL-18144, March 1968.

2. Jeffrey John Kelly.
   The Role of the Pigment Arrangement in Photochemistry and Kinetics of Photosynthesis, UCRL-18224, May 1968.

3. Harry Gus Ungar.
   Studies on the Control of Ribosomal Protein Synthesis in Escherichia coli, UCRL-18450, September 1968.

4. Kam-sik Ng.
   Quantum Requirement in Photosynthesis and the Effect of Light Quality on Photosynthetic Product Distribution, UCRL-18451, September 1968.

PERSONNEL LIST

Senior Staff

Melvin Calvin, Director
James A. Bassham
Edward L. Bennett
Paul M. Hayes
John E. Hearst
Melvin P. Klein
Richard M. Lemmon
Vivian Moses
Roderic B. Park
Henry Rapoport
Kenneth H. Sauer
Ignacio Tinoco, Jr.

Research Staff

Lelia M. Coyne
Wallace R. Erwin
Marie S. Hebert
Joyce S. Hsu
Ann M. Hughes
Kimiko Kanazawa
Martha R. Kirk
Chantal Lafont
Byrdie D. Mann
Lucy Marton
Hiromi Morimoto
Ann Orme
Donald E. Phelps
Dell H. Roadman
Stephanie L. Rosenbaum
Pamela B. Sharp

Postdoctoral Fellows

Albert Bobst
Kevin D. Cadogan
Ercole Cavalieri
Henry W.-S. Chan
Thomas R. Dehner
Anne-Lise Etienne
Paolo S. Ferruti
Eugene F. Friedman
David Gill
Michael A. Harpold
Barrie S. Hesp
Tamotsu Kanazawa
Gorge Kotowycz
Gotthard Krause
James R. Maxwell
Richard E. Moore
Brian C. Myhr
Amar Nath
Charles J. Norton
Harry C. Ottenheym
Robert A. Plane
Walter H. Riege
Igor A. Rybin
Hugo Sephton
Janet S. Splitter
Helmuth Springer-Lederer
Hans Steffen
V. Subramanyan
Shirley Tsai
Kern von Hungen
Howard H. Wang
Charles Weiss, Jr.

Laboratory Assistants

G. Stuart Baillie
Claire Broom
Mark Burnside
Franklin D. Collins
Burton P. Dorman
Ethel LeFall
Arthur F. Levit
William S. McAllister
J. A. McCammon
Patrick J. Williamson

Graduate Students

Rameshwar D. Agarwal
Algis Alkaitis
Robert A. Bazell
Loring K. Bjornson
Roberto Bogomolni
Marty E. Brewer
David E. Downie
Abdalla M. El-Badry
Gerald Entine
Marks S. Fischer
Jerry Han
George A. Havach
Walter A. Herzberg
Frederick A. Johnson
Jeffrey J. Kelly
Leo N. Kramer
Hung J. Lee
Tz-hong Lin
Robert M. Macnab
Robert Mann
Hugh R. Matthews
Robert J. Miller
Kam-si, Ng
Howard Ono
Jon C. Palmer
Harriet Parker
Gerald C. Peters
Kenneth D. Phillipson
Helmut Pohlit
Petrie M. Rainey
George C. Ruben
Alfrech J. Schultz
Lance L. Simpson
Jack Spiegelman
Alexander Sun
Nelson M. Teng
Harry G. Ungar
William Van Hoeven
Paul F. Wegfahrt, Jr.

Undergraduate Students (Research

Neal Adams
Joel Gottesfeld
Michael Mille

Shops

Electronics:	Robert Creedy John A. Despotakis
Carpenter:	Richard O'Brien
Glass:	William Hart

Office

Evelyn Litton
Johanna Onffroy
Marilyn Taylor
Gerryann Wulbern

PERMUTED INDEX